One-Dimensional Nanostructured Polyaniline: Syntheses, Morphology Controlling, Formation Mechanisms, New Features, and Applications

JINGPING WANG

College of Chemistry and Chemical Engineering, Shaanxi University of Science and Technology, Xi'an 710021, People's Republic of China

DONGHUA ZHANG

School of Materials and Chemical Engineering, Xi'an Technological University, Xi'an 710032, People's Republic of China

Received: January 30, 2012
Accepted: April 16, 2012

ABSTRACT: One-dimensional nanostructured polyaniline (1D nano-PANI), including nanofibers, nanowires, nanobelts, nanotubes, nanorods, nanoneedles, and nanosticks, has been extensively studied recently due to its unique properties

Correspondence to: J. Wang; e-mail: wangjingping@sust.edu.cn.
Contract grant sponsor: Natural Science Basic Research Plan in Shaanxi Province of China.
Contract grant number: 2011JM6003.
Contract grant sponsor: Doctor Startup Fund of Shaanxi University of Science and Technology.
Contract grant number: BJ12-05.
Contract grant sponsor: President Fund of Xi'an Technological University.
Contract grant number: XAGOXJJ0613.

Advances in Polymer Technology, Vol. 32, No. S1, E323–E368 (2013)

and many potential applications. As a continuation of our previous review on 1D nano-PANI (D. H. Zhang and Y. Y. Wang, *Mater Sci Eng* B 2006, 134(1), 9–19), the research and development of 1D nano-PANI, including both syntheses and applications, in the past 5 years (2006–2010) are reviewed in this paper. Newly invented chemical methods for fabrication of 1D nano-PANI, such as solid-state polymerization, seeding polymerization, UV light- and microwave-assisted polymerization, plasma-induced polymerization, porous membrane controlled polymerization, and vapor phase polymerization, are briefly reviewed, and morphology controlling of the nanostructures during several synthesizing processes are reported and discussed at first. The formation mechanisms and key factors that affect the morphology evolution of the 1D nano-PANI are discussed. Novel features of 1D nano-PANI, such as aligned or oriented, longer, self-doped, chiral, derivative, carbonized, and dendritic PANI, are summarized. Finally, newly exploited applications of 1D nano-PANI in the past few years, such as sensors (e.g., gases sensors, biosensors, moisture or humidity sensors, TNT sensors, taste sensors, and noble metal ion sensors), absorbents, catalysts, actuators, supercapacitors, batteries, fuel cells, solar cells, electrochromic devices, hydrogen storages, surface modifiers, field-effect transistors, and functional materials, are discussed in detail. Adv Polym Techn 32: E323–E368, 2013; View this article online at wileyonlinelibrary.com. DOI 10.1002/adv.21283

KEY WORDS: Nanofiber, Nanorod, Nanotube, Polyaniline, Sensor

Introduction

Since the first report by Kaner's group[1] that polyaniline (PANI) nanofibers with a diameter of 30–50 nm and a length of 500 nm to several micrometers can be facilely synthesized by an interfacial polymerization and showed significantly improved performance for gas sensing, great interest has been aroused in the area of one-dimensional nanostructured polyaniline (1D nano-PANI), as evidenced by the growing numbers of publications in the area (Fig. 1). This 1D nano-PANI includes not only nanofibers, nanowires, nanorods, nanotubes, nanofibrils, nanobelts, and nanoribbons, as we discussed before,[2] but also newly fabricated nanoneedles (Fig. 2)[3,4] and nanosticks (Fig. 3).[5] Research works focused on 1D nano-PANI can be roughly divided into the following four aspects, that is, (1) exploiting new and efficient methods for production of the nanostructures, (2) improving the quality of the nanostructures, (3) studying the new properties of the nanostructures and their applications, and (4) clarifying the formation mechanism of the nanostructures, especially in the no-template chemical procedures. For instance, on the one hand, longer and uniform PANI nanofibers, aligned or oriented PANI nanofibers and various substituted PANI nanofibers have been synthesized by different groups. On the other hand, novel properties like photoswitching and new applications include biosensor, catalyst, humidity and moisture sensor, actuator, and so forth, have been demonstrated. Furthermore, amended mechanisms that apply not only to PANI nanofibers but also to polypyrrole (PPY) and polythiophene (PTH) nanofibers have been proposed, and several key factors, such as aniline dimer, hydrogen bonding, aniline concentration, and solution acidity, in preparation of 1D nano-PANI have been identified and studied. To date, several outstanding review articles[2,6–15] and book chapters[16,17] have been published on 1D nano-PANI and conducting polymer nanostructures.[18] However, a more detailed and up-to date review paper on the syntheses, properties, and applications of 1D nano-PANI is still helpful and indispensable to the scientific community, owing to the myriad of studies and rapid development of the research in this area. The paper can be considered as further reading material to our previous mini review,[2] and so the works that are already summarized and cited in Ref. 2 are not discussed here again.

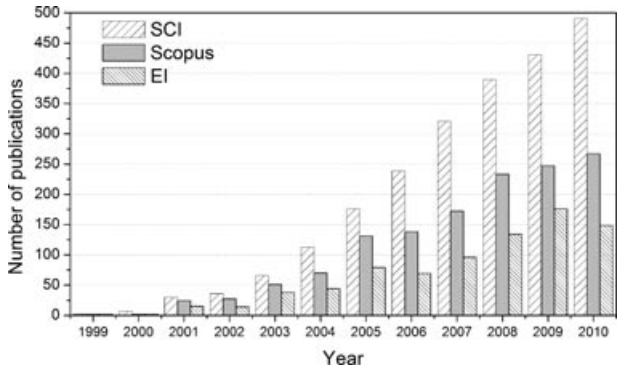

FIGURE 1. Number of papers with topic = (polyaniline) and topic = (nanofib* or nanowire* or nanobelt* or nanotube* or nanorod* or nanoneedle* or nanostick*) from both Web of Science, Scopus, and Engineering Village (as searched on Jan. 6, 2012).

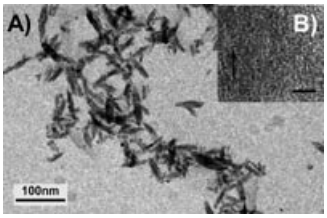

FIGURE 2. (A) TEM image of PANI nanoneedles; (B) HRTEM image of PANI nanoneedle. Scale bar = 3 nm (reproduced by permission of ACS Publications).[3]

The whole review is organized in two parts. In the first part, newly invented chemical methods for fabrication of 1D nano-PANI and morphology controlling the nanostructures during several synthesizing processes are briefly reviewed at the beginning. Furthermore, the formation mechanisms and key factors that affect the morphology evolutions of the 1D nano-PANI are discussed. Finally, novel features of 1D nano-PANI are reported and discussed.

In the second part, newly explored applications of 1D nano-PANI in the past 5 years (2006–2010) are emphasized and discussed in detail.

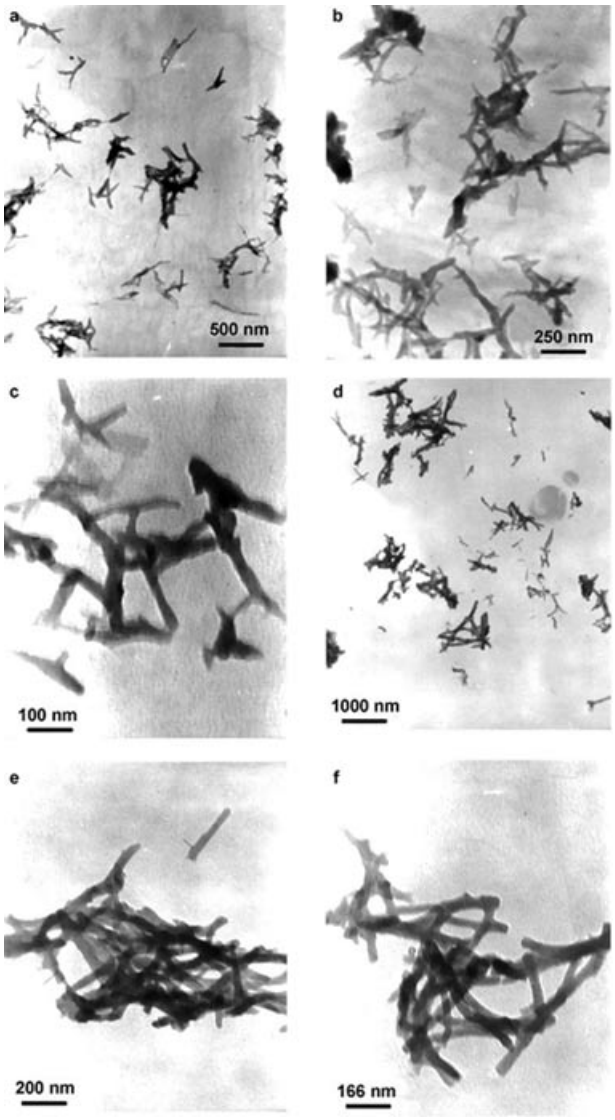

FIGURE 3. TEM images of PANI nanosticks synthesized in 0.5 M sulfuric acid ((a)–(c)) and 2 M nitric acid ((d)–(f)) (reproduced by permission of Wiley-VCH Verlag GmbH & Co. KGaA).[5]

Syntheses and Morphology Controlling of 1D Nano-PANI

SYNTHESES OF 1D NANO-PANI

Since each synthesizing method has its own advantages, 1D nano-PANI is still being synthesized by using various methods as discussed in our previous paper,[2] such as (1) hard template synthesis with templates of anodic aluminum oxide (AAO),[19–23] silica nanotubes,[24] halloysite nanotubes,[25] copper wires or rings,[26] fly ash,[27] polycarbonate track etched filtration membranes,[28] electrospun fibers,[29,30] NiO nanoparticles,[31] thin-glass tubes,[32] and eggshell membrane[33]; (2) soft template synthesis method with templates of crown ether,[34] tobacco mosaic virus,[35] naphthalene sulfonic acid (NSA),[36–38] aminobenzenesulfonic acid (SAN),[39] camphorsulfonic acid (CSA),[40–42] dodecylbenzenesulfonic acid

(DBSA),[43–45] molybdic acid,[46] amino acids,[47] poly(3-thiopheneacetic acid),[48] 3,5-dinitrosalicylic acid,[49] pyrene sulfonic acid,[50] 12-tungstophosphoric acid,[51] acid mordant yellow GG,[52] sucrose stearate or sucrose octaacetate,[53,54] sodium alginate,[55] polyethylene glycol,[56] β-cyclodextrin,[57,58] chitosan,[59] a mixture of cetyltrimethylammonium bromide (CTAB) and sodium dodecylbenzenesulfonate (SDBS),[31,60] CTAB or Triton X-100,[61,62] sodium dodecylsulfate (SDS),[63–66] 1-hexadecyl-3-methylimidazolium chloride,[67] 1-butyl-3-methylimidazoliumchloride,[68] 4-sulfobenzoic acid monopotassium salt,[69] and deoxyribonucleic acid (DNA)[70–73]; and (3) no-template synthesis, such as interfacial polymerization,[3,74–89] rapid mixing polymerization,[90–94] sonochemical synthesis,[95,96] and various electrochemical methods.[19,97–117]

The polymerization media covers not only the traditional acidic and neutral aqueous solution systems[118–121] or a hydrogel system[122] but also the alkaline aqueous solution systems.[120,123–125]

The starting materials for syntheses of 1D nano-PANI include not only aniline monomer and its derivatives[126] but also some aniline dimers such as *N*-phenyl-1,2-phenylenediamine and *N*-phenyl-1,4-phenylenediamine.[127] Copolymer PANI–PPY nanofibers were also successfully synthesized using cetyltrimethyl ammonium chloride or SDBS as the soft templates[128] or by an interfacial polymerization[82] with aniline and pyrrole as the starting materials. The composition of the copolymer nanofibers has a great effect on the morphology and/or size of metal nanoparticles formed through the redox reaction of the copolymer nanofibers.[128] With the addition of some nanoparticles such as nano-TiO_2 particles,[129–134] carbon black nanoparticles,[135] gold nanoparticles,[136] or inorganic salts[137,138] into the polymerization media or by chemical oxidative polymerization of aniline with some inorganic compounds that can deliver nanoparticles upon the redox reaction with aniline such silver nitrate,[139–141] chlorauric acid ($HAuCl_4$),[142,143] H_2PtCl_6,[75] CH_3SO_3Ag/H_2PtCl_6,[144] hybrid or composite PANI nanofibers or nanotubes, where these nanoparticles were dispersed inside the 1D nano-PANI structures, were also fabricated. Another kind of nanocomposite that is composed of pure 1D nano-PANI and a second nanomaterial, such as zeolite,[145] montmorillonite,[146] graphite nanosheets,[147,148] carbon nanotubes (CNTs),[149–151] or ferrite nanocrystals,[152] was also fabricated by adding a second nanomaterial in the polymerization media. These nanocomposites containing 1D nano-PANI are completely different from the hybrid or composite 1D nano-PANI.

In addition to the mostly used ammonium persulfate (APS), many other oxidants such as ferric chloride,[153–157] vanadic acid,[158] $HAuCl_4$ or tetrachloroaurate,[40,159–161] silver nitrate,[162] sodium chlorite,[163] manganese oxide,[164] hydrogen peroxide,[165–167] ferric sulfate ($Fe_2(SO4)_3{\cdot}xH_2O$),[168] or a binary oxidant system of APS/potassium dichromate,[169] APS/ferric chloride,[170,171] APS/silver nitrate,[141] APS/silver nitride,[172] CH_3SO_3Ag/H_2PtCl_6,[144] and potassium biiodate/sodium hypochlorite,[173,174] were employed for syntheses of 1D nano-PANI.

In addition to the no-template synthesis methods summarized in our previous paper,[2] novel methods invented and studied in the years followed are summarized in this section.

Solid-State Polymerization

By simply hand grinding of a mixture of aniline hydrochloride with either dehydrated ferric chloride ($FeCl_3$)[175] or hydrated ferric chloride ($FeCl_3{\cdot}6H_2O$)[176] for 40 min, branched PANI nanofibers (Fig. 4) with a diameter of 15–40 nm and a length of hundreds of nanometers were successfully synthesized by Zhou and Du and their coworkers. In both reaction systems, changing of the reaction time and molar ratio of monomer to oxidant, or dedoping with ammonia water, has no significant effect on the morphology of the PANI nanofibers. Although the formation mechanism of PANI nanofibers in solid-state polymerization is unclear, it is, as revealed by preliminary results, different from that in solution-based methods and is believed to be related to the mechanochemical

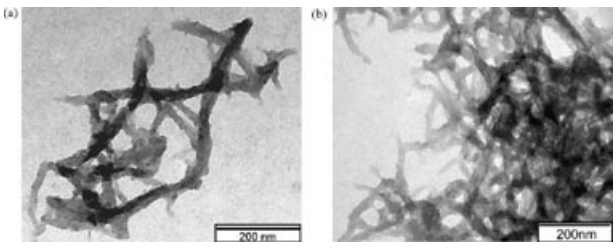

FIGURE 4. TEM micrographs of the products obtained (a) after grinding for 2 h and [$FeCl_3$]:[aniline] = 2:1 and (b) after grinding for 1 h and [$FeCl_3$]:[aniline] = 1:1 (reproduced by permission of Elsevier B.V.).[175]

oxidation polymerization process and the linear nature of PANI chains. Since no additional surfactants or organic solvents were used, the method was demonstrated to be a simple, facile, and practical one for the preparation and processing of PANI nanomaterials. In another study, PANI nanorods with a diameter of 30–60 nm and a length of 150–270 nm were also prepared by mixing solid APS and anilinium chloride crystals in equal molar ratios with a mortar and pestle.[177]

Seeding Polymerization

In addition to the insoluble nanomaterials initially used such as PANI nanofibers, CNTs, hexapeptide, and V_2O_5 nanofibers by Zhang et al.,[178] more and more seeds, including both insoluble and soluble ones, were reported for preparation of PANI nanofibers with improved quality. Insoluble seeds include nanosized alumina fibers,[179] whereas soluble ones cover various polymer solutions. For instance, by using solutions of conventionally synthesized PANI in various organic solvents such as dimethyl sulfoxide (DMSO), dimethyl formamide (DMF), dimethyl acetamide (DMA), and *N*-methyl-2-pyrrolidione (NMP) as seeds, Xing et al.[180] found that uniform PANI nanofibers with a relatively high conductivity (up to 34.5 S cm^{-1}) can be achieved with a PANI solution in DMSO as seeds. The lower acid concentration and PANI/DMSO solution amount and concentration all led to the aggregation of PANI nanofibers. It was also found that the size of PANI nanofibers increased with the aniline concentration, but not much with the reaction time. In a later study, solutions of aniline in either water miscible (DMSO, DMF, tetrahydrofuran (THF), and NMP) or immiscible (toluene, xylene, and carbon tetrachloride) organic solvents were used as seeds in an aqueous solution of APS for the preparation of PANI nanofibers by the same group.[181] Chlorophyllin (Fig. 5), a water soluble derivative of chlorophyll, was used as an in situ seed for the preparation of PANI nanofibers, since nanorods-like structures would be formed by the material under acidic conditions.[182] The chlorophyllin seed influenced the morphology (e.g., a higher concentration led to the aggregation of PANI), but not the molecular structure of the resulting PANI nanofibers, and was easily removed by washing with acetone or sodium hydroxide solution, rendering the method an alternative one for large-scale production of PANI nanofibers. Using Schiff bases such as *m*-phenylenediamine-glyoxal or *p*-phenylenediamine-glyoxal as seeds,

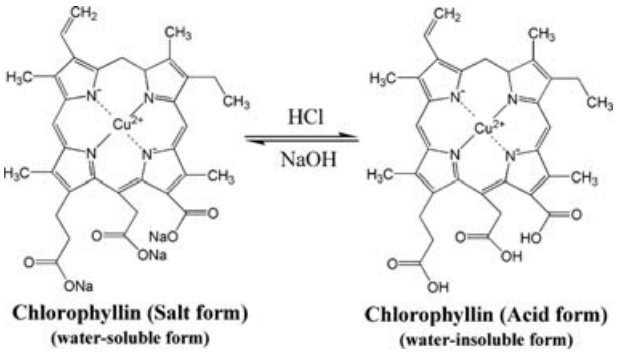

FIGURE 5. Chlorophyllin structures under acid–base conditions (reproduced by permission of Elsevier B.V.).[182]

PANI nanorods were successfully synthesized by Wang et al.[183] The average diameter of these PANI nanorods can be controlled by adjusting the Schiff base structure, dosage, and concentration of H^+ in the reaction medium. More importantly, the PANI nanorods showed unusual electromagnetic loss at the microwave frequency (f = 8.2–12.4 GHz), revealing the potential application for microwave absorption.

UV Light-Assisted Polymerization

In addition to the gamma ray assisted method for fabrication of PANI nanofibers,[184] UV light illumination was also employed for the synthesis of PANI nanofibers,[185,186] nanowires,[187] and nanotubes.[139] By illuminating the acidic solution of aniline and oxidants, a significant acceleration effect was observed and fine nanofibrous structures of PANI were achieved. The diameters of PANI nanofibers can be controlled and tuned by selecting the oxidants and the monomer/oxidant concentrations.[185,186] For instance, statistical transmission electron microscopy (TEM) measurements showed that the diameter range of the PANI nanofibers synthesized with an oxidant of ferric chloride, APS, and silver nitrate is 100–250, 40–70, and 10–25 nm, respectively.[185] Furthermore, uniform PANI nanofibers with smooth surfaces were achieved when lower concentrations of CTAB, which acted as the soft template, and hydrochloric acid (HCl) were used.[186]

Microwave-Assisted Polymerization

With microwave irradiation of an aqueous solution of aniline and 2-aminobenzoic acid or 2-aminosulfonic acid, nanofibers of the copolymers were successfully prepared by chemical polymerization with potassium iodate as the oxidant.[188,189]

In a comparison with the copolymers prepared by the conventional polymerization, where no other external irradiation such as microwave, ultrasonic, or UV light was applied, the copolymers achieved using microwave-assisted polymerization showed not only nanofibrous morphologies but also significantly increased yields. However, the structures of the copolymers were not significantly changed with microwave irradiation. Moreover, the nanofibers achieved by microwave-assisted polymerization exhibited 2.1–2.4 times better radical scavenger efficacy than the conventionally synthesized counterparts, revealing that the nanostructured copolymers can be used as promising radical scavengers. The authors also proposed a formation mechanism of the nanofibers by invoking the thermal and nonpurely thermal effects on the basis of classical nucleation theory.

Plasma-Induced Polymerization

Nanofibrous PANI films with nanofiber diameters ranging from 15 to 20 nm were prepared by plasma-induced polymerization and studied for nitrogen dioxide gas sensors.[190] An inductively coupled pulsed-plasma reactor at different radio frequency (RF) plasma pulsing, monomer injection, and substrate positions was used for the fabrication. A custom-built automotive injector with an oscilloscope was used to control the injection of vaporized aniline monomer under pressure ranging from 13 to 40 Pa. The optimum condition for preparation of the nanofibrous PANI thin film was established as fabrication on a glass substrate placed at a distance of 15.5 cm from the RF coil under 40 Pa pressure and 50 plasma pulses.

Porous Membrane Controlled Polymerization

In this method, the aqueous acidic solution of aniline or other derivative monomer was separated from the aqueous acidic oxidant solution by a permeable membrane (Fig. 6).[191] With diffusion of a monomer or oxidant through the membrane at controlled rates, PANI nanofibers formed at the membrane–solution interfaces and precipitated out of the aniline or oxidant solution. The pores of the membrane shrank simultaneously in diameter owing to the precipitation PANI and resulted in the termination of the polymerization. The termination time can be controlled by modifying the synthesis conditions such as monomer and oxidant concentrations, temperature, or stirring. Exclusive PANI nanofibers were formed with the early termination of the polymerization since secondary nucleation and growth of the initially formed PANI nanofibers were effectively prevented. PANI nanofibers can be collected directly both outside and inside the membrane without any further treatment. The diameters and lengths of the nanofibers can be facilely tuned by changing the pore diameters of the membrane at fixed synthesis conditions. The concept and methodology of the method are either different from that of hard template polymerization, since the nanofibers are not confined to the channels and no template removal step is needed, or different from the interfacial polymerization, since the method is free of organic solvents, low cost, and scalable. Other advantages of the method include a wide coverage of monomers and monomer concentrations, since not only nanofibers of PANI and PANI derivatives but also nanofibers of other conductive and nonconductive polymers can be prepared by this method.[191]

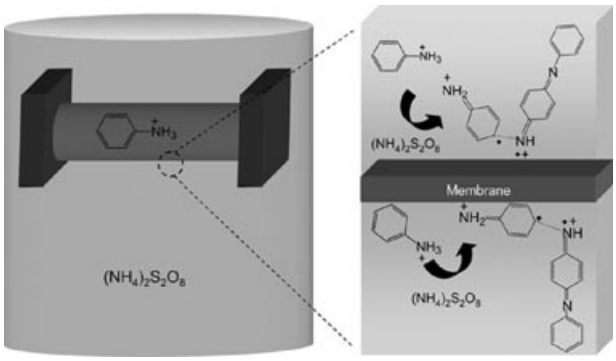

FIGURE 6. Schematic illustration of porous membrane controlled polymerization. A porous membrane is used to separate the monomer and oxidant solutions, resulting in careful control of nucleation and growth of nanofibers (reproduced by permission of The Royal Society of Chemistry.).[191]

Vapor Phase Polymerization

PANI nanofibers with a diameter of 20–100 nm and a length of 50–400 nm were also successfully synthesized by using vapor-phase polymerization.[192] In this method, aniline and a certain amount of aqueous HCl solution of APS were first placed into two round-bottomed fluxes, respectively. After these two round-bottomed fluxes were connected with a hollow glass tube, the one with aniline was heated at 200°C to generate aniline vapor. The aniline vapor thus produced was fed through

the hollow glass tube into the acidic APS solution in another round-bottomed flux and reacted there. PANI nanofibers were then formed with constant stirring of the aqueous solution. The as-prepared PANI nanofibers exhibited lower conductivity, but higher solubility and thermal stability, than the conventionally prepared PANI powders.

Others

Bulk quantities of PANI nanofibers in a fully reduced state (leucoemeraldine form) with a diameter of 20–50 nm were synthesized in one step by chemical oxidative polymerization of aniline with acetic acid instead of HCl and without use of any reducing agent or surfactants.[193] These nanofibers can be spontaneously oxidized by noble metal ions under mild aqueous conditions, leading to the deposition of various shapes, such as leaf, particulate, nanowires, and cauliflower for Ag, Pd, Au, and Pt, respectively, on the surface of the nanofibers. Furthermore, these nanofibers can also be used as seeds to prepare PANI nanofibers in a conventional HCl medium. By addition of a solid oxidant, such as APS, vanadium oxide, and potassium persulfate, into an unstirred aniline hydrochloride solution, which is completely different from the commonly used procedure of mixing solutions of oxidant and aniline, 1D and three-dimensional (3D) PANI nanostructures were easily prepared.[194] The slow release of the oxidant, via its solubilization and diffusion into the undisturbed solution, was considered the key step for formation of PANI nanofibers. PANI nanofibers or PANI nanoparticles can also be synthesized with the addition of varied concentrations of gadolinium chloride ($GdCl_3$) during the conventional chemical oxidative polymerization of aniline.[195]

Another method that must be mentioned is the Langmuir–Blodgett (LB) technique of molecular deposition,[196,197] in which a solution of an emeraldine base form of PANI was spread over the LB trough at an air/water interface at first. By either varying the acids used in the subphase, or adjusting the pH of the subphase in the LB trough, different doping induced nanostructures were formed. For example, at pH 1.5, nanorods with diameters less than 100 nm, nanoparticles with a diameter of 80 nm, and connected nanoparticles were obtained with acids of CSA, *p*-toluene sulfonic acid (*p*-TSA), and perfluoro-octanoic acid, respectively.[196] When *p*-TSA was used as the acid for adjusting the acidity of the subphase, nanorods with a diameter of 40 nm and a length of 400 nm, nanoparticles with a diameter of 15 nm, and connected lump-type nanostructures were formed at pH 1, 3, and 6, respectively.[197] In addition, a pseudo–high-dilution technique was also used for the synthesis of PANI nanofibers.[198] The aniline concentration was 0.4 M, 50 times higher than that in dilute polymerization as reported by Chiou and Epstein,[199] and a high yield can be achieved. The diameters of the nanofibers in the range of 18–110 nm can be tuned either by selecting different doping acids or by modulating the dropping rates of the oxidant solution to the aniline solution. With no stirring of the reaction mixture, PANI nanofibers with a high yield (93%) were also synthesized by a simple drop addition of APS solution to the aniline solution at a rate of one drop for every second at 0°C.[200]

MORPHOLOGY CONTROLLING OF 1D NANO-PANI

In addition to the study on the synthesis of 1D nano-PANI, the morphology controlling of the 1D nano-PANI is also studied.[201] Although the morphology controlling can be performed even after formation of PANI nanostructures, such as the transformation of a PANI nanofiber network to a continuous nanofilm by applying a local pressure of 28 MPa to the nanofiber network[202] and the fragmentation of the nanorods synthesized by using a porous alumina membrane template method into smaller nanowires with different bending shapes such as V and Y shapes,[203] only the measures taken during the synthesizing step, that is, before the formation of PANI nanostructures, are reviewed and discussed here for some specific synthesizing methods.

Interfacial Polymerization

Unlike the pioneering work by Huang et al.[1] in which PANI nanofibers formed at the interface are not affected by the polarity of the organic phase, He and Lu[204] reported that by finely controlling the polarity of the organic phase, the amount of APS, and the concentration of acid in an interfacial polymerization, nanostructured PANI with tubular, spherical polyhedral, and belt-like morphologies were prepared. For instance, nanobelts, a mixture of nanofibers and polyhedrons, and granular particles were formed, respectively, when the polarity of an organic solvent increased from hexane to toluene and to hexanol. The authors suggested that PANI nanostructures were formed by competing between the interfacial nucleation, which favors formation of PANI nanofibers, and aqueous nucleation, which

favors PANI granular particles. The polarity of organic solvents and concentration of acid influenced the diffusing rate of aniline from the organic to aqueous phase, whereas APS influenced the polymerization rate at the interface and in the aqueous phase. Therefore, the morphologies of the polymer can be controlled by tuning these factors. Wang et al.[205] also reported that by controlling the diffusion rate and polymerization induction time of aniline, which was achieved by adding a liquid paraffin layer between the organic and aqueous phases, PANI nanostructures such as nanosheets, nanofibers, and nanoparticles can be prepared at the interface. Using compressed carbon dioxide as the organic phase, PANI nanofibers with a fairly uniform diameter of 30–70 nm and the average length of 0.3–1 μm were synthesized with a high yield of 63.04% (Fig. 7).[206] The nanofibers can be well dispersed in various solvents such as water, ethanol, 2-propanol, *m*-cresol, and toluene with concentrations as high as 1000 mg L^{-1} due to their uniform size, offering profound possibilities for processing and applications of PANI nanofibers.

Rapid Mixing Polymerization

Various oxidants with different redox potentials were used for the synthesis of PANI nanofibers by chemical oxidative polymerization, and it was found that the diameters of PANI nanofibers increased with increasing oxidant redox potentials, obeying an equation given by the authors.[207] For instance, PANI nanofibers with a diameter of ca. 12 nm were achieved with copper chloride whose redox potential is 0.56 V, whereas a diameter of ca. 130 nm was achieved with APS, whose redox potential is 2.05 V.

Wang et al.[208] reported that by simply changing the molar ratios of *p*-TSA to aniline in the reaction mixture, in which only aniline and *p*-TSA were dissolved, the morphologies of PANI nanostructures can be controlled, rendering the method a novel and facile one among the others. For example, nanosheets were obtained when aniline/*p*-TSA increased from 3/1 to 5/1 and a mixture of nanosheets and microspheres was achieved when the molar ratio increased to 6/1, whereas PANI nanofibers were formed when an aniline/*p*-TSA ratio was kept at 1/3. Furthermore, other parameters such as temperature, APS concentration, and stirring also have an important influence on the morphology of PANI nanostructures.

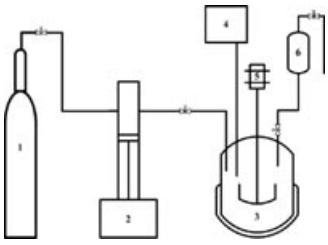

FIGURE 7. Schematic diagram of the experimental apparatus: (1) CO_2 cylinder, (2) syringe pump, (3) high-pressure reactor, (4) temperature controller, (5) magnetic drive, and (6) injector (reproduced by permission of Elsevier B.V.).[206]

By studying the polymerization of aniline in a high-viscosity reaction media, which was created by codissolving a high molecular weight polyethylene oxide (PEO) with aniline or the oxidant, it was found that well-dispersed 1D nano-PANI was formed even at high concentrations of aniline, irrespective of the oxidants and doping acids used.[209] With increasing of the viscosity of the reaction media, both sizes and aspect ratios of the 1D nano-PANI decreased significantly. The reason was ascribed to the suppressed mass transfer with the addition of PEO to the reaction media, which retarded the nucleation and growth of PANI nanostructures. Uniform PANI nanofibers were produced at a much lower aniline concentration (0.005 M), as reported by Wang and Jing,[249] by stirring the highly viscous reaction media.

In addition to the generally prepared cylinder nanotubes, PANI nanotubes with rectangular holes and outer contours were also fabricated by qualitatively and purposely controlling the reaction rates, which were realized by adjusting the acid and oxidant concentrations during the polymerization.[210] It was also found that the formation and orderly aggregation of the intermediates, that is, tetragonal prisms, played a key role in the formation of the PANI nanotubes with rectangular inner and outer cross sections. Using a redox initiator of APS/Fe^{2+} as the oxidant, high-quality PANI nanofibers with smooth surface and uniform diameters of 15–30 nm were prepared by Li et al.[211] The redox initiator suppressed effectively the secondary growth of PANI due to the accelerated polymerizing rate of aniline as compared with other oxidants, leading to formation of high-quality PANI nanofibers.

Soft Template Polymerization

An amphiphilic dopant 4-[4-hydroxy-2((*Z*)-pentadec-8-enyl) phenyl]-azobenzene sulfonic acid was used as the structure-directing agent for

preparation of PANI nanostructures since it forms a stable emulsion in a wide range of dopant/aniline ratios from 1/1 to 1/1500 by Jayakannan et al.[212–218] The acid was developed from cardanol, an industrial waste and pollutant from cashew nut, rendering the synthesis strategy renewable and environmentally friendly. Two supermolecular aggregates of the dopant exist in water depending on its concentration: One is a bilayer, and the other is a micelle. By simply controlling the dopant/aniline ratios in feed, PANI morphologies can be easily tuned. For instance, PANI nanostructures such as hollow spheres, dendritic nanofibers, and linear nanofibers were achieved by subsequent oxidation when the concentration of the dopant/aniline complex was above the critical micelle concentration since it exists as either aggregated or isolated micelles and a mixture of nanotubes plus nanofibers, or nanotubes was formed if below the critical micelle concentration since the complex is in the form of bilayers. The large-scale synthesis of PANI nanofibers, with a diameter of 130–200 nm and a length of up to 5 μm, up to 100 g quantity was successfully achieved by using the cylindrical micellar template of a renewable resource amphiphilic azo benzenesulfonic acid.[217] Since the amphiphilic azo benzenesulfonic acid dopant was found not to be suitable for dispersion polymerization, a novel amphiphilic dopant 4-(3-dodecyl-8-enylphenyloxy) butane sulfonic acid, which was synthesized by a ring opening of 1,4-butanesultone with cardanol under basic conditions, was used as the structural directing agent for fabrication of PANI nanofibers and nanotapes by the same group.[219] In the emulsion polymerization route, PANI nanofibers were achieved with the cylindrical micellar soft template formed between dopant and aniline, whereas in the dispersion polymerization route PANI nanotapes were obtained with the vesicular template of aniline and toluene. Very recently, another kind of amphiphilic dopant molecule, 4-(3-pentadecylphenoxy) butane-1-sulfonic acid, was synthesized from renewable resource 3-pentadecyl phenol via a ring opening of 1,4-butane sultone and used as a soft template for preparation of PANI nanofibers by the same group.[220] The acid has a hydrophobic long tail and a hydrophilic acid head, and stable organo-gel nanotube gels were formed by self-assembly of the acid in high polar solvents. With the addition of aniline, the acid molecules also self-assembled as gels with the aniline molecules preferentially trapped inside the nanotubes, and PANI nanofibers were prepared with oxidation of the gel-template using APS. In addition to its structure-directing effect on the formation of PANI nanofibers, the gel template also affected some other properties such as conductivity, solubility, percent crystallinity, and solid-state ordering of the as-prepared PANI nanofibers.

With stearic acid as the soft template, Wang et al.[221] found that by simply controlling the concentration of aniline and stearic acid, the morphology of PANI can be tuned from linear nanotubes to dendritic fibers and to network structures. For instance, PANI nanotubes with inner and outer diameters of 2–3 and 180–220 nm were obtained when 0.2 M aniline and 0.04 M stearic acid were used, respectively. However, interconnected 3D dendritic PANI fibers with a branch diameter of 160–200 nm resulted when the stearic acid concentration was decreased to 0.02 M and a further decrease of the stearic acid concentration to 0.001 M lead to dendritic PANI rods with a diameter of 80–120 nm. In another study, various nanostructures ranging from nanoflakes to nanorods and nanospheres were prepared by changing the molar ratios of selenious acid to aniline in chemical oxidative polymerization.[222] For example, PANI nanoflakes, nanorods, and nanospheres were obtained when the selenious acid to aniline molar ratio was 0.03, 0.5, and 2, respectively.

By changing either the chain lengths of dicarboxylic acids ($HOOC(CH_2)_nCOOH$, $n = 0$–4) or a molar ratio of the acids to aniline monomer, the average diameters as well as crystallinity and conductivity, of the chemically prepared PANI nanofibers and nanotubes were successfully controlled.[223] For instance, using malonic acid ($n = 1$) as the dopant (and also the soft template), the average diameter of the nanostructures increased from 100 to 170 nm with the molar ratio of dopant/aniline changed from 0.01 to 0.5, whereas conductivity increased from 0.048 to 0.94 S cm^{-1} with the molar ratio of dopant/aniline changed from 0.1 to 1.0. Keeping the molar ratio of dopant/aniline fixed at 0.25 and increasing the chain lengths of the dopant, that is, increasing the number of $–CH_2–$ groups in dicarboxylic acids from 0 to 4, the average diameter of the PANI nanostructures increased from 80 to 170 nm whereas the conductivity decreased from ca. 6.5×10^{-2} to ca. 2.4×10^{-2} S cm^{-1}. The strong peak at $2h = 6.50^{\circ}$ in the X-ray diffraction pattern revealed the orientation of dicarboxylic acids in the PANI chains. The interchain distance perpendicular to the polymer chains increased chain lengths of the dicarboxylic acid dopant. Similar results were reported by Zhang et al.,[224] where the morphology, diameter, crystallinity, and conductivity of the PANI micro/nanofibers were affected by

the alkyl chain lengths of saturated fatty acids used for the synthesis of the polymer. For instance, with an increase in the alkyl chain length from acetic acid to hexanoic acid, lauric acid, and stearic acid, the diameters of the PANI fibers increased monotonously from 190 to 450 nm.

PANI nanowires or submicro/nanostructured dendrites were also synthesized and immobilized on the surface of polyacrylic acid (PAA) grafted polypropylene (PP) films, rendering high hydrophilicity to the PP films.[225] PAA-grafted PP films were first immersed in an aqueous solution of aniline, PAA, and SDS, followed by stirring the solution for ca. 8 h. After keeping them at low temperature for 2 h, an aqueous APS solution was added. PANI nanowires with a diameter of 60–100 nm and a length of ca. 1 μm were achieved with continuous stirring, whereas PANI dendrites were achieved with stirring for only 20 min after the addition of APS solutions, showing that stirring plays an important role in forming PANI nanostructures. In a later study, shape-controllable PANI micro/nanostructures from spherical particles to nanowires and eventually to nanoribbons were deposited onto surfaces of the PP film by tuning the conformation of the surface-grafted PAA brushes and the ratio of acrylic acid to aniline by the same group.[226] Superhydrophobicity was exhibited by the PANI nanowires and nanoribbons grafted PP films, which is different from the hydrophilic PP films obtained in their first study.[225] In both studies, the grafted PAA acted not only as a template but also as a dopant to PANI.

By controlling the molar ratios of 5-sulfosalicylic acid to aniline during chemical oxidative polymerizing aniline in the aqueous solution of 5-sulfosalicylic acid, the morphology, molecular structure, molecular weight distribution, and conductivity of 5-sulfosalicylic acid doped PANI were studied.[227] With the molar ratio kept at 1 or 0.5, granular agglomerates were obtained. While decreasing the molar ratio to 0.25, nanotubes with a typical outer diameter of 100–250 nm, an inner diameter of 10–60 nm, and a length of 0.4–1.5 μm, and the nanorods with a diameter of 80–110 nm and a length of 0.5–0.7 μm were synthesized. The formation of nanotubes was explained on the basis of the precipitation–dissolution of oligomer templates, whereas nanorods were explained on the basis of stacking of low-molecular-weight-substituted phenazines.

Using a CTAB–lauric acid complex coacervate gel as the template, 1D nano-PANI was easily tuned from nanotubes to nanofibers and to 3D networks by changing the physical state of the initiator, that is, the APS solution or APS powder, and that of the gel template, that is, sol or gel, during polymerization.[228] The one-step method is reproducible even in the large-scale synthesis of 1D nano-PANI and might also be a general route for fabrication of some other polymers with nanostructures according to the authors.

Sonochemical Synthesis

With ultrasonic irradiation of the mixture of aniline and oxidants in varied acidic solutions, 1D nano-PANI can be successfully synthesized since the secondary growth can be effectively prevented by ultrasonic irradiation.[95,96,229,230] By polymerizing aniline in the presence of different doping concentrations of mineral or organic acids (hydrochloric, nitric, sulfuric, phosphoric, perchloric, and CSA) under ultrasonic irradiation, it was found that PANI nanotubes were formed with a lower concentration of dopant acids (Fig. 8), whereas PANI nanofibers were formed with a higher concentration of dopant acids, no matter which one was used.[96] Furthermore, the diameters of the nanotubes or nanofibers can be roughly controlled by using different kinds of dopant acids. For instance, nanotubes with the average diameter of ~200, 160–180, 180, and ~150 nm and nanofibers with the average diameter of ~50, ~60, ~70, and ~110 nm were achieved with lower and higher concentrations of nitric acid, CSA, perchloric acid,

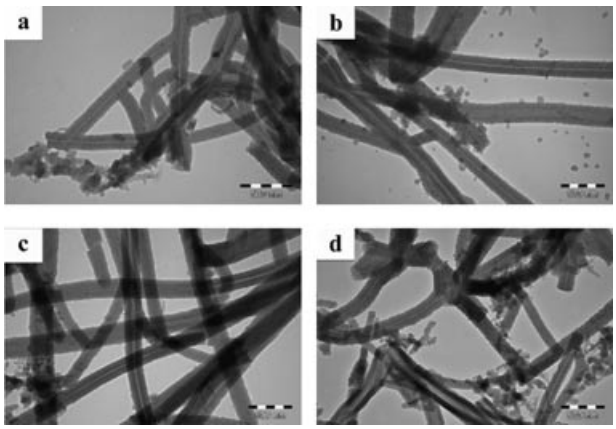

FIGURE 8. TEM images of PANI nanotubes synthesized under ultrasonic irradiation doped by the following acids (0.05 M): (a) phosphoric, (b) nitric, (c) perchloric, and (d) camphorsulfonic acid (reproduced by permission of WILEY-VCH Verlag GmbH & Co.).[96]

and phosphoric acid, respectively. By systematically examining the effects of ultrasonic power, ultrasonic frequency, and reaction temperature on the morphologies of PANI, Li et al.[231] found that both increased ultrasonic power (up to 250 W) and reaction temperature (up to 75°C) were favorable for formation of PANI nanofibers with smoother surfaces and uniform diameters. For example, at a fixed ultrasonic frequency of 40 kHz, nearly exclusive nanofibers with a diameter of 40–80 nm and a length of 300–700 nm were obtained when ultrasonic power was increased from 100 to 250 W; otherwise, PANI nanofibers to a certain extent with irregular agglomerates resulted at lower power levels. Although the purity of PANI nanofibers increased generally with increasing ultrasonic frequency from 20 to 100 kHz, an optimal frequency of 50 kHz was determined in achieving PANI nanofibers with the highest uniformity and smoothest surfaces at a fixed ultrasonic power of 250 W. At a fixed ultrasonic power of 100 W and frequency of 40 kHz, high-purity PANI nanofibers with smoother surfaces, more uniform diameters, and larger aspect ratios were produced at 75°C, with the highest temperature range of 0–75°C.

Formation Mechanisms of 1D Nano-PANI

Among the various synthesizing methods for the preparation of 1D nano-PANI, the no-template method is the most favored one owing to not only the facility or feasibility of the synthesis process but also the pureness of the final achieved products. The last aspect has proved much more important than the former one since the very beginning by research.

Studies on the formation mechanism of 1D nano-PANI prove its significant importance,[120,232–239] and several important mechanisms have been put forward by Kaner et al.,[240–243] Chiou and Epstein,[199,244] Manohar et al.,[245] Travas-Sejdic et al.,[246,247] Stejskal et al.,[248] Wang and Jing,[249] Huang and Lin,[250,251] and Ho et al.[43] However, all these mechanisms cannot explain why the intrinsic fibrillar growth is applicable only to PANI[242,252,253] but not to other intrinsically conducting polymers such as PPY and PTH.[254] Also, the mechanism proposed by Manohar et al.[245] is not applicable to the finer PANI nanofibers or nanofibers/nanotube mixtures prepared with hydrogen peroxide as the oxidant.[165–167]

To answer the above-mentioned first question, Li et al.[254] proposed a new model based on a combination of the classical nucleation/growth theory and electric double layers model (Fig. 9). According to this mechanism, the initially formed PANI chains and nanofibers are positively charged owing to both the protonation and partial oxidation of PANI chains and are surrounded by "electric double layers," which consist of an inner dense layer and an outer diffusion layer. If only the diffusion of reactants such as reactive aniline radicals and oligomers overcomes the repulsion from the double layers, initial polymer chains or nanofibers can grow larger or longer. Aniline monomers, oligomers, and polymers are all very easily protonated in acidic solutions, and their diffusion was limited by the repulsion force; PANI nanofibers were then easily formed because reactants are available only at the ends of the nanofibers. While in the case of PPY, the reactive reactants will easily penetrate the electronic layer and react at the surface of the initially formed nanoseeds, leading to a granular structure rather than a fibrillar one. Therefore, it is concluded that the

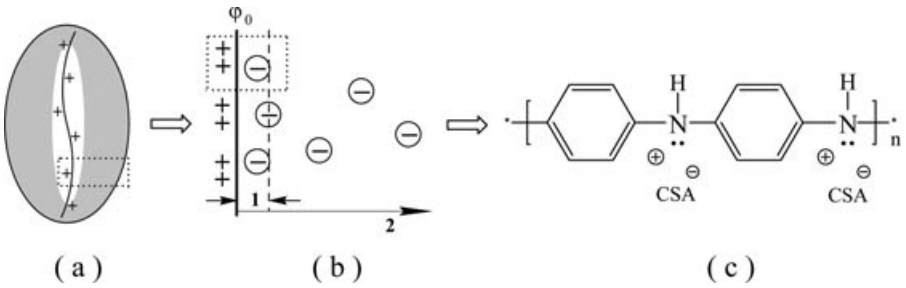

FIGURE 9. (a) Schematic diagram of electric double layers on a positively charged PANI chain. (b) Charge profile near the PANI/solution interface, where regions 1 and 2 represent the inner dense layer and the diffusion layer, respectively. (c) Simplified chemical structure illustrating the protonation and charging on a PANI chain (reproduced by permission of American Chemical Society).[254]

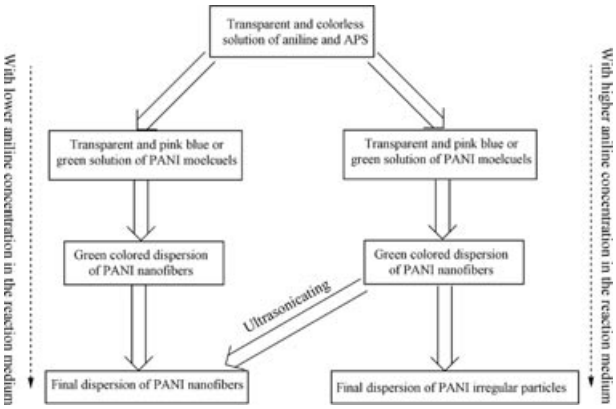

FIGURE 10. Schematic illustration of the formation of PANI with different morphologies (reproduced by permission of American Chemical Society).[249]

intrinsic fibrillar growth of PANI resulted from both the easy protonation of PANI chains and the function of the electric double layer structure. Furthermore, the aniline concentration dependent PANI morphology can be explained on the basis of the electric double layer structure. If two particles move close to each other, a repulsion force results due to the overlapping of the diffusion layers, and congregation is happened only when the potential barrier was overcome. Therefore, repulsion force dominates over attraction force in a dilute solution and formation of PANI nanofibers is favored; whereas attraction force dominates in a solution of high aniline concentration, leading to the formation of granular PANI. This explanation was also corroborated by Wang and Jing[249] that PANI nanofibers were formed and preserved with a lower aniline concentration whereas with an increase in the aniline concentration large-sized PANI particles or agglomerates were obtained (Fig. 10).

In addition to the proposed mechanism mentioned above, several synthesizing parameters that play an important role in facilitating formation of 1D nano-PANI have been identified and reported, including aniline dimer, hydrogen bonding, aniline concentration, and solution acidity, as discussed in detail below.

ANILINE DIMER

Although the effect of some mediators like *p*-phenylenediamine on the morphology of PANI was first reported by Stejskal et al. in 1999,[255] the importance of it on formation of PANI nanofibers or substituted PANI nanofibers was stressed again recently by Tran and coworkers[256,257] and Surwade et al.[258] According to Tran et al.,[257,259,260] less entangled and longer PANI nanofibers were formed when either aniline dimer or *p*-phenylenediamine was added during the polymerization process in a catalytic amount under conditions that typically do not favor nanofiber morphology. A mechanism based on classical nucleation theory was then proposed as such. With addition of these promoters, the polymerization rate is significantly accelerated and supersaturation is quickly achieved, resulting in the homogeneous nucleation dominated reaction, which leads to PANI nanofibers. Most importantly, successful syntheses of both PPY and PTH nanofibers by simply adding minutes of their dimers in the reaction revealed the mechanism may be applicable to a wide range of semirigid rod, precipitation polymerizations.

By studying the morphology evolution of PANI on the walls of different reaction vessels and intentionally added surfaces, Surwade et al.[258] found that PANI nanofibers were formed through coupling of aniline dimers, whereas PANI granules were formed through coupling of an aniline dimer and monomer. A mechanism based on a double heterogeneous nucleation process, instead of the classical homogeneous/heterogeneous nucleation process, was proposed. For instance, if the polymerization of aniline was carried out in a glass beaker containing a piece of a polyethylene terephthalate (PET) sheet, PANI nanofibers formed on the surface of the PET sheet; and if the polymerization was performed in a vessel with "no surface," like stainless steel vessel or ice vessel, no nanofibers were found. However, if a PET sheet was immersed in the ice vessel, nanofibers were also achieved, indicating that these surfaces have played a dramatic role in determining the morphology of PANI. Furthermore, nanofibers of aniline tetramer were successfully fabricated by oxidation of aniline dimer alone, showing that very long nanofibers can be formed with extremely short chains. It was proposed then that nanofibers (PANI or tetramer) form when surface conditions favor a high concentration of aniline dimers, like the reaction with a PET sheet, and granules of PANI form when the surface concentration of a dimer is low, like the one in an ice vessel.

In a further study on their previous finding that the morphology of PANI depends on the acidity conditions during the reaction rather than on the chemical nature of the acids,[261] Stejskal et al. investigated the polymerization of aniline in both water[262] and in 0.4 M acetic acid.[263] It was found that the

acidities of the reaction media increased in two steps. The crystal- or needle-like structured oligomers formed in the first step of polymerization acted as templates for the subsequent formation of PANI nanotubes in the second step of polymerization. It was proposed further that phenazinium units act as discotic molecules that guide the stacking of oligomers and provide the necessary organization and order that predetermine the growth of nanotubes. The nanotubular structures were further stabilized by the hydrogen bonding and ionic interactions between the neighboring PANI chains.

HYDROGEN BONDING

The hydrogen-bonding interaction, as well as some others, like $\pi-\pi$ stacking and hydrophobic interactions, affects significantly the final morphology of PANI. A reduction in the interaction during polymerization of aniline is favorable for formation of 1D nano-PANI. However, hydrogen bonding between the substituents on the monomer and the polymer backbone was found as one of the key factors in forming the aligned bundles of poly(*o*-methoxyaniline) nanowires.[260]

According to Wu et al.,[264] with addition of 0.01 mol% of phenol during oxidative polymerization of aniline with agitation, PANI nanofibers with thinner diameters and longer lengths than those without addition of phenol during polymerization were synthesized, showing that the effect of inter- and/or intrachain hydrogen bonding is important on the morphology of PANI nanofibers since it was revealed that the function of phenol is to avoid formation of the hydrogen bonding during the growth of PANI chains. The hydrogen bonding, $\pi-\pi$ stacking, and hydrophobic interactions provided by perfluorosebacic acid (PFSEA) are also considered as the driving forces for self-assembly of 1D nanofibers to 3D-boxlike PANI nanostructures when using PFSEA as both the dopant and soft template for preparation of 3D boxlike PANI nanostructures because of the low surface energy of the perfluorinated carbon chain and the two hydrophilic carboxyl acid groups.[265,266] In another study, PANI nanofibers with a diameter of 16–23 nm were prepared by adding inorganic salts such as NaCl, LiCl, $MgCl_2$, and $AlCl_3$ into the reaction mixtures and the nanofibers aggregated into chrysanthemum flower like microstructures with an increased concentration of the salts.[267] The aggregation might have resulted from physical entanglements, hydrogen bonding, and "pseudodoping" of PANI by the ions of the salts.

In the synthesis of PANI nanostructures by a soft template method, Petrov et al.[268] found that mainly aggregated nanotubes dendrites or coral-like structures of PANI were obtained if salicylic acid was used only as the template, irrespective of its molar ratio to aniline, while with even a little SDS added as the cosoft template, isolated PANI nanotubes were achieved. It was then proposed that SDS reduced the hydrogen-bonding interactions between the amine nitrogen of PANI chain and the –OH group of salicylic acid, which is responsible for the aggregation of PANI nanotubes. The intermolecular hydrogen bonding between methanol and PANI was also reported as the facilitating force in the construction of PANI nanofibers during an electrochemical polymerization.[102]

By adding a small amount of different organic solvents such as DMF, DMSO, THF, and NMP into the reaction medium during polymerization of aniline, Xing et al.[269] reported that the hydrogen-bonding interaction between PANI and the solvents played an important role in the preparation of uniform PANI nanofibers with a relatively high conductivity and good water dispersiblity. However, aggregation of the nanofibers resulted when excessive organic solvents were added.

ANILINE CONCENTRATION

By studying the morphology evolution of PANI during solution precipitation, rapid mixing polymerization, and interfacial polymerization, Wang and Jing found that the key factor that determines the formation and growth of PANI nanofibers during chemical oxidative polymerization is the aniline concentration.[249] At lower concentrations of aniline, PANI nanofibers were formed and preserved and collected as the final product, whereas at higher concentrations, large-sized PANI particles or agglomerates were obtained, owing to the growth of PANI nanofibers. However, with the application of ultrasonic irradiation on the reaction media, PANI nanofibers were also prepared at higher concentrations of aniline. The effect of the aniline concentration, as well as the ratio to doping acid, on the morphology and microstructure of PANI obtained was also reported by Liu et al.[270] For example, nanospheres and nanorods, nanofibers with smooth surfaces, and sea cucumber–like PANI nanofibers were synthesized with aniline concentrations of 0.15, 0.20, and 0.30 mol L^{-1}, respectively. However, with a further increase in aniline concentrations, nanofibers with smooth

surfaces and nanorods were obtained at aniline concentrations of 0.35 and 0.40 mol L^{-1}, respectively.

SOLUTION ACIDITY

The acidity, or pH, of the polymerization environment was also considered as one of the important parameters in synthesizing 1D nano-PANI.[236,250,271] For polymerization of aniline in a lower acidity medium (e.g., ≤0.1 M HCl), PANI nanotubes were achieved through curling of the initially formed flake-like intermediates as the reaction proceeded, where the phenazine-like aniline units served as the axis for PANI nanotube curling. While for polymerization at higher acidity (≥0.2 M HCl), PANI nanofibers were obtained with the help of the para-linked emeraldine base PANI templates formed in the initial reaction stage due to their linear nature and expanded chain structure. The PANI nanofibers would grow into irregular agglomerates with a prolonged reaction, as observed by other groups.[249] Based on the findings, the authors concluded then that the solution acidity is the primary determining factor in the formation of various PANI molecular structures, and therefore PANI nanofibers or nanotubes with different mechanisms.[250] With the introduction of methanol to the acid-free reaction media with concentrations up to 1 M, PANI nanotubes were successfully synthesized; without methanol, primarily irregular agglomerates PANI was obtained.[272] It was revealed that with an increase in the solution acidity, aniline monomers linked to phenazine-like units and polymerized through head-to-tail coupling. PANI nanotubes were formed through a self-curling process of the PANI intermediates, where the protonation of the para-coupling PANI is the primary driving force for the transformation. Controlling the acidity profile during polymerization of aniline was considered to be the key factor in producing PANI nanotubes.[273] With initial pH >3, aniline was oxidized to nonconducting oligomers, which acted as the template for formation of nanotubes. With pH <2, granular PANI was obtained.

New Features of 1D Nano-PANI

In addition to the significant progress achieved in the preparation of 1D nano-PANI, studying the formation mechanisms, and controlling of morphologies, some new features and novel applications of 1D nano-PANI were also explored and developed in the past 5 years with further functionalization, characterization, and theoretical studies on the 1D nano-PANI.[274–286]

ALIGNED OR ORIENTED 1D NANO-PANI

Although great potential has been demonstrated by 1-D nano-PANI for optoelectronic nanodevices ranging from single-molecular transistors and electron-emitting flat panel displays to chemical nanosensors and artificial actuators,[7,8,287–290] the controlled orientation of the nanostructures is the critical step for all these applications. Therefore, fabrication of highly oriented or aligned 1D nano-PANI has always been a challenging task for researchers worldwide.

Nandan et al.[289] reported a simple, environmentally friendly, and effective method for fabricating highly oriented PANI nanowires by hierarchical self-assembly of PANI in an emeraldine base form with ω-methoxy poly(ethylene oxide)phosphates (PEOPA), a phosphoric acid terminated PEO. PANI nanowires have a fairly uniform diameter of ca. 30 nm and a length of up to several micrometers. Since OsO_4 was used as a staining agent in the TEM examination, a dark image in the TEM micrographs is predominantly of the poorly doped PANI, whereas the bright regions are the well-doped PANI with PEOPA, which accounts for the main composition in this phase.[291] The formation mechanism of the oriented PANI nanowires is still not clear, but the authors speculated that the orientation was probably due to the highly directional hydrogen bonding between the hydroxyl and the ether groups or among the hydroxyl groups within the PEO layers in the lamellar structure.

Urchin-like PANI hollow spheres consisting of highly oriented nanofibers with a length of 50–180 nm and diameter of 15–20 nm were synthesized by oxidize aniline loaded polystyrene (PS) hollow spheres, which were prepared by mixing an aniline solution in HCl with the hollow spheres for aniline uptake, with ferric chloride at room temperature.[292] The hollow spheres play a crucial role in formation of the urchin-like PANI structures, since they provide not only the interface to separate the reactants but also the nucleation sites to grow the nanofibers. On the other hand, if the PS hollow spheres were first loaded with ferric chloride and then mixed with aniline, PANI is only formed inside the cavity of the hollow spheres.

Without using any organic solution, radially oriented PANI nanofibers with a diameter of

300–500 nm and a length of 15–20 μm were prepared by Chen et al.[293] in a novel interfacial polymerization, where the organic phase was made up of aniline and salicylic acid. The morphology and size of the PANI nanostructures can be adjusted by simply changing the concentration ratios of aniline to salicylic acid, providing a novel method to design and synthesize PANI nanostructures. Using a hydrophilic crown ether derivative (CE-SO_3K) as the structure-directing agent (soft template), oriented arrays of PANI nanotubes with a diameter of 60–150 nm and a length of micrometers were synthesized by Xia et al.,[34] with an optimal ratio of aniline to crown ether derivatives of 25.

Following their previous studies that PANI nanofibers can be easily formed by the novel dilute polymerization,[199,244] Chiou et al.[294] found that aligned PANI nanofibers with a diameter of 10–40 nm and a length of 70–360 nm can be simultaneously formed on the available substrates present in the reaction media during dilute polymerization (Fig. 11). Various substrates, including those nonconductive plastic ones and conducting ones, with different geometries have been successfully coated with the aligned PANI nanofibers, indicating the robustness of the method in preparing aligned PANI nanofiber films. More interestingly, with exposure to trifluoromethane or tetrafluoromethane plasma, superhydrophobicity was exhibited by the aligned PANI films, completely different from the initially demonstrated superhydrophilicity. Potential applications of the aligned PANI nanofiber films include antifog coatings, self-cleaning surfaces, DNA manipulation, transparent electrodes for low-voltage electronics, and chemical and biological sensors, as pointed out by the authors.[294] A vertically aligned PANI nanofiber array with individual fiber diameters of ca. 100 nm, heights of ca. 600 nm, and a packing density of ca. 40 pieces μm^{-2}, on the Au surface was facilely prepared by pretreating the Au surface using 4-aminothiophenol before the chemical oxidative polymerization of aniline.[295] It was found that the self-assembled monolayer (SAM) of 4-aminothiophenol molecules on the Au surface served not only as the anchoring site to initiate the in situ polymerization of aniline but also as the nucleation site to form the nucleation center for the formation of PANI nanofibers. The aligned growth of PANI nanofibers was guided by the normally aligned 4-aminothiophenol SAM on the Au substrate.

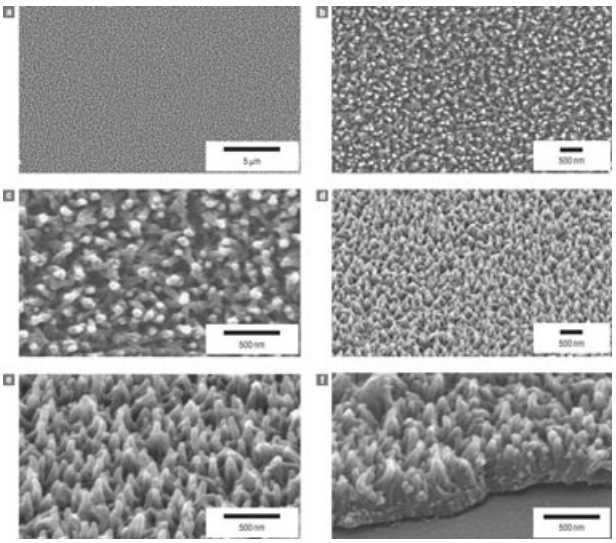

FIGURE 11. SEM images of aligned polyaniline nanofibers grown on an overhead transparency. (a): Top view, low magnification. (b) and (c): Top view, high magnification. (d) and (e): Tilted view, high magnification. (f): Tilted view for the edge of the partially removed thin film (reproduced by permission of Nature Publishing Group).[294]

A large area of oriented PANI nanorods with a uniform diameter of 50–60 nm and length of 150–250 nm was also prepared on an aluminum plate by using a one-step electrodeposition method without the use of any template.[296] Ordered PANI nanowires with a diameter of 30–50 nm and a length of 100–200 nm were successfully deposited on the surface of platinum, gold, and carbon substrates by using a three-step method under a nitrogen atmosphere, and remarkably increased capacitance was demonstrated by the PANI nanowires deposited substrates owing to the increased specific surface areas and the ordered nanostructures, indicating the great potential in fabrication of high efficient electrochemical capacitors or rechargeable batteries.[297] Arrays of oriented PANI nanostructures with different shapes and sizes were also fabricated on transparent indium tin oxide (ITO) substrates using a block copolymer nanotemplate during a single-step electropolymerization.[298] The orientation was still maintained even after the removal of the template by dissolving in chloroform.

In addition to the aligned or oriented 1D nano-PANI nanostructures, an aligned bundle of poly(*o*-methoxyaniline) nanowires was also synthesized by chemical oxidative polymerization of *o*-methoxyaniline in the presence of aniline dimers.[260] The presence of aniline dimers, a prolonged reaction

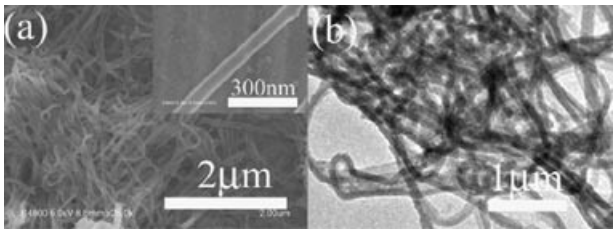

FIGURE 12. PANI nanowires prepared in the presence of CTAB: (a) SEM image at a low magnification and at a high magnification (inset), and (b) TEM image (reproduced by permission of Elsevier Inc.).[299]

time, and careful tuning of reaction conditions were found, which are some of the crucial parameters in the preparation of aligned poly(*o*-methoxyaniline) nanowires.

LONGER 1D NANO-PANI

With CTAB as the soft template in the neutral aqueous solution, PANI nanowires with the average diameter of 60 nm and a length of up to tens of micrometers were fabricated by Wang et al. (Fig. 12).[299] About four times of an increase in conductivity was exhibited when the nanowires, which were connected with two Au electrodes beforehand, were moved from a dark box to irradiation of an incandescence lamp. The unique photosensitive conductivity of the nanowires showed great application potential in photoswitching nanodevices. Preliminary results of such a device showed high sensitivity, reproducibility, and stability.

SELF-DOPED 1D NANO-PANI

Self-doped PANI nanofibers with a diameter of 60–70 nm and lengths up to several micrometers were successfully prepared by copolymerizing aniline with SAN in an aqueous acidic solution,[300] where CTAB was the soft template. It was revealed that both the pH of the solution and concentration of CTAB have important effects on the morphology of the final product. For example, if no acid was used, PANI in irregular aggregates containing a small quantity of nanofibers was obtained, and with an increase in CTAB concentration from 0.005 to 0.01 mol L^{-1}, the diameters of the nanofibers increased from 60–70 to 90–110 nm. Nanotubes of self-doped PANI, as well as hollow microspheres and aligned pearls, were also prepared by the same authors by copolymerization of aniline and SAN without the aid of any template and surfactant.[301] The molar ratio of aniline to SAN also has a significant effect on morphologies of PANI, as confirmed by another study,[302] in which self-doped PANI with morphologies from nanoclusters to nanotubes and coral reef–like nanostructures was achieved by simply increasing the molar ratio of aniline to SAN in the copolymerization reaction.

In another study, self-doped poly(anilineboronic acid) (PABA) nanostructures with varied shapes and forms were also easily synthesized by controlling the self-doping degree, external doping, polymerizing rate, and polarity of the polymerization solvent.[303] For instance, PABA nanoparticles with an average diameter of 2–15 nm were prepared without using surfactants or stabilizers as a template, whereas the average diameters of nanofibers can be controlled by adjusting the reaction conditions such as the polymerizing rate and polarity of the solvent. A self-doped copolymer of poly(aniline-*co*-anthranilic acid) nanorods in bundles was successfully synthesized by chemical oxidative polymerization of aniline and anthranilic acid in a neutral alcohol/aqueous media with APS.[304] Self-doped PANI nanotubes, as well as nanoparticles, were also synthesized by oxidative copolymerization of aniline and 1-amino-2-naphthol-4-sulfonic acid in the presence of TSA, which served as an external dopant.[305] The nanostructured copolymers were blended with low-density polyethylene with loading of 1 wt% for electrostatic charge dissipation applications, where the static decay time of the film was 0.1–0.31 s on recording the decay time from 5000 to 500 V.

CHIRAL 1D NANO-PANI

The chirality of PANI originates only from the helical conformation of polymer backbones and/or from the helical packing of the polymer chains induced by chiral acids since dedoped PANI has no asymmetric carbon. Therefore, chiral PANI was synthesized usually by either codissolving PANI and chiral acids in common solvents or polymerizing aniline in the presence of chiral acids. However, the chirality of most of the chiral PANI synthesized from these methods is relatively low.[306] For the synthesis of chiral PANI nanofibers, the mostly used inducing chiral acid is (+)- or (–)-CSA.[161,306–309] For example, by using an aniline oligomer to accelerate the polymerization reaction and adding an APS solution to the aniline solution incrementally, Li and Wang[306] prepared chiral PANI nanofibers, with very high optical activity comparable to that of helical peptides or proteins, for the first time in a concentrated (+)- or

(–)-CSA solution. By systematically studying the effect of experimental parameters on the polymerization reaction and properties of the nanofibers in a later study, it was found by the same group[310] that a maximized interaction of CSA with the growing polymer chain and the use of oligomer molecules to catalyze the polymerizing reaction are the key requirements for preparation of highly chiral PANI nanofibers. The chiral nanofibers were stable against thermal treatment up to 90°C for 1 h and repeated doping–dedoping treatment with 0.1 M ammonium hydroxide and 1.0 M HCl. Right- and left-handed helical PANI nanofibers were also prepared by chemical oxidative polymerization of aniline in the presence of chiral D- or L-CSA.[307] Chiral PANI nanorods, as well as nanostructured gold microparticles, were synthesized in one pot by Zhang et al.[161] in the presence of (+)- or (–)-CSA using potassium tetrachloroaurate as an oxidant. The results showed that the chiral organization of the PANI nanorods was strongly affected by the molar ratio of aniline/tetrachloroaurate, and the ratio for the highest optical activity is ca. 5/2. In a later study, binary oxidants of potassium tetrachloroaurate and APS, which were added subsequently in different portions to the aniline solution, were used by the same authors to synthesize chiral PANI nanofibers.[308] The optical activity of the as prepared chiral nanofibers depended on the mass ratio of potassium tetrachloroaurate to APS, and the highest optical activity was observed in the ratio range of 1.0–2.5. Aqueous dispersions of chiral PANI nanobundles were also prepared by interfacial polymerization, where the PANI chains intertwined over interconnected units of cyclodextrin sulfate.[311]

The helicity of the PANI nanofibers, as always induced by chiral dopant during polymerization, can also be tuned with copolymerization of aniline with different substituted aniline.[312] For instance, by copolymerization with *m*-toluidine, reversed helicity was found for both the conformation and nanofibers as compared to PANI, whereas copolymers with a similar helicity to that of PANI were obtained by copolymerization with *o*-toluidine. Theoretical simulations revealed that the steric hindrance of the methyl group at the metaposition of the phenyl ring played a dominant role in the helical inversion as observed.

DERIVATIVE 1D NANO-PANI

In comparison with parent PANI, PANI derivatives are also intensively studied in both academic and industrial research areas due to their enhanced properties like improved solubility in organic solvents.[313]

Successful synthesis of a variety of substituted PANI nanofibers, including alkyl-, methoxyl-, fluoro-, and thiomethyl-substituted PANI, was first reported by Tran and Kaner[256] in 2006. The authors demonstrated a general route for fabrication of substituted PANI nanofibers by introducing an initiator like *p*-phenylenediamine into the reaction mixture of the rapidly mixed monomers and oxidant mixture. Without adding these initiators, irregular-shaped agglomerates or spheres are obtained, whereas with adding nanofibers with lengths as long as several micrometers and diameters ranging from 25 to 120 nm were formed. The reason for this morphology transformation was attributed, in large part, to the improved polymerization rate and also to the nucleation sites formed because the oxidation of the initiators is lower than that of the monomers.

Lately, both poly(*o*-toluidine) and poly(*o*-methoxyaniline) nanofibers were successfully synthesized through rapid mixing polymerization using $HAuCl_4$ as the oxidant,[314] instead of the commonly used APS. The diameters of the nanofibers, as well as that of the gold nanoparticles, increased with the concentration of $HAuCl_4$ and can be tuned in the range of 10–200 nm. It was considered that the gold nanoparticles formed acted as a catalyst to the oriented growth of substituted PANI nanofibers, and the method was claimed to be a general chemical route to nanofibers of PANI derivatives.

Poly(*N*-methylaniline) nanowires with adjustable diameters of 40–80 nm were synthesized with CTAB as the soft template without the use of any acid in the reaction media by Mao et al.[315] It was found that the morphology of the final polymer can be controlled by adjusting the concentration of the monomer. For example, nanowires with a diameter of 70–80 and 40–60 nm were prepared when monomer concentrations were kept at 0.024 and 0.012 M, respectively. When the monomer concentration was decreased to 0.006 M, microspheres with a diameter of 200 nm–1 μm were obtained instead.

Poly(aniline-*co*-*o*-aminophenol) interwoven nanofibers were synthesized by using the repeated potential cycling method in the presence of ferrocenesulfonic acid.[316] The average diameters of the copolymer nanofibers increased from 70 to 107 nm with the cycling numbers increased from 8 to 18. However, little change was observed with a further increase in the cycling numbers. Better

electrochemical activity at pH $\leq$9.0, larger usable potential window, and faster electron transfer ability were exhibited by the nanofibers prepared in the presence rather than that in the absence of ferrocenesulfonic acid. Poly(luminol-aniline) nanowires films were synthesized on the surface of a graphite electrode by electrooxidizing the mixture of luminol with aniline in sulfuric medium and studied for an electrogenerated chemiluminescence biosensor for glucose due to their large specific surface area, excellent conductivity, high porosity, rapid electron transfer, and better electrogenerated chemiluminescence properties than polyluminol film alone.[317]

CARBONIZED PANI NANOTUBES

Highly carbonized PANI nanotubes, as well as microtubes, were prepared by heating the soft template synthesized PANI nanotubes and microtubes at 800°C or higher for 120 min without traces of oxygen.[318] No evident morphology change was observed after the heating carbonization process, except for tube diameters decreased by 50%. In addition, the electrical conductivity decreased from 7.4 $\times$ 10^{-5} S cm^{-1} for the starting material to 4.8 $\times$ 10^{-9}, 1.3 $\times$ 10^{-11}, and finally 2.4 $\times$ 10^{-6} S cm^{-1} for samples obtained at room temperature: 250, 500, and 800°C, respectively. The carbonized PANI micro- and nanotubes with stable units of modified chemical structure and physical properties can be expected to find applications in nanoelectronics and molecular electronics according to the authors. By heating of the chemically synthesized PANI nanotubes in a nitrogen atmosphere to ca. 800°C, carbonized nanotubes were prepared in either a milligram scale by using a thermogravimetric analyzer [319,320] or gram scale by using a horizontal tube furnace.[320] The carbonized PANI nanotubes, with a nitrogen content of ~9 wt%, showed a specific surface area of the order of 100 m^2 g^{-1} and slightly lower thermal stability than that of the commercial multiwalled carbon nanotubes (MWNTs). A conductivity of 0.7 S cm^{-1} was displayed by the carbonized PANI nanotubes. However, if 1D nano-PANI was heated in the presence of oxygen, such as heating of NSA-doped PANI nanofibers at a rate of 10°C min^{-1} from room temperature up to 300°C under air atmosphere,[321] only cross-linking structures were formed without changing the nanofiber morphology. The carbonized PANI nanotubes, or PANI-based CNTs, were studied as electrode materials for supercapacitors in a potassium hydroxide solution.[322] High specific capacitance of 163 F g^{-1} at a current density of 0.1 A g^{-1} and excellent cyclic stability were exhibited by the as-prepared supercapacitors. Carbonized PANI nanotubes obtained by heating in vacuum at different temperatures (300–800°C) were dispersed into silicone oil to prepare carbonaceous electrorheological fluids.[323] It was shown that the fluids possessed versatile electrorheological performance such as high electrorheological efficiency, good dispersion stability, and temperature stability. Furthermore, the electrorheological effect of the fluids depended on the heat treatment temperatures and those nanotubes obtained at around 600°C exhibited the maximum electrorheological effect.

DENDRITIC PANI

Using poly(acrylamide-*co*-acrylic acid) with an acid unit content of 1.5 and 70 wt% as the soft template in a chemical oxidative polymerization of aniline with APS, dendritic "coral reef" flower patterned PANI nanostructures were prepared.[324] The radially spread "flowers" contained many nanorods in a diameter of ca. 170 nm, and the leaf was ca. 2.0 μm in width and ca. 400 nm in thickness. A hyperbranched structure can also be observed along the dendritic growth direction. In another report, when the concentration of the soft template, stearic acid, decreased from 0.04 M to 0.02 M and 0.01 M, interconnected 3D dendritic PANI fibers with branch diameters of 160–200 nm and dendritic PANI rods with a diameter of 80–120 nm, respectively, were formed instead of the nanotubes at a higher concentration of stearic acid.[221]

Dendritic PANI nanostructures with PANI nanorods lying on the surface of nanofibers were also synthesized using ferric chloride as the oxidant, without use of any other hard or soft templates.[325] The diameters and surface roughness of PANI nanofibers were tuned by changing the reaction time and temperature. For instance, PANI nanofibers with a diameter ca. 150 nm and length up to 1 μm were obtained at 25°C, whereas smoother nanofibers with a diameter of 30–50 nm and lengths to several micrometers were achieved at 60°C. Branched PANI nanofibers with a diameter of 15–40 nm and a length of hundreds of nanometers were also successfully synthesized by the solid-state polymerization as mentioned above,[175,176] in which ferric chloride or hydrated ferric chloride were used as the solid oxidant.

New Applications of 1D Nano-PANI

The conductivity of PANI can be easily controlled by either the protonation state or the oxidation state of the main chain[326] (Fig. 13) or by the combined doping and soft lithography process, where a semiconducting dopant (tris(8-hydroxiquinoline-5-sulfonic acid)Al) enhanced the conductivity of the amorphous PANI by promoting the formation of crosslinked networks with PANI chains while good processability was also retained.[327] The tunable conductivity and reversible dop–dedope and redox features render PANI a promising candidate for its tremendous applications. More importantly, the poor processability of PANI, that is, insolubility in common organic solvents and infusibility on heating, can be significantly overcome by the improved dispersability of 1D nano-PANI. Therefore, more and more applications are being explored for 1D nano-PANI and these will be discussed in the following sections.

GAS SENSOR

The study on 1D nano-PANI for gas sensors can be roughly divided into two groups according to the acidity or alkalinity of the gases, that is, one for strong acidic or basic gases such as HCl and NH_3,[328–331] and another for weak acidic or basic and neutral gases.[185,332,333] As far as the first group is concerned, the research has covered not only the improved sensitivity of the sensors but also integrated sensors with a readout circuit instead of the initially adopted resistance changing recording. For instance, Liu et al.[334] successfully manufactured an ammonia sensor integrated readout circuit using the commercial 0.35-μm complementary metal oxide semiconductor process and the postprocess by using a PANI nanofiber film as the sensing film and a polysilicon layer as the sensing resistor. Sensitivity of ca. 0.88 mV ppm^{-1} was exhibited by the sensor at room temperature with a bias and input voltage of 3.3 and 3 V, respectively. A PANI nanowire film prepared by using the soft template method showed good sensitivity and a rapid response to trimethylamine.[335] Although a slight difference was easily observed in the gas sensitivity and response rate to trimethylamine, triethylamine, and ammonia, distinguishing the three gases from one another is still difficult for the PANI nanowire film. For the second group of gases, great progress has also been achieved, and these gases are discussed below, one by one, in detail.

Hydrogen Sulfide Sensor

PANI nanofibers were modified with metal or metals salts for sensing of hydrogen sulfide, a weak acidic gas that is also toxic, corrosive, and flammable. With the deposition of Au nanoparticles onto PANI nanofibers,[336] hydrogen sulfide with a concentration as low as 0.1 ppb can be detected, showing a significantly improved sensing limit compared to that of pure PANI nanofibers, where no response was observed with a hydrogen sulfide concentration as high as 500 ppm.[337] Although the exact mechanism of the

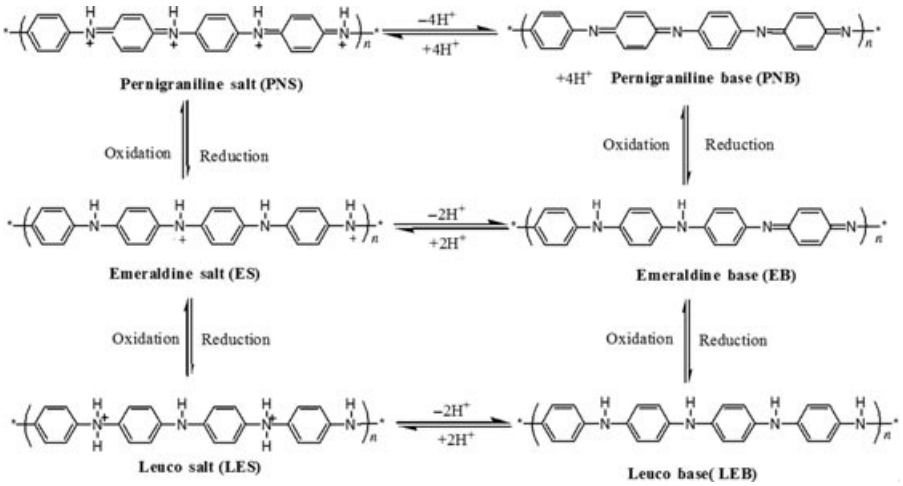

FIGURE 13. Redox and dop–dedope processes of PANI.[326]

improved response is unclear, the sensor showed a fast response time (<2 min), recovery time (<5 min), excellent sensitivity (13.78% per ppb), good reproducibility, and selectivity (over NH_3).

On the other hand, transition-metal salts such as copper chloride, copper acetate, zinc chloride, and cadmium chloride were also incorporated into PANI nanofibers to improve their sensing performance, and an enhanced response, as much as or greater than four orders of magnitude, was achieved.[337,338] As far as the mechanism is concerned, it was proposed that the metal cations coordinate weakly to the imine and amine nitrogens of the PANI backbone and the PANI backbone acts like a weak ligand; therefore, the metal cations react easily with hydrogen sulfide to form metal sulfides and an acid by-product that dopes PANI.[338]

Nitrogen Dioxide Sensor

PANI nanofibers were used for fabrication of nitrogen dioxide gas sensors for the first time by Yan et al.[339] Upon exposure to nitrogen dioxide, the resistance of the PANI nanofiber film increased slightly in the first 100 s, and then increased sharply in the following several seconds. The slight increase resulted from the removal of adsorbed water molecules on the nanofiber surface and the dramatic increase in the oxidation of PANI. The resistance increased, while the turn-on time and response time decreased with increasing of the nitrogen dioxide concentration for the PANI nanofiber sensor. Compared to the PANI film, PANI nanofiber sensors showed a much faster response and higher sensitivity and both the response and sensitivity were not affected by the thickness of the PANI nanofiber film, which is different from a PANI film sensor whose response time decreased with the film thickness. Furthermore, the PANI nanofiber sensor exhibited relative selectivity for nitrogen dioxide against hydrogen, oxygen, and carbon dioxide with the same concentration of 200 ppm. The nitrogen dioxide gas sensing behavior of plasma-polymerized nanofibrous PANI films was also studied by measuring the resistance change in PANI films with exposure to the nitrogen dioxide gas concentration and exposure time.[190] The sensitivity factor of the films was dependent on their thickness, and the optimal sensitivity factor was found at the film thickness of 100 nm.

Hydrogen Sensor

By deposition of PANI nanofibers/In_2O_3 composite or PANI nanofibers/WO_3 composite, which were prepared by chemical oxidative polymerization of aniline in the presence of In_2O_3 or WO_3 nanoparticles, onto a layered ZnO/64° YX $LiNbO_3$ transducer, PANI nanofiber composite based surface acoustic wave (SAW) sensors were fabricated and studied for their response to hydrogen, nitrogen dioxide, and carbon monoxide first by Sadek et al.[340,341] (Fig. 14). The PANI nanofibers/In_2O_3 composite–based sensor produced repeatable responses of the same magnitude with a good baseline stability for hydrogen and carbon monoxide, but not for nitrogen dioxide for its poisoning effect on the nanocomposite film. The sensor response, defined as the variation in resonant frequency, of PANI nanofibers/In_2O_3 composite and PANI nanofibers/WO_3 composite–based SAW sensors is 11.0 and 7.0 kHz, respectively, toward 1% hydrogen in synthetic air. Although the sensitivity of the latter sensor is not as good as the former one, the latter is more stable.[341] The sensing mechanism for hydrogen is still unclear. Highly ordered PANI nanofibers were also electrochemically deposited on a 36° lithium tantalate ($LiTaO_3$) surface to fabricate SAW sensors by the group.[342] The frequency shift of the sensor increased with the thickness of PANI nanofiber films for the hydrogen concentration below 0.5%, and sensors with a PANI nanofiber film thickness of ~3.5 μm exhibited the biggest frequency shift for a 1% hydrogen concentration. By replacing the nanoparticles with diamond nanoparticles with the average diameter of 3.2 nm, composite PANI/diamond nanofibers with the average diameter of 50 nm were prepared onto a layered ZnO/64° $LiNbO_3$ SAW transducer for hydrogen gas sensing by the same group.[343] The gas sensor showed a response more than 750 kHz to 1% hydrogen gas in synthetic air, indicating a higher response than those reported in Ref. 340 and 341.

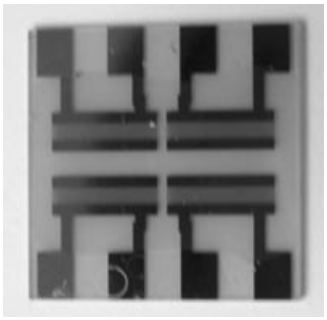

FIGURE 14. Typical SAW sensor, showing two sets of identical resonators (reproduced by permission of Elsevier B.V.).[341]

In a later study, two kinds of PANI nanofibers, one is HCl-doped nanofibers with a diameter of 30 nm and the other is CSA-doped one with a diameter of 50 nm, were deposited onto a layered ZnO/64° YX $LiNbO_3$ transducer to fabricate a SAW sensor for hydrogen.[344] Both sensors demonstrated a relatively fast response and recovery time with good repeatability and baseline stability, but the sensitivity of the CSA-doped PANI nanofiber sensor is greater than that of the HCl-doped sensor, especially for higher hydrogen concentrations. The sensor response is 3 and 14.6 kHz toward 1% of hydrogen at room temperature for HCl- and CSA-doped PANI nanofiber sensors, respectively. Very recently, CSA-doped PANI nanofibers with a diameter of 50 nm were deposited on an aluminum nitride modified YX $LiNbO_3$ transducer for fabrication of the hydrogen SAW sensor.[345] The sensor exhibited a fast response and recovery with a stable baseline frequency and repeatable and large response toward different concentrations of hydrogen at room temperature. For instance, the registered frequency shifts of the sensor to 0.25%, 0.5%, and 1% hydrogen gas are approximately 17.7, 30.3, and 34.6 kHz, respectively.

Conductometric hydrogen sensors were also fabricated by the same group by deposition of either HCl-doped or -dedoped PANI nanofibers onto conductometric sapphire transducers.[346] The conductivity of both doped and dedoped PANI layers increased with exposure to hydrogen. Sensitivity, defined as the ratio of resistance of the sensor in air to that in the presence of hydrogen, of the doped and dedoped PANI sensors is 1.11 and 1.07, respectively, showing that the doped sensor is more sensitive than the dedoped one. However, the dedoped sensor showed a more stable baseline and better repeatability than the doped one and the instability of doped sensor is attributed to the volatility of HCl.

According to the study by Virji et al.,[347] CSA-doped PANI nanofibers deposited on a gold electrode can be used as a good room temperature hydrogen sensor in a dry atmosphere, since PANI interacted with hydrogen to enhance charge transfer, decrease resistance, and the response increased monotonically with the hydrogen concentration. Although humidity suppressed the hydrogen signal, oxygen did not interfere with the interaction of hydrogen with PANI. The responses of hydrogen and deuterium were also studied, with the hydrogen response being about four times larger than the deuterium response. Better performance was demonstrated by the PANI nanofiber film than the conventional PANI film owing to the better interaction of hydrogen with a small diameter and large surface area of the PANI nanofibers. In a later study, the authors found that the responses of PANI nanofiber hydrogen sensors were affected by the electrode materials and completely different from each other (Fig. 15).[348] On gold electrodes, ohmic behavior and a small increase in conductivity were shown upon exposure to the hydrogen of PANI nanofibers. On platinum electrodes, ohmic contacts were shown without hydrogen; upon exposure to hydrogen, nonlinear behavior was observed due to the formation of

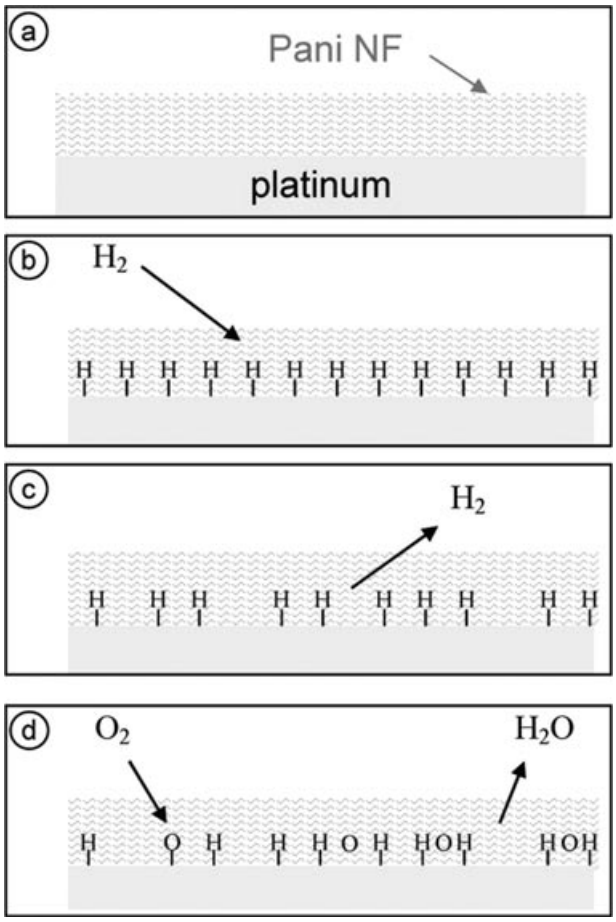

FIGURE 15. Possible mechanism for the response of polyaniline on platinum to hydrogen. (a) The sensor consists of a porous mesh of polyaniline nanofibers (Pani NF) cast upon platinum electrodes. (b) Upon exposure to hydrogen gas, the gas migrates through the nanofibers and forms a hydride with the platinum. (c) After purging the hydrogen away, some of the platinum hydride is persistent. (d) Oxygen removes hydrogen from the platinum by a catalytic reaction to form water resulting in a pristine Pt polyaniline interface as in (a) (reproduced by permission of American Chemical Society).[348]

platinum hydride, which then resulted in a large increase in resistance. The reason for the different responses is that the nature of the metal–PANI nanofiber contacts was changed on exposure to hydrogen, inducing Schottky barrier formation and giving rise to a dramatic change in sensing behavior. The sensitivity of the platinum–PANI nanofiber sensor was much greater than that of the gold–PANI nanofibers and can be used to detect hydrogen at concentrations as low as 10 ppm. Nanocomposites of chemically prepared graphene and PANI nanofibers were fabricated by in situ polymerization of aniline in the presence of graphene and studied for hydrogen gas sensing.[349] The sensitivity to 1 wt% of hydrogen gas is 16.57%, which is larger than the sensitivities of the sensors based on only PANI nanofibers (9.38%) and much larger than that of only graphene (0.83%).

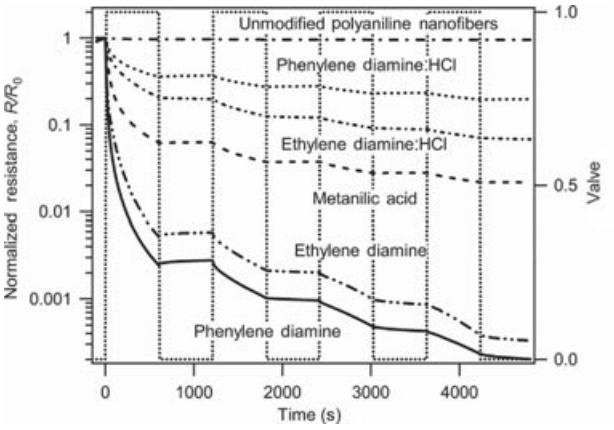

FIGURE 16. Response of polyaniline nanofiber amine composites to phosgene. The concentration of phosgene is 2 ppm at room temperature with 50% relative humidity (reproduced by permission of Springer).[350]

Phosgene Sensor

By modification of PANI nanofibers with amines, such as amines ethylenediamine, phenylenediamine and metanilic acid (3-aminobenzenesulfonic acid), and amine salts such as phenylenediamine dihydrochloride and ethylenediamine dihydrochloride, which was completed by mixing aqueous amine solutions with PANI nanofiber dispersions followed by casting and drying, PANI nanofibers were also studied for the detection of phosgene with concentrations lower than 0.01 ppm.[350] The detection mechanism is based on the nucleophilic substitution reaction of phosgene with the amine to produce an isocyanate and an acid, which dopes with the PANI nanofibers and results in resistance changes in the composites with over two orders of magnitude. The more basic the amine, the more reactive the nucleophilic substitution reaction, and the larger the response to phosgene (Fig. 16).

Arsine Sensor

Arsine gas (AsH_3) is another commonly used toxic industrial gas in addition to the abovementioned phosgene. PANI nanofibers incorporated with a series of metal salts, including $CuCl_2$, $CuBr_2$, CuF_2, $Cu(O_2CCH_3)_2$, $Cu(NO_3)_2$, $EuCl_2$, $NiCl_2$, $FeCl_3$, and $CoCl_2$, were studied for detection of AsH_3.[351] Since AsH_3 is a well-known strong reducing agent, the metal salts ions would be reduced to metals, generating simultaneously an acid. The latter would then dope the PANI nanofibers and lead to large changes in resistance. The response of the sensor is affected not only by the redox chemistry of the metals and the catalytic activity of the counterion of the metals salt but also by some environmental conditions such as temperature and humidity. Among the examined metal salts, the best response with greater than an order of magnitude change in resistance was yielded by the $CuBr_2$/PANI nanofiber composite upon exposure to AsH_3.

Alcohol Sensor

Most of the PANI gas sensors are mechanically based on the conductivity changes on exposure to the sensing gas, whereas an ethanol vapor sensor was fabricated based on changes in the absorption of an evanescent wave on a core-modified cladding interface where PANI nanofibers were used as the modified cladding in a fiber optic methanol sensor.[352] The response of the sensor was studied by measuring the intensity of transmission light, and response and recovery times of 35 s and 15 s, respectively, were found for the sensor. The fast response of the sensors was attributed to the effective penetration of ethanol into the modified cladding of PANI nanofibers. The sensor also showed good reversibility and repeatability.

Methane Sensor

Composites consisting of PANI nanofibers with the average diameter of 30–100 nm and palladium oxide (PdO) nanoparticles were prepared by in situ

chemical oxidation polymerization of aniline in the presence of PdO at room temperature, and methane gas sensors were fabricated through a layer-by-layer self-assembly deposition of the composite on mass-type quartz crystal microbalance (QCM) devices.[353] By measuring the frequency responses of the composite-based QCM sensor to methane gas at room temperature and 50°C, it was found that the sensor had a better response at room temperature than at 50°C. Since the response of the sensor reduced with an increase in humidity at room temperature, it was suggested by the authors that temperature and humidity compensation must be taken into consideration in practical use of the sensor and a dual QCM structure, with one bare QCM used as a reference sensor for compensation of the temperature and humidity effect.

BIOSENSOR

In addition to the research studies for various gases, 1D nano-PANI was also studied for biosensors, either as labels or as transducers.[354−361] PANI nanofibers or nanotubes are prominent candidates for supports in enzyme immobilization and biosensors because of, on the one hand, several advantages including the excellent matrix for immobilization of biomolecules and rapid electron transfer for signals,[362−365] and two redox couples in the right potential range that facilitate the enzyme–polymer charge transfer[366] demonstrated by PANI; on the other hand, the large surface area and nanopores of PANI nanofibers or nanotubes into which enzymes and other target species can be immobilized.[367−369] A glucose biosensor was fabricated by the immobilization of glucose oxidase and dendrimer-encapsulated Pt nanoparticles onto PANI nanofibers through the electrostatic layer-by-layer adsorption method.[366] The sensor exhibited excellent performances such as a low detection limit of 0.5 μM, a response time of 5 s, a wide linear range of 10 μM–4.5 mM, high sensitivity of 39.63 μA/ $(\text{mM cm}^2)^{-1}$, and good stability. Glucose oxidase was also immobilized onto a nanocomposite of Au nanoparticles and PANI nanofibers, which was prepared by in situ polymerization of aniline in the presence of Au nanoparticles, with the help of a Nafion solution to fabricate a glucose biosensor.[370] The biosensor exhibited an amperometric response that was about six times enhanced as compared with the one modified with pure PANI nanofibers due to the facilitated electron transfer between the electrode and hydrogen peroxide, and good selectivity against other electroactive species such as ascorbic acid, uric acid, and glutathione because of the permselective barrier effect of Nafion. Considering the rapid response, low detection limit, high stability, excellent reproducibility, and the close values recorded by the biosensor to that by the automatic analyzer, the biosensor is suitable for practical glucose detection. An amperometric glucose biosensor for glucose oxidase was also developed by electrochemically entrapping glucose oxidase onto the inner wall of highly ordered PANI nanotubes.[371] The biosensor is based on the direct electron transfer of glucose oxidase, as revealed by cyclic voltammetry (CV). The biosensor showed a rapid response of ca. 3 s, low detection limit of ca. 0.3 μM, a higher sensitivity and biological affinity, as well as good repeatability and stability. Besides, no interference was caused by the common interfering species such as ascorbic acid, uric acid, or acetamidophenol, since a low detection potential was employed, showing it can be used for the detection of glucose content in real clinical samples. By coating glucose oxidase immobilized PANI nanofibers onto the monolith surface, a monolith reactor for enzymatic bioconversion was reported by Joo and Lee.[372] The monolith reactor showed an increase in the conversion ratio of up to 83% at increasing residence time and excellent enzyme activity and long-term stability. However, rapid enzyme deactivation and detachment were observed if the enzymes were immobilized without the PANI nanofibers.

By subsequent deposition of a layer of self-doped PANI nanofibers[300] and Fe_2O_3 microspheres on a carbon ionic liquid electrode, a novel architecture electrode for sensing of DNA hybridization was fabricated.[373] The synergistic effect of Fe_2O_3 microspheres, self-doped PANI nanofibers, and ionic liquid lead to the greatly enhanced immobilization of DNA on the surface of the electrode and sensitivity of DNA hybridization recognition. A wider dynamic range from 1.0×10^{-13} to 1.0×10^{-7} mol L^{-1} for detecting the sequence-specific DNA of the phosphoenolpyruvate carboxylase gene from transgenically modified rape and lower detection limit of 2.1×10^{-14} mol L^{-1} was exhibited by the as-fabricated DNA biosensor.

Employing PANI nanofibers as one kind of doping material, Zhou et al.[374] prepared a modified carbon paste electrode, which served as an excellent affinity interface for further immobilization of CNTs and Au nanoparticles due to its high electric conductivity. The as-fabricated nanocomposite film greatly enhanced the loading of a DNA probe and hence improved remarkably the sensitivity for the

DNA target, owing to the synergistic effect of PANI nanofibers, CNTs, and Au nanoparticles. An electrochemical DNA biosensor was also fabricated by modification of a carbon paste electrode with PANI nanofibers, multiwalled CNT, and chitosan.[359] Immobilization of the probe DNA on the surface of the electrode was improved greatly owing to the unique synergistic effect of PANI and MWNT, that is, the superior electron-transfer ability of MWNT and the excellent reversible redox centers of PANI. In another study,[375] a PANI nanotube array was fabricated on the graphite electrode with the help of an alumina hard template and studied as the signal enhancement element of an ultrasensitive biosensor for DNA hybridization detection. This DNA electrochemical biosensor demonstrated both extremely high sensitivity to readily detect the presence of a target nucleotide at a concentration as low as 1.0 fM (ca. 300 zmol of target molecules) and good hybridization specificity, even at the ultralow concentration of 37.59 fM. The ultrasensitive property was related to the collective effect of PANI nanotubes, the enhanced PANI conductivity, and the faster hybridization kinetics of oriented nanostructure. Composite membranes of gold nanoparticle/PANI nanotubes on the glassy carbon electrode were also studied for the electrochemical sensing of the immobilization and hybridization of DNA.[376] The sensitivity to the DNA hybridization recognition was dramatically enhanced by the synergistic effect of gold nanoparticles and PANI nanotubes. The dynamic detection range from 1.0×10^{-12} to 1.0×10^{-6} mol L^{-1} and detection limit of 3.1×10^{-13} mol L^{-1} were observed for the biosensor for a phosphinothricin acetyltransferase gene, a sequence-specific DNA.

Electrochemically synthesized PANI nanowires were also studied for the detection of DNA hybridization, with methylene blue as an indicator.[103] The fabricated sensor effectively discriminated complementary from a noncomplementary DNA sequence, with a detection limit of 1.0×10^{-12} mol L^{-1} and very good sensitivity. By covalently immobilizing lipase onto PANI nanotubes, which were electrochemically deposited onto an ITO electrode, using glutaraldehyde (Glu) as the cross-linker, biosensor for detecting triglyceride using the impedimetric technique was reported by Dhand et al.[377] The charge transfer resistance of the PANI nanotube film changed with varying triglyceride concentrations, owing to the fatty acid molecules released during triglyceride hydrolysis. A chronocoulometric DNA sensor based on a doped screen-printed electrode that was constructed with chitosan, chemically synthesized PANI nanotubes, and ionic liquids was reported by Ren et al.[378] The complementary target DNA at a low concentration from the three-base mismatched DNA at a higher concentration was distinguished by the sensor.

In addition to DNA sensing, 1D nano-PANI was also studied for sensing of microRNAs or RNAs.[379] Following immobilization of peptide nucleic acid capture probes in nanogaps of a pair of interdigitated microelectrodes and hybridization with their complementary target microRNA, PANI nanowires were deposited by an enzymatically catalyzed method, and the electrostatic interaction between anionic phosphate groups in miRNA and cationic aniline molecules was found for guiding the formation of PANI nanowires onto the hybridized target microRNAs. Target microRNA can be quantified in a range from 10 fM to 20 pM, with a detection limit of 5.0 fM under optimized conditions, and the PANI nanowires–based biosensor array was applied to direct detection of microRNA and RNA extracted from cancer cell lines.

A simple electrochemical oligonucleotide (ODN) sensor was constructed by depositing PANI nanotubes, which were chemically synthesized using poly(methyl vinyl ether-*alt*-maleic acid) as the soft template and APS as the oxidant,[380,381] onto an electrode surface and subsequently attaching ODN probes via simple carbodiimide chemistry between residual carboxylic acid functionalities on the nanotubes and end-modified ODNs.[382] The potential pulse amperometry technique was used to obtain a direct and fast electrochemical readout, and a detection limit of 3.4×10^{-10} mol L^{-1} of complementary ODN was found for the ODN sensor.

Biosensors for the detection of hydrogen peroxide were also reported by using 1D nano-PANI. The sensors were prepared either by a layer-by-layer assembly of chemically synthesized PANI nanofibers with PAA on an electrode[383] or by modification of a glassy carbon electrode with Au–Pt alloy nanoparticles loaded PANI nanotubes film, and followed by immobilization of horseradish peroxidase in chitosan.[384]

A freestanding PANI nanofibril network was formed in a microgap between two gold electrodes by the electrochemical oxidation of aniline to fabricate a fast and sensitive analytical device for detecting microorganisms in a flowing liquid. The detection limit of the device is about 300 and 1.9×10^5 mL^{-1} for yeast (*Saccharomyces cerevisiae*) and bacteria cells (*Lactobacillus rhamnosus*), respectively, and the linear response is within the range of 0–5000

and (0–15) $\times 10^6$ cells injected for yeast and bacteria, respectively. The system is self-cleaning, needs no special procedure for regenerating the baseline, and can be useful in biomedical applications, environmental protection, and antibioterrorism systems, including "online" monitoring.[385] A novel nanobiodetector was also reported by electrochemically depositing a limited number of PANI nanofibers between two Au electrodes.[386] Several bacteria, including *Klebsiella pneumoniae, Pseudomonas aeruginosa, Escherichia coli*, and *Enterococcus faecalis*, suspended in either water or a physiological solution, were easily detected by the nanobiodetector in an "on–off" switch mode, that is, the nanobiodetector at state "off" is insensitive at a low population of cells (state) and state "on" is activated suddenly with a linear response above a threshold number of cells in the suspensions. The novel detector would be very useful in bioalarm systems, environmental monitoring, and medical applications, as pointed out by the authors. Using glutaraldehyde as the cross-linker, cholesterol oxidase was immobilized onto either PANI nanotubes films fabricated by using the electrophoretic technique onto the ITO-coated glass plates[387] or PANI-carboxymethyl cellulose (PANI–CMC) nanocomposite film deposited onto an ITO-coated glass plate.[388] Good performances, such as a wide detection range (25–500 mg dL^{-1}), high sensitivity (3.36 mA mg^{-1} dL), and a fast response time (30 s) were exhibited by the PANI nanotube based bioelectrodes, and a wide linearity range (0.5–22 mM), low detection limit (1.31 mM), high sensitivity (0.14 mA mM^{-1} cm^2), and fast response time (10 s) were exhibited by the PANI–CMC nanocomposite based bioelectrodes for the detection of cholesterol.

MOISTURE OR HUMIDITY SENSOR

Venancio et al.[389] described a new simple method to fabricate cheap and "throw-away" sensors for air moisture. In the first step, a 16-finger interdigitated graphite pattern was introduced onto a PET film or a copy paper by a specific procedure. In the second step, either a coating of PANI nanofibers was deposited on the pattern by dipping into the aqueous dispersion of 2-acrylamido-2-methyl-1-propane-sulfonic acid doped PANI nanofibers or an HCl-doped PANI film by in situ deposition. Sensitivity to moisture, which is given as the resistance change ratio of the sensors, of the sensor with PANI nanofibers ($\Delta R = 93.3\% \pm 19\%$) is much higher than the one with in situ deposited PANI film ($\Delta R = 5.05\% \pm 0.79\%$), which, as explained, resulted from the higher active surface area of PANI nanofibers than the in situ deposited PANI film.

PANI nanofibers were deposited on a SAW resonator as a selective coating to enhance the sensitivity of the humidity sensor.[390] In comparison with the uncoated oscillator, which did not show an obvious frequency change on humidity changes, the PANI nanofiber coated one exhibited a larger frequency shift. The sensitivity, in terms of $\Delta f/f$, was at least 16.8 ppm/ $(\%RH)^{-1}$ at room temperature, about two times higher than the best reported for SAW humidity sensors in publications.

PANI nanofiber films were fabricated onto screen-printed electrodes by using the chemical deposition method and investigated for humidity sensors.[391] At a lower relative humidity (<50% RH), the electrical resistance of the sensor decreased with increasing humidity. While at a higher relative humidity, the electrical resistance of the sensor increased with humidity. The reversed behavior was attributed to the distortion of the nanostructure or change in the oxidation state of PANI with the absorption of water molecules.

TNT SENSOR

In addition to the above-mentioned gas sensors, biosensors, and moisture or humidity sensors, PANI nanofibers were also studied for the electrochemical detection of an ultratrace amount of 2,4,6-trinitrotoluene (TNT) in various electrolytes such as NaCl solution, river water, tap water, and artificially prepared seawater.[392] Copolypeptide-doped PANI nanofibers, synthesized by chemical oxidative polymerization of aniline in the presence of the copolypeptide, which comprises glutamic acid (Glu) and lysine (Lys) units, were applied onto a glassy carbon electrode to fabricate the sensing electrode. A sensitive electrochemical response to TNT with a linear dynamic range of 0.5–10 μM and a detection limit down to 100 nM were exhibited by the sensing electrode. Most importantly, selectivity of the sensing electrode is very good, since two other nitroaromatic analogues examined, that is, 2,4-dinitrotoluence and trinitrobenzene, showed different redox behaviors from TNT, which can be used to distinguish these compounds from one another (Fig. 17).

TASTE SENSOR

A taste sensor for a quality assessment of commercial and freshly squeezed orange juices using

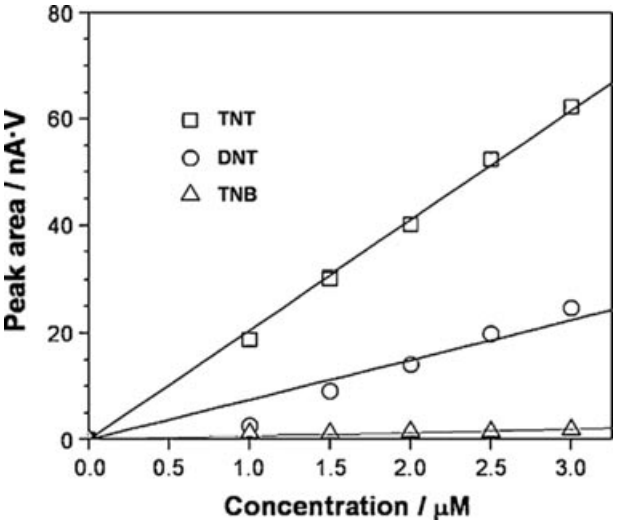

FIGURE 17. The plots of the areas of the first reduction peaks versus the concentrations of TNT, DNT, and TNB for poly(Glu–Lys)-doped nanofibers (reproduced by permission of Elsevier B.V.).[392]

PANI nanofibers as the sensoactive layer was reported by Medeiros et al.[393] Doped PANI nanofibers, synthesized by interfacial polymerization, were dispersed in DMA and DMF. Thin PANI nanofiber films or PANI/sodium polystyrene sulfonate bilayer films were deposited onto interdigital microelectrodes containing 20 pairs of digits by self-assembly and casting. Capacitance was measured in analyzing the aqueous solutions of citric acid and eight types of orange juice, including four commercial brands of ready-to-drink juice, two commercial brands of artificially reconstituted juices, and freshly squeezed orange juice from sweet lime. Changes in the citric acid concentration up to as low as 2 ppm can be detected by the sensors. Although the sensitivity of the self-assembled films was slightly lower than that of the cast films, a more regular increase in the capacitance with concentrations of analyte and a faster recovery were shown by the self-assembled films. More importantly, not only were the different types of orange juice distinguished but also the influence of storage conditions on the juice degradation process was detected and differentiated, indicating the potential application of the sensor array for the quality monitoring of types of orange juice.

NOBLE METAL ION SENSOR

On exposure to some noble metal ions like silver ions, PANI would reduce the metal ions to the corresponding metals. Recently, a noble metal ion sensor was reported by Ayad et al.,[394] where a PANI nanotubular film was deposited onto an electrode of the QCM. Silver nanoparticles were produced at the film surface on introducing the electrode to a solution of silver nitrate, and a detectable crystal frequency decrease was resulted with a mass increase in silver on the electrode, indicating that the sensor can be used for the detection of sliver ions. Since some other noble metal ions can be reduced by PANI like silver ion as well, simple sensors for detecting the presence of noble metals ions can be constructed with the PANI nanotubes deposited QCM electrode.

ADSORBENT

PANI nanotubes were studied for the first time as an adsorbent for the removal of cationic dyes such as methylene blue from the aqueous solution by Ayad and Abu El-Nasr.[395] By using the QCM and UV–visible spectroscopy, it was found that the adsorption of methylene blue onto the PANI nanotubes was much more noticeable than that onto the conventional PANI powder. The reason was attributed to the increased surface area of PANI nanotube substrates as compared with the conventional PANI powder substrates. By fitting the adsorption equilibrium data to Langmuir, Freundlich, and Tempkin isotherms and applying the data to various kinetic models, it was observed that the Langmuir isotherm fitted best the adsorption of methylene blue to PANI nanotubes and the process was best described by the pseudo–second-order kinetic model. The study revealed that PANI nanotubes could be used as a much more efficient adsorbent than the conventional PANI powder for dye removal from water.

CATALYST

Owing to its high surface area and porosity, PANI nanofibers are always used for fabrication of metal/PANI nanocomposites, especially in the field of catalysis.[141,396–400] By simply mixing palladium nitrate with PANI nanofibers, palladium nanoparticle decorated PANI nanofibers were successfully prepared by Gallon et al.[401] and studied as a semiheterogeneous catalyst in water. It was shown that the nanocomposites are active catalysts for Suzuki coupling between aryl chlorides and phenylboronic acid and for phenol formation from aryl halides and potassium hydroxide in water and air.

PANI nanotubes with Pd nanoparticles attached in the inner walls were fabricated by a three-step

procedure, that is, coating Pd nanoparticles onto surfaces of electrospun PS nanofibers, in situ deposition of PANI onto the Pd nanoparticles attached PS nanofibers, and finally the removal of the PS nanofibers.[402] The Pd nanoparticles attached PANI nanotubes showed improved catalytic efficiency than both the Pd/carbon composite and Pd/MWNT composite on catalytic reduction of *p*-nitroanilinum. Ag nanoparticles loaded PANI nanotubes were immobilized on the surface of an ITO substrate to construct a sensor, and the sensor exhibited higher electrocatalytic activity toward the reduction of dopamine than pure PANI.[141]

Nanocomposites of Pd- or Pt-deposited nanorods of poly(*N*-acetylaniline) were also fabricated by using the electrochemical method and studied for electrocatalytic reduction of oxygen[403] and oxidation of methanol,[404] respectively. For electrocatalytic reduction of oxygen, the Pd-deposited nanorods composite-modified electrode has higher electrocatalytic activity than the Pt-modified MWNT electrode. The mechanism was demonstrated as a 1-step 4-electron process. For electrocatalytic oxidation of methanol, the Pt-deposited nanorods composite-modified electrode showed not only enhanced electrocatalytic activity but also greatly reduced the poisoning effect. It was suggested that the synergistic effect of the nanostructured polymer and Pt nanoclusters provides a nanothickness hydrophobic and conjugative environment for accumulating methanol, stabilizing the nanostructure, extracting intermediates, and poisoning species. PANI nanofibers supported Pt nanoparticles, prepared by using an ethylene glycol (EG) reduction method, were also studied for an electrochemical catalyst for direct methanol fuel cells.[405] The catalyst showed both higher electrocatalytic activity and catalyst tolerance for the methanol oxidation reaction than that of the carbon black-supported platinum catalyst, which were attributed to the unique properties and morphology of PANI nanofibers. The half-cell results revealed that this catalyst is one of the most promising candidates for direct methanol fuel cells. In a later study, Liu et al.[406] found that by changing the electrodeposition sequence of Pt and Ru particles onto PANI nanofibers, both the electrocatalytic activity and catalyst-poisoning tolerance for the methanol oxidation were changed, that is, a better catalytic performance and diminished poisoning effect for CO were demonstrated by the catalyst with first deposition of Ru and then Pt particles.

To improve the electrochemical oxidation of cysteine, an important amino acid in biology, a PANI nanofiber film electrode with Pt nanoparticles loaded was prepared electrochemically and optimal Pt loading of 600 $\mu g\ cm^{-2}$ and pH 4.5 was observed for the electrode in terms of its electrocatalytic performance.[407] The electrode exhibited greatly improved electrochemical oxidation behavior in comparison with the Pt electrode, and it was shown that, together with the good sensitivity, selectivity, reproducibility, and stability, the electrode can be used to detect L-cysteine after further investigation.

By in situ deposition of a layer of poly(3,4-ethylenedioxythiophene) onto the surfaces of PANI nanofibers, a bilayer nanostructured conducting polymer composite was prepared by Zhang et al.[408] The composite showed not only two orders of magnitude increased electrical conductivity but also stronger electrocatalytic activity for oxidation of ascorbic acid than PANI nanofibers, showing promising uses in electrochemical sensors for biomedical applications and polymer electronics and devices.

Ferrocenesulfonic acid doped PANI nanofibers coated with polycatechol were also studied for catalytic electrochemical oxidation of ascorbic acid, and it was found that the catalytic activity of the coated nanofibers with small diameters (70–90 nm) is higher than that of the nanofibers with large diameters (140–210 nm).[409] In another study, by comparing the catalytic activity of vanadium-doped PANI nanoparticles, nanotubes, and nanorods for selective oxidation of sulfides to sulfoxides in water, Sreedhar et al.[125] found that the nanotubes and nanorods showed higher activity and selectivity than nanoparticles, indicating that the special morphology of nanostructures plays an important role in enhancing the catalytic activity of PANI. Ferric chloride doped PANI nanofibers were prepared by mixing PANI nanofibers with a solution of ferric chloride at a low temperature and studied for selective acylation of alcohols and amines using acetic acid as an acylating agent under solvent-free conditions to produce the corresponding acetates and acetamides in high yields.[410] By introducing PANI nanofibers to the gas diffusion electrode in proton exchange membrane fuel cells, the catalyst utilization in the oxygen reduction reaction was increased from 57% to 84% and the polarization resistance of the electrode was reduced, leading to improved electrode performance.[411]

Poisoning tolerance is equally important to improve catalytic activity for any catalyst. With incorporation of some nanoparticles such as neodymium oxide into PANI nanofibers, which were then

deposited on the Pt electrode, not only was the catalytic activity of the electrode on methanol oxidation enhanced but also the tolerant ability of the Pt catalyst to CO-like species increased.[412] What is more, neodymium oxide showed one more effect of inhibition on the electrochemical degradation PANI, in addition to its inducing effect for formation of PANI nanofibers by chemical polymerization.

Cuprous iodide (CuI) supported PANI nanofibers were prepared, characterized, and evaluated as a catalyst for the N-arylation of aliphatic, aromatic, and (*N*)*H*-heterocyclic amines with aryl iodides at an ambient temperature (25°C) and aryl chlorides at 80°C by Arundhathi et al.[413] Enhanced activity was achieved by the catalyst without using high temperatures, ancillary ligands, and high catalyst loading, and the reason is the high basicity and size of PANI nanofibers. It was foreseen by the authors that the new catalyst will find widespread applications in synthesizing a wide variety of pharmaceutically and industrially important secondary and tertiary amines with a wide variety of functionalities in a one-pot coupling of aryl halides and amines.

ACTUATOR

PANI nanofibers were investigated as a novel compliant electrode material for fault-tolerant dielectric elastomer actuators because of their high aspect ratio, moderate conductivity, and ease of processablity.[414] Electrodes with varied thicknesses were fabricated by spraying PANI nanofibers. Actuators with electrode thicknesses of 1.1, 1.3, and 1.5 μm showed relatively high actuation strains under an electric field of 3–3.5 kV, and optimal results were achieved for actuators with an electrode thickness of 1.1 μm and performed with an electric field of 3 kV. Preliminary results, including the pulsed voltage testing and mechanical compliance, revealed PANI nanofibers as a promising material for dielectric actuators. By painting a viscous Nafion solution on the surface of the composite film, which was prepared by solution blending and casting of Nafion and PANI nanorods, sandwiching with another composite film and pressing, followed by silver plating, a three-layer membrane actuator was constructed.[415] The actuator showed a higher angular distance and displacement than that based on a pure Nafion membrane.

A novel monolithic actuator based on an asymmetric film of flash-welded PANI nanofibers (Fig. 18) was reported by Baker et al.,[416] and fabrication of the coherent monolithic porous microstructures through the electrophoretic deposition of PANI nanofibers was demonstrated in a later study.[417] Several advantages such as ease of synthesis, a large degree of bending, patternability, and no delamination were demonstrated by the continuous single component bending/curling actuator over the conventional dual component, bimorph actuator. By immersing in a 0.5 M CSA solution, the asymmetric film bent to the flash-welded surface due to larger swelling of the fibers compared with the cross-linked flash-welded surface for an approximately 720° rotation from its original position in 20 s, more rapid than the asymmetric films driven by chemically induced proton exchange and the conventional PANI bimorph actuators. By placing in a 0.5 M sodium hydroxide solution, the acid-coiled asymmetric film reversed to the flat original state in ca. 2 min, due to the removal of repulsive charges, dopant ions, and

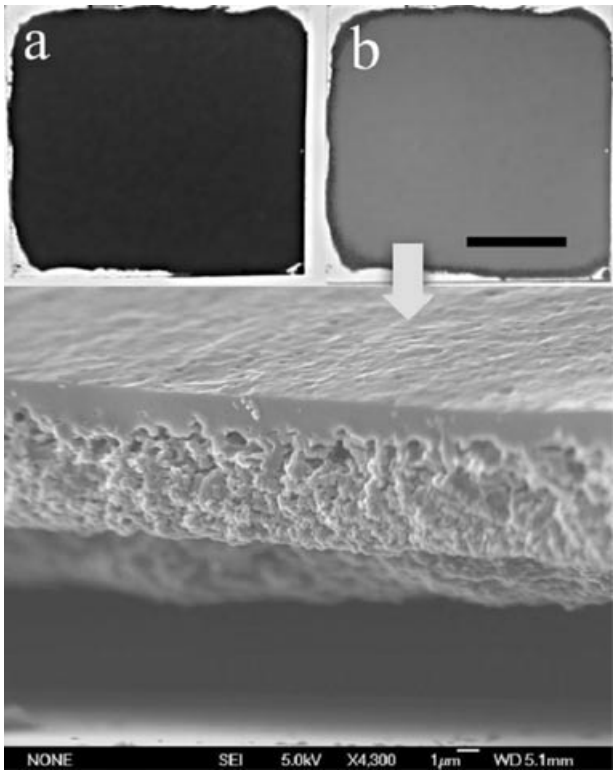

FIGURE 18. Dedoped polyaniline nanofibers drop cast from a concentrated polyaniline nanofiber suspension form a uniform film as imaged by an optical microscope (a) before and (b) after flash welding (scale bar = 1 cm). (c) A scanning electron micrograph of a fractured cross section of a flash-welded polyaniline nanofiber film with a 1-μm thick upper flash-welded layer, and a 5-μm thick nanofibrillar active layer (scale bar = 1 μm) (reproduced by permission of Wiley-VCH Verlag GmbH & Co.).[416]

solvent resulting from deprotonation. The bending actuator could be developed for use in microtweezers, microvalves, artificial muscles, chemical sensors, and/or patterned actuator structures. Free-standing and asymmetric polyvinyl alcohol (PVA) composite films with the PANI nanofiber content of 68–90 wt% were fabricated by drop cast of a mixture of the two components in water followed by a dry and flash welding technique and studied for high-performance monolithic actuators.[418] The composite actuators showed superior bending/recovery responsive properties toward acid/base and more enhanced mechanical properties than pure PANI nanofiber actuators. The bending degree and actuation speed can be controlled by changing contents of PANI nanofibers and the pH of the external media, respectively, and a reversible repeatability of beyond 100 cycles was exhibited. More interestingly, monolithic boxes were fabricated by using asymmetric stripes as hinges between faces and a controlled folding/unfolding movement in acid/base was demonstrated.

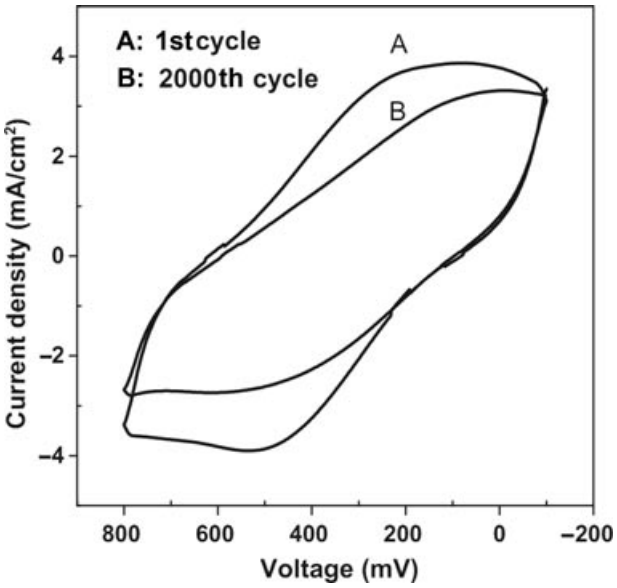

FIGURE 19. The C–V curves for stability of polyaniline electrode at (a) first and (b) 2000th cycles. The scanning rate and concentration of H_2SO_4 electrolyte were 100 mV/s and 1 M, respectively (reproduced by permission of Elsevier B.V.).[428]

SUPERCAPACITOR

1D nano-PANI, especially PANI nanofibers, has been extensively investigated for electrode materials or supercapacitors in considering the distinctive characteristics of conducting pathways, surface interactions, nanoscale dimensions, good thermal and chemical stability, large surface areas, and high electrical conductivity in a doped state.[148,171,419–425]

With hydrolysis of triethoxysilylmethyl *N*-substituted aniline and the subsequent condensation reaction with silanol groups on surfaces of silica nanoparticles, a nanofibrous PANI with chains chemically anchored to silica nanoparticles was prepared by a one-step electrodeposition process.[426] The nanocomposite showed an average specific capacitance of 380 F g^{-1}, which is 40% higher than that of a simple composite of PANI and silica. The improved stability resulted from the chemical bonding between organic and inorganic moieties, and the nearly symmetric chronopotentiogram also showed that the nanocomposite is a promising candidate as a material for supercapacitors.

PANI nanowires with a diameter of 30–60 nm or PANI nanofibers with a diameter of 120–125 nm were electrochemically deposited on a stainless steel electrode and characterized for supercapacitor application by CV in 1 M H_2SO_4 (Fig. 19).[427,428] Highly capacitive behavior (e.g., specific capacitance of 775 F g^{-1} for PANI nanowires[427] and 861 F g^{-1} for PANI nanofibers[428] were measured at a scan rate of 10 mV s^{-1}) and stable supercapacitive characteristics, as well as long-term stability, showed the great potential of PANI nanowires and nanofibers for the high-performance supercapacitor. In another study, PANI nanowires (with a diameter of 30 nm) arrayed electrodes were prepared electrochemically by using the AAO template and constructed for an electrochemical supercapacitor.[429] A specific capacitance of about 1142 F g^{-1} was shown by performing CV of the electrodes in a 2 M H_2SO_4 aqueous solution. Fuzzy nanofibrous interconnected PANI films were electrochemically deposited on stainless steel substrates and studied as electrodes for supercapacitors, where the highest specific capacitance of 839 F g^{-1} at the voltage scan rate of 10 mV s^{-1} was achieved.[430]

Using supramolecular assemblies of block copolymer as the nanotemplate, highly dense arrays of ordered and highly aligned PANI nanorods with a diameter of 10 nm and spacing and height of around 27 nm were electrodeposited on transparent ITO substrates.[431] Although the electrochemical capacitance was as high as 3407 F g^{-1}, limited electrochemical stability was demonstrated by the ordered PANI nanorods. In another study, an ITO substrate was first modified with a self-assembled monolayer of 3-(triethoxysilyl)-propyl isocyanate followed by aniline to form aniline-primed substrates.[432] In the

following step, polymerization was carried out to fabricate nanostructured PANI-coated electrodes, where the pendant aniline groups on the surface acted as initiation sites for polymerization. It was demonstrated by CV that an electrode composed of PANI nanorods showed a much higher specific capacitance of 592 F g^{-1} than 214 F g^{-1} by the nanospheres-coated electrode measured at 10 mV s^{-1}, which was attributed to the larger surface area for redox reactions in nanorods than nanospheres.

Nanocomposites of vertically aligned PANI nanowire arrays on a graphene oxide substrate, which were prepared by dilute polymerization of aniline in the presence of graphene oxide, showed a higher electrochemical capacitance and better stability than each individual component when used as supercapacitor electrode materials, indicating a synergistic effect of PANI and graphene oxide.[433] Vertically aligned PANI nanowires were also synthesized on various conducting substrates such as an Au plate, Pt plate, and stainless steel plate by using a galvanostatic current method and studied for supercapacitor electrodes by the same group.[434] The aligned nanowire arrays showed a higher capacitance than both the disordered nanowire and nanowire arrays prepared using a hard template of AAO.[23] The highest specific capacitance of 950 F g^{-1} was measured and can be fixed at 780 F g^{-1} at a high charge–discharge current density of 40 A g^{-1} for the PANI nanowire arrays.

PANI nanofibers synthesized by rapid mixing polymerization were drop-coated onto a pretreated graphite electrode to fabricate PANI nanofiber coatings. An ideal capacitive response between 0.2 and 0.7 V (Ag/AgCl) in 1 M HCl was demonstrated by the PANI nanofiber films, such as a high-specific capacitance (ca. 490 F g^{-1}), high-power capability, excellent capacitance retention, and high-frequency capacitive responses. Using the PANI nanofiber electrode as a cathode and a graphene electrode as an anode, an asymmetric supercapacitor was built. The energy and power densities of the asymmetric supercapacitor were ca. 4.86 Wh kg^{-1} and 8.75 kW kg^{-1}, respectively, at 500 mV s^{-1}, indicating promising applications for the next generation of supercapacitors.[435] Freestanding and flexible composite films of chemically converted graphene and PANI nanofibers, which were synthesized by interfacial polymerization, were prepared by using vacuum filtration of the mixed dispersions of both components in deionized water and studied for construction of symmetric supercapacitors.[436] The conductivity of the composite film was as high as 5.5 S cm^{-1}, one order of magnitude higher than that of pure PANI nanofiber film. A high capacitance of 210 F g^{-1} was exhibited by the supercapacitor at a discharging current density of 0.3 A g^{-1}. By increasing the discharging current density from 0.3 to 3 A g^{-1}, this capacitance can be maintained for about 94% (197 F g^{-1}). Moreover, a high capacitance of 155 F g^{-1} was maintained even after 800 charging/discharging cycles at a current density of 3 A g^{-1}, showing good stability of the symmetric supercapacitor. A flexible electrode was fabricated by the electrochemical deposition of PANI nanofibers onto the surface of carbon cloth, and symmetrical capacitors were assembled with a cellulose film as a separator by sandwiching the electrodes.[437] The supercapacitor showed high gravimetric capacitance of 1079 F g^{-1} at a specific energy of 100.9 Wh kg^{-1} and a specific power of 12.1 kW kg^{-1} and also an exceptionally high-area-normalized capacitance of 1.8 F cm^{-2}. Flexible electrodes were also fabricated by deposition of PANI nanofibers onto gold-sputtered polyvinylidene fluoride-*co*-hexafluoropropylene membranes.[438] The specific capacitance of 235 F g^{-1} and a discharge capacitance of 245 F g^{-1} at 100 mVs^{-1} were exhibited by the electrodes. By coating the electrodes with the Nafion solution, the stability of the electrodes was enhanced and the specific capacitance of 180 F g^{-1} was obtained after 10,000 cycles at 100 mV s^{-1}. Symmetric supercapacitors based on the electrodes had the specific capacitance of 125 F g^{-1} at 100 mV s^{-1} and 95 F g^{-1} after 10,000 cycles.

Dedoped PANI nanofibers were also studied as electrode materials for supercapacitors.[439] The as-fabricated electrochemical capacitor showed a specific capacitance of 593 F g^{-1} at a constant current density of 2.5 A g^{-1} in a 1 M H_2SO_4 aqueous solution and can be subjected to repeated charge/discharge over 5000 cycles in the voltage range of 0–0.65 V. In comparison to the supercapacitor based on doped PANI nanofibers, the one using dedoped PANI nanofibers as electrode materials showed an increase of about 29% of the capacitance retention ratio. In another study, using dedoped PANI nanofibers, which were synthesized by interfacial polymerization, and super-p as conducting materials, a mixture of CMC and styrene–butadiene rubber as a binding material, a composite electrode for an aqueous redox supercapacitor was prepared by casting the mixture on a Ti electrode after ball-milling.[440] An initial specific capacitance of 554 F g^{-1} was demonstrated at a current loading of 1.0 A g^{-1}. However, owing to the polymer degradation and mechanical stress on PANI

nanofibers, the capacitance decreased rapidly with continuous cycling. By replacing the PANI nanofibers with a composite of PANI/CNT, which was synthesized by in situ chemical polymerization, the high initial specific capacitance of 606 F g^{-1} and good capacitance retention in the voltage range of 0–0.4 V were obtained, indicating that the PANI/CNT composite might be more practical for fabrication of a supercapacitor than PANI nanofibers.

BATTERY

Owing to its good redox reversibility and stability in air and aqueous media, PANI has been studied for cathodic material for preparation of either aqueous or lithium batteries.[424] A Li/PANI battery exhibits several advantages such as longer cycle life, lower self-discharge rate, and resistance to overdischarge over the conventional Li battery, and a theoretical specific capacity of 95.2 mA h g^{-1} was reported for $HClO_4$-doped PANI.[19] A Li/PANI cell constructed with PANI nanotubes showed a much higher discharge capacity (75.7 mA h g^{-1} at the 20th cycle), as well as longer charge and discharge plateau, than that of the commercial doped PANI powder (54.2 mA h g^{-1} at the 20th cycle), indicating promising applications of the doped PANI nanostructures in Li/PANI rechargeable batteries. The better performance of the Li/PANI rechargeable battery might, as stated, have resulted from the higher specific surface area, higher conductivity, and relatively flexible alignment of PANI nanotubes than the commercial powders.

In another study, PANI nanofibers synthesized by interfacial polymerization were doped by $HClO_4$ (1.0 M) and used to prepare the polymer cathode of the Li/gel polymer electrolyte (GPE)/PANI cell.[441] A maximum discharge capacity of 69 mA h g^{-1} at the 20th cycle and 48 mA h g^{-1} at the 100th cycle and a coulombic efficiency of 95% at the 20th cycle were exhibited by the cell. Both the discharge capacity and coulombic efficiency were lower than that of the Li/PANI nanofiber cell reported by Cheng et al.[19] The enhanced performance of the Li/GPE/PANI nanofiber cell was considered to have resulted from both the facilitated easy access of the electrolyte with PANI nanofibers and the higher ionic conductivity of the GPE. A decrease in discharge capacity with cycling was attributed to degradation of the PANI nanofiber electrode, which can be overcome by using a composite of PANI with CNTs.[441]

PANI nanofibers deposited electrode by normal pulse voltammetry was directly used as a cathode without any further treatment in a PANI–Zn secondary battery, where a Zn electrode was used as the anode.[100] A maximum capacity of 235.6 mA h g^{-1} was demonstrated at the first charge–discharge cycle, but the capacity decreased significantly to 159.03 mA h g^{-1} at the 100th cycle and 141.5 mA h g^{-1} at the 120th cycle, with an average capacity loss of 0.4% per cycle. The reduction in battery capacity was caused by not only the degradation of PANI nanofibers but also the zinc passivation, as revealed by the study. A coulombic efficiency of 97%–100% was also shown by the battery over a wide range of current density of 0.3–5.6 mA cm^{-2}. The better performance of the battery, as compared with the one using PANI nanofibers synthesized by CV, was related to the higher porosity and surface area of the PANI nanofibers synthesized by using the normal pulse voltammetry.

FUEL CELL

Platinum nanoparticle loaded PANI nanofibers were sprayed through a layer-by-layer assembly technique to fabricate membrane electrode assemblies for hydrogen/oxygen full cells.[442] Membranes with the nanoscale structure can be produced quickly with the technique, adequately addressing the specific tuning of their porosity, platinum loading, electronic conductivity, and proton conductivity. The layer-by-layer structures boosted performance significantly, accelerating the charge transport of the proton exchange membrane due to the high conductance of PANI nanofibers as well as ion/gas transport due to their fibrous morphology. A power density of 63 mW cm^{-2} was demonstrated by the as-prepared membrane electrode assemblies, and a Pt utilization of 437.5 W g^{-1} Pt was calculated, which is comparable to the traditional fuel cell using carbon black as a Pt support. PANI nanofibers were introduced into the catalyst layer of the electrode for both the proton exchange membrane fuel cell and direct methanol fuel cell by Zhiani et al.[443,444]. It was found that, for the former fuel cell, the addition of PANI nanofibers improved the homogeneity distribution of the ionomer in a catalyst layer and increased the performance of gas diffusion electrodes in the oxygen reduction reaction, and for the latter fuel cell, PANI nanofibers improved the catalyst activity in methanol oxidation, hindered and prevented the catalyst from more poisoning by intermediate products of methanol oxidation, and

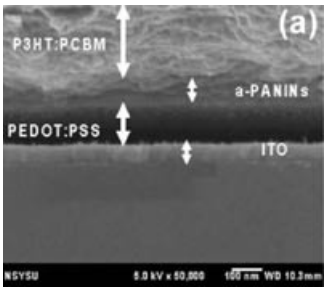

FIGURE 20. FE–SEM cross-sectional image of the ITO/PEDOT:PSS/a-PANINs/P3HT:PCBM layers (reproduced by permission of Elsevier B.V.).[445]

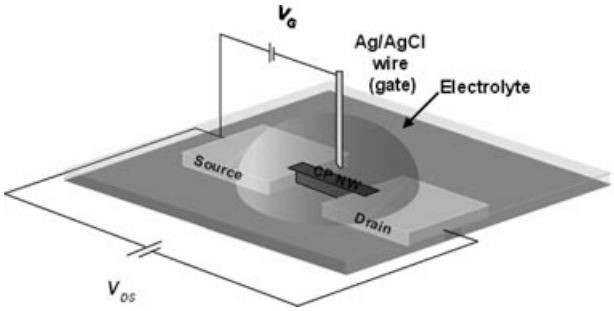

FIGURE 21. Schematic illustration of the single conducting polymer nanowire based electrolyte/liquid ion-gated FET device (reproduced by permission of American Chemical Society).[448]

improved the mechanical properties of the catalyst layer.

SOLAR CELL

PANI nanotubes were used as an interfacial layer in poly(3-hexylthiophene):[6,6]-phenyl-C_{61}-butyric acid methyl ester (P3HT:PCBM)-based polymer bulk heterojunction solar cells to collect holes efficiently from the active layer and transport them to the buffer layer under the internal electric fields of the fabricated ITO/buffer/a-PANINs/P3HT:PCBM/Al devices (Fig. 20).[445] The enhanced holes collection was ascribed in part to geometrical field enhancement at the PANI nanotube layer, and a power conversion efficiency of 4.26% under AM 1.5 G (100 mW cm^{-2}) illumination was observed for an annealed device, ca. 26% higher than that of the one without an interfacial layer of PANI nanotubes. Sulfamic acid doped PANI nanofibers, synthesized by interfacial polymerization, were studied as new counterelectrodes materials for fabrication of highly efficient dye-sensitized solar cells by Ameen et al.[446] The solar cell based on the emeraldine base form of PANI nanofibers exhibited a solar-to-electricity conversion efficiency of ~4.0%, whereas the one based on sulfamic acid doped PANI nanofibers showed a ~27% improvement in the solar-to-electricity conversion efficiency. The enhancement in the conversion efficiency was attributed to the improved electrocatalytic activity for the I^{3-}/I^{-} redox reaction with incorporation of sulfamic acid into the PANI nanofibers. The solar-to-electricity conversion efficiency for the dye-sensitized solar cells based on sulfamic acid doped PANI nanofibers counterelectrode is 5.5% under 100 mW cm^{-2}. Very recently, a flexible counterelectrode for the reduction of tri-iodide was developed by electrochemical deposition of PANI nanofibers on graphitized polyimide carbon films, which exhibited a very low charge transfer resistance and series resistance owing to the high electrocatalytic activity of PANI nanofibers and the high conductivity of the flexible graphitized polyimide film.[447] An energy conversion efficiency of 6.85% under 1 sun illumination was demonstrated when the electrode was combined with a dye-sensitized titanium dioxide photoelectrode and electrolyte.

FIELD-EFFECT TRANSISTOR

Single conducting polymer nanowires based field-effect transistors (FET) in a width of 100 nm and a length of 2.5 μm were fabricated using PANI or PPY nanowires, which were electrochemically grown between two electrodes (Fig. 21).[448] The FET device can be turned on and off by electrical or chemical signals. By tuning the electrochemical gate potential of the nanowires, a large modulation in the electrical conductivity of up to three orders of magnitude was demonstrated by the transistors. In comparison with the FETs based on conducting polymer nanowire electrode junctions and thin films, the single conducting polymer nanowires FETs showed a higher electrical performance. Most importantly, comparable performance was demonstrated in comparison with the silicon nanowire FETs. Furthermore, sensitivities of the single conducting polymer nanowires can be easily tuned by simple control of the electrolyte/liquid ion gate potentials. PANI nanotubes were also used to fabricate FET.[449] A p–n junction diode behavior was exhibited by the nanotube-based FET, where the forward-bias current was turned on at a negative gate voltage and off by applying a positive gate voltage. Further studies on an electrolyte-gated conducting PANI nanowire FET by sweeping in a cyclic potential

mode showed not only significant hysteresis during reduction/oxidation in the electrolyte gate, where the conductivity on the positive sweep was typically larger than that on the negative sweep[450] but also a clear irreversible degradation of the current–voltage characteristics.[451] The reasons for the hysteresis and degradation were attributed to the changes in the PANI structure and the effects of coulombic repulsion in PANI nanowires during the oxidation process, and the intensity of coulombic repulsion in the cycle mode, respectively. Two comprehensive and detailed reviews on FET sensors using 1D nanostructured conducting polymers are presented by Myung et al.[452,453] very recently, where the recent developments were reviewed, the advantages and disadvantages of various fabrication, functionalization, and assembling techniques were discussed, and the future directions of the research field were predicted.

ELECTROCHROMIC DEVICE

Using a PANI nanofiber deposited ITO glass substrate as the electrochromic electrode, an ITO substrate as the counterelectrode, and 1-ethyl-3-methylimidazolium tetrafluoroborate as the electrolyte, an electrochromic device (ECD) with a dimension of 2×1.5 cm^2 was fabricated by Yu et al.[454] At the bleached state, that is, by applying a voltage of -1.5 V to the PANI nanofiber electrode, the ECD showed excellent transparency in the range of 490–800 nm, whereas at the colored state, the color changed from transparent to light blue, and eventually to deep blue when voltages of 0.5 to 1.5 V were applied. Contrast ratios of 93% at $+1.5$ V (vs. -1.5 V) and 77% at $+0.5$ V (vs. -1.5 V) were also demonstrated, making the ECD a promising candidate for E-paper displaying. The dynamic response times, including both the bleaching and coloring response time, of the ECD are much shorter than the one fabricated with a regular PANI thin film instead of PANI nanofibers. The reason was ascribed to the large surface area of PANI nanofibers, which enhanced the implantation and intercalation abilities of the ions by offering a much shorter diffusion distance during the redox process.

A self-powered photoelectrochromic cell with a dimension of 1×1 cm^2 was also fabricated[454] by using a dye-sensitized nanocrystalline TiO_2 layer as one electrode and PANI nanofibers as the counterelectrode. The cell exhibited a short circuit current of 0.47 mA and an open circuit voltage of 0.58 V when exposed to light. Although the color change of the cell cannot be observed by the naked eye, the reversible transformation from the colored state (open circuit) to the bleached state (short circuited) of the cell can be easily detected by an irradiatometer and a photoswitch effect was demonstrated under irradiation. Several potential applications, such as photoswitches, light sensors, and information storage devices, were suggested for the cell provided the two states are defined as "0" and "1."

HYDROGEN STORAGE

The reversible hydrogen storage behavior of PANI nanofibers at room temperature was first reported by Niemann et al.[455] It was found that 95% of the total capacity (3-4 wt% of PANI nanofibers) was achieved in less than 10 min at a high hydrogen pressure of ca. 80 bar, and ca. 1–2 wt% of the absorbed hydrogen was released when desorbed against 1 bar. Pressure-composition-temperature measurement at room temperature clearly showed that the hydrogen absorption and desorption was reversible, and no deterioration in hydrogen sorption kinetics and overall storage capacity of 3–4 wt% was observed during the 25 tested cycles. Although the detailed hydrogenation and dehydrogenation mechanism in PANI nanofibers is not clear, the reversible hydrogen sorption capacity of 3–4 wt% at room temperature was attributed to the unique nanofibrous microstructure and surface properties of PANI nanofibers.

SURFACE MODIFIER

Perpendicularly oriented PANI nanowires were electrodeposited on a Ti/Si substrate with the aid of an AAO template, rendering the surface both conductive and superhydrophobic, even in corrosive solutions such as acidic and basic ones over a wide range of pH.[456] The hydrophobocity of the PANI nanowire film can be further enhanced by treating the sample in a solution of perfluorooctanoic acid and *N,N′*-dicyclohexylcarbodiimide in ethanol for surface fluorination. For example, the contact angle of the PANI nanowire film increased from $105^\circ \pm 1^\circ$ to $160^\circ \pm 1^\circ$ after the surface treatment. More importantly, either hydrophobic or hydrophilic PP films can be readily fabricated by deposition of shape-controllable PANI nanostructures on the PAA-grafted PP films as mentioned above.[225,226] Superamphiphilic behavior was also demonstrated by electrochemical deposition of PANI nanofibers on a stainless steel electrode.[457] More importantly, by grafting hydroxyl groups onto PANI molecule chains, which was achieved by

reacting leucoemeraldine state PANI with epichlorohydrin and then followed by hydrolyzing in a basic solution, the lasting time of the superhydrophilic behavior increased from 1 month to more than 2 months, indicating the significantly improved stability of the superhydrophilic property of the PANI nanofiber deposited surface. A large-area PANI nanofiber network was also deposited on the surfaces of diatomite by in situ polymerization of aniline without stirring.[458] Electrodes modified by the composite showed good redox reversibility in the aqueous media ranging from pH 1.0 to 7.0 and good electrochemical cycling stability in the aqueous media of pH 4.0, indicating promising applications of the materials with an increased operating pH window in the aqueous media and good conductivity.

By simply casting the water dispersion of PANI nanofibers on glass slides, green-colored uniform PANI nanofiber film with a relatively smooth surface was prepared by Li and Kaner.[459] In the same way, even and compact coating of PANI nanofibers in the emeraldine-based form was formed by casting an alcohol dispersion with 10% of PANI nanofibers on a pretreated carbon steel coupon.[460] The film showed improved corrosion protection performance over that of the control sample, which was prepared with aggregated PANI, since a better passive layer was formed on the surface of carbon steel. Uniform, compact and strongly adherent poly(aniline-*co*-amino-naphthol-sulfonic acid) nanowire coatings were electrochemically deposited onto an iron electrode and studied for corrosion protection of iron in an acidic solution.[461] Improved protection efficiency was demonstrated by the nanowire film compared to that of PANI due to the better adhesion and adsorption of the copolymer film onto the iron surface, which were facilitated by the morphology, π-electron conjugation, quaternary nitrogen atom, good interaction of the side groups, and the larger molecular size of the copolymer nanowires. After studying the anticorrosion performance of different 1D nano-PANI coatings cast on the surface of mild steel electrodes, Yang et al.[462] found that PANI nanofibers with uniform diameters of 60–100 nm synthesized by a direct mixed reaction had more excellent protective properties than that synthesized by conventional polymerization and interfacial polymerization, revealing that the anticorrosion performance of PANI is influenced not only by nanostructure but also morphology.

In forming the nanoscale thin films, a simple and scalable solution-based method, a flash dry deposition method, was introduced by Hu et al.[463] with CNT and PANI nanofibers as the examples, where uniform films over macroscale areas (8 in. $\times$ 8 in.) with homogeneous structures in the microscale were obtained by controlled drying of the applied CNT or PANI nanofiber solutions.

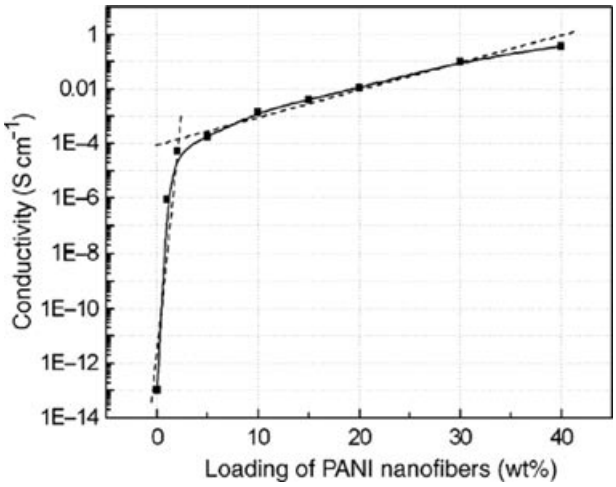

FIGURE 22. Conductivities of the PMMA/PANI nanofibers composites (reproduced by permission of American Chemical Society).[464]

FUNCTIONAL ADDITIVES

Excellent dispersiblity is one of the key features demonstrated by 1D nano-PANI since stable dispersions can be formed not only in various organic solvents but also in water. This key feature renders 1D nano-PANI a novel additive for fabrication of various functional materials.

Conductive Composite

By mixing the dispersion of sulfuric acid doped PANI nanofibers and a solution of poly(methyl methacrylate) (PMMA), simultaneously transparent and conductive films were fabricated by casting and drying (Fig. 22).[464] The composite film has good stability in air and solvents, showing great promising applications such as antistatic charge and electromagnetic interference shielding. Both the dielectric behavior and charge transport of PANI nanofibers, which were synthesized by interfacial polymerization, filled PMMA composites were studied by Banerjee and Kumar.[465] It was found that the dielectric constant was dependent on temperature and frequency only in the low-frequency region (<1 kHz) and this increased with the PANI nanofiber

content, and also the charge transfer process, in giving rise to ac conductivity, is dominated by the correlated barrier hopping mechanism. Conductive composites of PANI nanorods and cyanoresin[466] and conductive PANI nanofiber filled epoxy resin composites[467] were also reported. Improved thermal stability was shown with the increase of cyanoresin content owing to the hydrogen bonding formed between TSA-doped PANI nanorods and cyanoresin, whereas the lowest percolation threshold was demonstrated by the PANI nanofibers filled than PANI particles or fibers filled epoxy resin composites. Conductive HCl-doped PANI nanofibers were later dispersed in polyacrylate coating and studied for electromagnetic interference shielding in the frequency range of 100 kHz to 10 GHz, and a shielding effectiveness as high as 63 dB was achieved with PANI nanofiber loadings of 45%.[468] DBSA-doped PANI nanofiber filled polyethylene composites were prepared by melt processing, with a lower conductive percolation of 4 wt% due to the easily formed conducting paths by PANI nanofibers inside the polymer matrix.[469] A conductive PANI nanorod filled composite was also fabricated by dispersion polymerization of aniline in the presence of PVA.[470]

Most importantly, biocompatible conductive composites were fabricated using PANI nanofibers and collagen, which was completed by spreading the mixture of PANI nanofiber dispersion and collagen solution.[471] Conductivity of the as-prepared composite films increased with PANI nanofiber loadings, as observed for other filled conductive composites. Furthermore, porcine skeletal muscle cells were successfully cultured on the composite films as on pure collagen reference, indicating the suitability of the composites for biomedical applications. In a very recent study,[472] conductive composites of PANI nanofibers and polycaprolactone were fabricated by solution casting and investigated as platforms for cardiac tissue regeneration, where both conductive and biological recognition properties are required to assure more efficient electroactive stimulation of cells. It was found that a more efficient transfer of electrical signals was provided by short PANI nanofibers due to their spatial organization to form the percolative network. Furthermore, biological assays clearly indicated that the electrical signals offered by PANI nanofibers stimulate the cardiogenic differentiation of human mesenchymal stem cells into cardiomyocite-like cells, showing that the electroactive biodegradable substrates can be potentially used as novel synthetic patches for regeneration of cardiac muscle.

With the addition of conductive PANI nanofibers to vinylidene fluoride-trifluoroethylene copolymers, a kind of ferroelectric polymers significantly improved dielectric constant as high as 50 times and percolation threshold as low as 2.9 wt% were demonstrated by the filled composite films.[473] More importantly, the leakage current at low-frequency was suppressed and the electric field strength required to switch spontaneous polarization of the ferroelectric polymers was drastically reduced. All these improved properties revealed potential application of the nanocomposites in fields such as high-energy density capacitors, thin-film transistors, nonvolatile ferroelectric memories, and some electromechanical devices.

Dedoped PANI nanofibers were added into a composite electrolyte either of a PEO-P(VdF-HFP)-$LiClO_4$ or of P(VdF-HFP)-(PC + DEC)-$LiClO_4$ system with different loadings.[474,475] It was found that the ionic conductivity of the polymer electrolytes increased with increasing loading of PANI nanofibers to 15 wt% but it decreased with further loading to 25 wt%. The increase in ionic conductivity was attributed to formation of better connectivity for ion motion through the liquid electrolyte due to the improved porous structure of the GPEs after the addition of PANI nanofibers, and the decrease was due to the formation of insulating clusters that resulted from phase separation of PANI nanofibers from the composite electrolytes. The PANI nanofiber loaded composite electrolytes are particularly attractive for technological applications such as for rechargeable lithium batteries, owing to the enhanced properties such as higher ionic conductivity at ambient temperatures and improved interfacial stability.

Ultrafiltration Film

Nanocomposite ultrafiltration membranes of PANI nanofibers and polysulfone were fabricated by using a simple filtration process[476] or phase inversion process.[477] The nanocomposite membranes showed similar rejection performance to the polysulfone membrane, but better permeability and hydrophilic property than the polysulfone membrane. For the blended film prepared by using the phase inversion process, the slower flux decline rate and higher flux recovery after a simple water flush than polysulfone membrane were exhibited, suggesting that PANI nanofibers are promising materials for the preparation of ultrafiltration membranes with high flux and low fouling.

Stabilizer

Composite films (in a thickness of 0.1 mm) of PMMA and HCl-doped PANI nanofibers were prepared by casting mixtures of dispersion of PANI nanofibers and a solution of PMMA in butanone, and effects of gamma irradiation stabilizing performance of PANI nanofibers on the composite films were assessed.[478] With loading as low as 0.15%, an inhibition factor of 93% at a sterilization dose of 25 kGy was demonstrated by PANI nanofibers; with increasing the sterilization dose to 60 kGy or higher, mild deprotonation of PANI nanofibers was observed but the oxidation state was not affected, indicating that PANI nanofibers are an effective protection agent against structural damage of PMMA to gamma irradiation.

Antioxidant

The antioxidant activity of PANI nanofibers was higher than the conventional PANI and increased with decreasing of average diameters of the nanofibers due to increased surface areas.[479] Therefore, inclusion of PANI nanofibers in biological media might be very favorable in tissues suffering from oxidative stress, since the excessive levels of reactive radical species are need to be decreased or eliminated. The antioxidant activity of the PANI nanofibers synthesized by interfacial polymerization was studied by using a 1,1-diphenyl-2-picrylhydrazyl (DPPH) scavenging assay, and it was found that hematolysis of red blood cells from cytotoxic agents can be protected with PANI nanofibers.[480] The antioxidant activity of PANI nanofibers can be enhanced by swift heavy ion irradiation.[481] The increased antioxidant activity with increasing fluence was attributed to the availability of more reaction sites as a result of fragmentation of the PANI nanofibers that compensates for the benzenoid to quinoid transition after irradiation, though the quinoid unit has no hydrogen for DPPH scavenging. Hemolysis prevention capability and biocompatibility of PANI nanofibers also increased with irradiation fluence. The results showed the possibility of employing swift heavy ion irradiation as a potential technique to enhance the antioxidant activity and biocompatibility of conducting polymer nanostructures for biomedical applications.

Reductant

PANI nanofibers are always used as the reducing agent and/or supporting materials for various metal nanoparticles due to their specific redox property. Suprahigh density Pt nanoparticles or Pt/Pd hybrid nanoparticles were produced by mixing PANI nanofibers with aqueous solutions containing the related metal precursors and formic acid.[482] The metal nanoparticles were grown directly onto the surface of the PANI nanofiber, and no additional linker was used. Different electrochemical devices, such as a catalyst for the methanol oxidation reaction, hydrogen peroxide and glucose sensors, using the nanocomposites as a signal enhancement element all showed enhanced electrocatalytic activities toward the related molecules. Palladium[401] and gold[483,484] nanoparticles decorated PANI nanofibers were also fabricated by simply mixing PANI nanofibers with aqueous palladium nitrate or $HAuCl_4$ solutions. In the case of gold nanoparticles decorated PANI nanofibers, diameters of the gold nanoparticles ranged from 2 to 10 nm by changing the concentration of $HAuCl_4$,[483] and the gold nanoparticles loaded PANI nanofibers were studied for hydrogen peroxide sensing due to the strong interaction between gold nanoparticles and PANI nanofibers, which enhanced the electroactivity of PANI nanofibers and the electrocatalytic activity of gold nanoparticles for the oxidation of hydrogen peroxide.[484] The size and morphology of gold can be well controlled by using external electrochemical deposition methods on the mixture.[485] PANI nanotubes, common granular PANI, as well as aniline oligomers were mixed with silver nitrate in nitric acid to prepare PANI–Ag composites.[486,487] The conductivity of the composites was affected by not only the silver content but also the types of PANI used. For example, the common granular PANI-based composites showed a conductivity of $\sim 10^{-2}$ S cm^{-1}, irrespective of their silver content in the range of 3–6 wt%; whereas for the PANI nanotube based composites the conductivity depended strongly on the content of silver; the aniline oligomer based composites were completely nonconducting, though the oligomers served as the best reductant and produced the highest content of silver in the composites. The highest conductivity of 943 S cm^{-1} was demonstrated by the PANI–Ag composite with a silver content of 17.3 wt%, which was produced by reducing silver nitrate with a PANI nanotube base in 0.1 M nitric acid.

Electrorheological Fluid

Electrorheological fluids are commonly composed of 0.05–0.5 vol% electrically polarizable particles with sizes of 1–100 μm dispersed in insulating

oils such as mineral or silicone, and various intrinsically conducting polymers have been studied as electrorheological materials to overcome the drawbacks such as device corrosion, water evaporation, narrow operational temperature range, and dispersion instability in applications, of those hydrous electrorheological materials used earlier, such as silica, alumina, and composited celluloses. Among these, PANI and its derivatives in various structures, e.g., PANI nanoparticles, PANI nanofibers, and microencapsued PANI, are the most popular ones of dry-based electrorheological materials.[488,489]

After being dedoped with aqueous ammonia and dried, PANI nanofibers, nanoparticles and microparticles were dispersed, respectively, in silicone oil (dielectric constant of 2.7–2.9, viscosity of 50 mPa s, density of 0.998–1.005 g cm^{-3} at 25°C) with stirring and ultrasonicating to study the effect of morphology on the electric, electrorheological, sedimentation, and temperature properties of the as-produced electrorheological fluids.[490] A significantly improved suspended stability was observed for the suspensions dispersed with nanofibers and nanoparticles as compared to that of PANI microparticles. Under electric fields, the strongest electrorheological effect was demonstrated by the PANI nanofiber suspension. For instance, stress and shear moduli about 2.5–3.0 times as high as those of PANI nanoparticle suspension and 1.3–1.5 times as high as that of the PANI microparticle suspension were observed for the PANI suspension. The shear stress of the PANI nanofiber suspension maintained a more stable level in a wide shear rate region of 0.1–1000 s^{-1} than that of the PANI nanoparticle and microparticle suspensions. More importantly, the PANI nanofiber suspension showed a electrorheological effect as good as the PANI microparticle suspension in a broad operating temperature range of 5–115°C, whereas the PANI nanoparticle suspension showed reduced temperature stability.

Polymer Electrolyte

Dedoped PANI nanofibers with varied loadings were incorporated into poly(vinylidene fluoride-*co*-hexafluoropropylene)-(ethylene carbonate+diethyl carbonate)-$LiClO_4$ (P(VdF-HFP)-(PC+DEC)-$LiClO_4$) GPE to a novel composite GPE.[491] It was found that incorporation of PANI nanofibers to a certain concentration (e.g., no higher than 6 wt%) enhanced significantly the ionic conductivity and interfacial stability of the composite polymer electrolytes. With a further increase in the PANI nanofiber loadings (e.g., 8 and 10 wt%), the ionic conductivity decreased due to the insulating clusters formed by phase separation. The enhanced interfacial stability and improved ionic conductivity with incorporation of PANI nanofibers rendered the composite polymer gel electrolyte membranes as promising candidates for some technological applications like rechargeable batteries.

Others

Some other applications of 1-D nano PANI, like support for the lipase-mediated reaction,[92] a precursor for nanocarbons,[41] a reducing agent for gold nanoparticles with controlled sizes,[492] were also reported but are not elaborated on here.

Concluding Remarks

1D nano-PANI is such an interesting type of material that more and more attention has been focused on it. The advancement in syntheses, morphology controlling, formation mechanisms, novel features, and new application of the nanomaterial in the past 5 years were reviewed in this paper. Several chemical methods have been invented for fabrication of 1D nano-PANI with various novel features and properties, making it a promising candidate for many more new applications. Although the formation mechanisms are still not clear, some plausible ones have been advanced, with a number of key factors that affect the morphological evolution of 1D nano-PANI being identified. The nanomaterials combine both features of intrinsically conductive PANI and that of 1D nanomaterials, rendering them one of the most promising candidates for various novel applications. Applications of the nanomaterials, ranging from different kinds of sensors to display devices, energy storage, surface modifiers, various functional fillers, and so on, are also reviewed and discussed in this paper. It can be estimated that practical applications of 1D nano-PANI in some of the fields will be achieved in the near future.

References

1. Huang, J. X.; Virji, S.; Weiller B. H.; Kaner, R. B. J Am Chem Soc 2003, 125(2), 314–315.
2. Zhang, D. H.; Wang, Y. Y. Mater Sci Eng B 2006, 134(1), 9–19.

3. Nuraje, N.; Su, K.; Yang, N. L.; Matsui, H. ACS Nano 2008, 2(3), 502–506.
4. Su, K.; Nuraje, N.; Zhang, L. Z.; Chu, I. W.; Matsui, H.; Yang, N. L. Macromol Symp 2009, 279, 1–6.
5. Li, X. G.; Li, A.; Huang, M. R. Chem-Eur J 2008, 14(33), 10309-10317.
6. Huang, J. X. Pure Appl Chem 2006, 78(1), 15–27.
7. Aleshin, A. N. Adv Mater 2006, 18(1), 17–27.
8. Aleshin, A. N. Phys Solid State 2007, 49(11), 2015–2033.
9. Li, D.; Huang, J. X.; Kaner, R. B. Acc Chem Res 2009, 42(1), 135–145.
10. Tran, H. D.; Li, D.; Kaner, R. B. Adv Mater 2009, 21(14–15), 1487–1499.
11. Sapurina, I.; Stejskal, J. Polym Int 2008, 57(12), 1295–1325.
12. Wan, M. X. Adv Mater 2008, 20(15), 2926–2932.
13. Cho, C. P.; Perng, T. P. J Nanosci Nanotechnol 2008, 8(1), 69–87.
14. Liu, P.; Zhang, L. Crit Rev Solid State Mater Sci 2009, 34(1–2), 75–87.
15. Wan, M. X. Macromol Rapid Commun 2009, 30(12), 963–975.
16. Jang, J. Adv Polym Sci 2006, 199, 189–259.
17. Huang, J. X.; Kaner, R. B. In Handbook of Conducting Polymers, 3rd ed.: Conjugated Polymers, Theory, Syntheses, Properties, and Characterization; Skotheim, T. A.; Reynolds, J. R. (Eds.); CRC Press, Boca Raton, FL, 2007; Ch. 7, pp. 7–1 to 7–49.
18. Jackowska, K.; Biegunski, A. T.; Tagowska, M. J Solid State Electrochem 2008, 12(4), 437–443.
19. Cheng, F. Y.; Tang, W.; Li, C. S.; Chen, J.; Liu, H. K.; Shen, P. W.; Dou, S. X. Chem-Eur J 2006, 12(11), 3082–3088.
20. Drury, A.; Chaure, S.; Kroell, M.; Nicolosi, V.; Chaure, N.; Blau, W. J. Chem Mater 2007, 19(17), 4252–4258.
21. Xiong, S. X.; Wang, Q.; Chen, Y. H. Mater Lett 2007, 61(14–15), 2965–2968.
22. Qi, L.; Zhou, J. Z.; Weng, S. H.; Cai, C. D.; Yao, G. H.; Lin, Z. H. Chem J Chin Univ 2007, 28(3), 562–564.
23. Cao, Y.; Mallouk, T. E. Chem Mater 2008, 20(16), 5260–5265.
24. Kim, T. H.; Kim, Y.; Lee, S. J.; Han, W. S.; Jung, J. H. Chem Lett 2008, 37(6), 598–599.
25. Zhang, L.; Liu, P. Nanoscale Res Lett 2008, 3(8), 299–302.
26. Gao, Y.; Wang, F. C.; Gong, J.; Su, Z. M.; Qu, L. Y. J Nanosci Nanotechnol 2008, 8(11), 5972–5976.
27. Iwuoha, E. I.; Mavundla, S. E.; Somerset, V. S.; Petrik, L. F.; Klink, M. J.; Sekota, M.; Bakers, P. Microchim Acta 2006, 155(3–4), 453–458.
28. Palys, B.; Celuch, P. Electrochim Acta 2006, 51(20), 4115–4124.
29. Xue, B.; Qi, S. Y.; Gong, J.; Gao, Y.; Yao, S.; Yin, R.; Qu, L. Y. J Nanosci Nanotechnol 2007, 7(12), 4515–4521.
30. Zhou, T.; Chen, J. L.; Chen, D.; Zhang, W.; Guo, J. X.; Gong, J. Chem J Chin Univ 2007, 28(11), 2210–2213.
31. Song, G. P.; Han, J.; Guo, R. Synth Met 2007, 157(4–5), 170–175.
32. Gao, Y.; Yao, S.; Gong, J.; Qu, L. Y. Macromol Rapid Commun 2007, 28(3), 286–291.
33. Gao, Y.; Li, X.; Gong, J.; Fan, B.; Su, Z. M.; Qu, L. Y. J Phys Chem C 2008, 112(22): 8215–8222.
34. Xia, H. B.; Cheng, D. M.; Lam, P. S.; Chan, H. S. O. Nanotechnology 2006, 17(15): 3957–3961.
35. Niu, Z.; Liu, J.; Lee, L. A.; Bruckman, M. A.; Zhao, D.; Koley, G.; Wang, Q. Nano Lett 2007, 7(12), 3729–3733.
36. Li, X.; Shen, J. Y.; Wan, M. X.; Chen, Z. J.; Wei, Y. Synth Met 2007, 157(13–15), 575–579.
37. do Nascimento, G. M.; Silva, C. H. B.; Temperini, M. L. A. Macromol Rapid Commun 2006, 27(4), 255–259.
38. Huang, K.; Meng, X. H.; Wan, M. X. J Appl Polym Sci 2006, 100(4), 3050–3054.
39. Yang, C. H.; Chih, Y. K.; Tsai, M. S.; Chen, C. H. Electrochem Solid State Lett 2006, 9(2), G49–G52.
40. Huang, K.; Zhang, Y. J.; Long, Y. Z.; Yuan, J. H.; Han, D. X.; Wang, Z. J.; Niu, L.; Chen, Z. Chem-Eur J 2006, 12(20), 5314–5319.
41. Kyotani, M.; Goto, H.; Suda, K.; Nagai, T.; Matsui, Y.; Akagi, K. J Nanosci Nanotechnol 2008, 8(4), 1999–2004.
42. Ayad, M.; Prastomo, N.; Matsuda, A. Mater Lett 2010, 64(3), 379–382.
43. Hsieh, B. Z.; Chuang, H. Y.; Chao, L.; Li, Y. J.; Huang, Y. J.; Tseng, P. H.; Hsieh, T. H.; Ho, K. S. Polymer 2008, 49(19), 4218–4225.
44. Ding, X. F.; Han, D. X.; Wang, Z. J.; Xu, X. Y.; Niu, L.; Zhang, Q. J Colloid Interf Sci 2008, 320(1), 341–345.
45. do Nascimento, G. M.; Silva, C. H. B.; Izumi, C. M. S.; Temperini, M. L. A. Spectrochim Acta A 2008, 71(3), 869–875.
46. Zhang, L. X.; Zhang, L. J.; Wan, M. X. Eur Polym J 2008, 44(7), 2040–2045.
47. Zhang, L. J.; Peng, H.; Zujovic, Z. D.; Kilmartin, P. A.; Travas-Sejdic, J. Macromol Chem Phys 2007, 208(11), 1210–1217.
48. Zhang, Z. M.; Wang, L. Q.; Deng, J. Y.; Wan, M. X. React Funct Polym 2008, 68(6), 1081–1087.
49. Janosevic, A.; Ciric-Marjanovic, G.; Marjanovic, B.; Trchová, M.; Stejskal, J. Mater Lett 2010, 64(21), 2337–2340.
50. Shinde, S. D., Jayakannan, M. J Phys Chem C 2010, 114(36), 15491–15498.
51. Ciric-Marjanovic, G.; Holclajtner-Antunovic, I.; Mentus, S.; Bajuk-Bogdanovic, D.; Jesic, D.; Manojlovic, D.; Trifunovic, S.; Stejskal, J. Synth Met 2010, 160(13–14), 1463–1473.
52. Ren, L.; Zhang, X. F. Synth Met 2010, 160(7–8), 783–787.
53. Qiu, H.; Qi, S. H.; Wang, J.; Wang, D. H.; Wu, X. M. Mater Lett 2010, 64(18), 1964–1967.
54. Qiu, H.; Qi, S. H.; Wang, D. H.; Wang, J.; Wu, X. M. Synth Met 2010, 160(11–12), 1179–1183.
55. Yu,Y. J.; Si, Z. H.; Chen, S. J.; Bian, C. Q.; Chen, W.; Xue, G. Langmuir 2006, 22(8), 3899–3905.
56. Zhao, W. J.; Ma, L.; Lu, K. J Polym Res 2007, 14(1), 1–4.
57. Li, X. W.; Zhao, Y. P.; Zhuang, T.; Wang, G. C.; Gu, Q. Colloid Surf A 2007, 295(1–3), 146–151.
58. Li, X. W.; Zhuang, T.; Wang, G. C.; Zhao, Y. P. Mater Lett 2008, 62(8–9), 1431–1434.
59. Li, Y. M.; Zhang, C. Q.; Li, G. C.; Peng, H. R.; Chen, K. Z. Synth Met 2010, 160(11–12), 1204–1209.
60. Li, G. C.; Wang, Z. B.; Xie, G. W.; Peng, H. R.; Zhang, Z. K. J Dispersion Sci Technol 2006, 27(7), 991–995.
61. Kumar, S.; Singh, V.; Aggarwal, S.; Mandal, U. K. Soft Mater 2009, 7(3), 150–163.

62. Kumar, S.; Singh, V.; Aggarwal, S.; Mandal, U. K. Colloid Polym Sci 2009, 287(9), 1107–1110.
63. Jeevananda, T.; Lee, J. H.; Siddaramaiah. Mater Lett 2008, 62(24), 3995–3998.
64. Han, Y. G., Kusunose, T.; Sekino, T. J Polym Sci, Polym Phys 2009, 47(10), 1024–1029.
65. Mallick, K.; Witcomb, M.; Erasmus, R.; Strydom, A. J Appl Polym Sci 2010, 116(3), 1587–1592.
66. Arenas, M. C.; Andablo, E.; Castano, V. M.; J Nanosci Nanotechnol 2010, 10(1), 549–554.
67. Miao, Z. J.; Wang, Y.; Liu, Z. M.; Huang, J.; Han, B. X.; Sun, Z. Y.; Du, J. M. J Nanosci Nanotechnol 2006, 6(1), 227–230.
68. Pahovnik, D.; Zagar, E.; Vohlidal, J.; Zigon, M. Synth Met 2010, 160(15–16), 1761–1766.
69. Park, J. K.; Jeon, S. S.; Im, S. S. Polymer 2010, 51(14), 3023–3030.
70. Yang, T.; Wei, G.; Niu, L.; Li, Z. Chem J Chin Univ 2006, 27(6), 1126–1130.
71. Datta, B.; Schuster, G. B. J Am Chem Soc 2008, 130(10), 2965–2973.
72. Houlton, A.; Pike, A. R.; Galindo, M. A.; Horrocks, B. R. Chem Commun 2009, (14), 1797–1806.
73. Li, X.; Wan, M. X.; Li, X. N.; Zhao, G. L. Polymer 2009, 50(19), 4529–4534.
74. Liu, S. W.; Zhu, K. Z.; Zhang, Y.; Xu, J. R. Polymer 2006, 47(22), 7680–7683.
75. Liu, F. J.; Huang, L. M.; Wen, T. C.; Gopalan, A.; Hung, J. S. Mater Lett 2007, 61(22), 4400–4405.
76. He, Y. J. Appl Surf Sci 2006, 252(6), 2115–2118.
77. Goel, S.; Gupta, A.; Singh, K. P.; Mehrotra, R.; Kandpal, H. C. Mater Sci Eng A 2007, 443(1–2), 71–76.
78. Li, W.; Zhang, Q. H.; Chen, D. J.; Li, L. J Macromol Sci A 2006, 43(11), 1815–1824.
79. Su, C.; Wang, G. C.; Huang, F. R.; Li, X. W. J Mater Sci 2008, 43(1): 197–202.
80. Ding, S. H.; Mao, H.; Zhang, W. J. J Appl Polym Sci 2008, 109(5), 2842–2847.
81. Xing, S. X.; Zheng, H. W.; Zhao, G. K. Synth Met 2008, 158(1–2), 59–63.
82. Xing, S. X.; Zhao, G. K.; Yuan, Y. Polym Compos 2008, 29(1), 22–26.
83. Sun, Q. H.; Deng, Y. L. Mater Lett 2008, 62(12–13), 1831–1834.
84. Li, J. B.; Jia, Q. M.; Zhu, J. W.; Zheng, M. S. Polym Int 2008, 57(2), 337–341.
85. Dallas, P.; Stamopoulos, D.; Boukos, N.; Tzitzios, V.; Niarchos, D.; Petridis, D. Polymer 2007, 48(11), 3162–3169.
86. Su, B. T.; Tong, Y. C.; Bai, J.; Lei, Z. Q.; Wang, K.; Mu, H. M.; Dong, N. Indian J Chem A 2007, 46(4), 595–599.
87. do Nascimento, G. M.; Kobata, P. Y. G.; Temperini, M. L. A. J Phys Chem B 2008, 112(37), 11551–11557.
88. Mu, S. L. Synth Met 2010, 160(17–18), 1931–1937.
89. Wang, X. Z.; Wang, X. F.; Wu, Y. T.; Bao, L.; Wang, H. Mater Lett 2010, 64(17), 1865–1867.
90. Zhou, C. Q.; Han, J.; Song, G. P.; Guo, R. Macromolecules 2007, 40(20), 7075–7078.
91. Qiang, J. F.; Yu, Z. H.; Wu, H. C.; Yun, D. Q. Synth Met 2008, 158(13), 544–547.
92. Lee, G.; Joo, H.; Lee, J. J Mol Catal B, Enzym 2008, 54(3–4), 116–121.
93. Hu, Z. C.; Xu, J. J.; Tian, Y. A.; Peng, R.; Xian, Y. Z.; Ran, Q.; Jin, L. T. Carbon 2010, 48(13), 3729–3736.
94. Huang, Y. F.; Lin, C. W. Synth Met 2010, 160(5–6), 384–389.
95. Lu, X. F.; Mao, H.; Chao, D. M.; Zhang, W. J.; Wei, Y. J Solid State Chem 2006, 179(8), 2609–2615.
96. Lu, X. F.; Mao, H.; Chao, D. M.; Zhang, W. J.; Wei, Y. Macromol Chem Phys 2006, 207(22), 2142–2152.
97. Wang, J.; Bunimovich, Y. L.; Sui, G. D.; Savvas, S.; Wang, J. Y.; Guo, Y. Y.; Heath, J. R.; Tseng, H. R. Chem Commun 2006, (29), 3075–3077.
98. Wei, D.; Kvarnstrom, C.; Lindfors, T.; Ivaska, A. Electrochem Commun 2006, 8(10), 1563–1566.
99. Wen, J. B., Zhou, H. H.; Luo, S. L.; Pang, X. Y.; Chen, J. H.; Kuang, Y. F. Chem J Chin Univ 2006, 27(5), 948–950.
100. Ghanbari, K.; Mousavi, M. F.; Shamsipur, M. Electrochim Acta 2006, 52(4), 1514–1522.
101. Choi, J.; Kim, S.J.; Lee, J.; Lim, J.H.; Lee, S.C.; Kim, K.J. Electrochem Commun 2007, 9, 971–975.
102. Zhou, S.; Wu, T.; Kan, J.Q. Eur Polym J 2007, 43, 395–402.
103. Zhu, N. N.; Chang, Z.; He, P. G.; Fang, Y. Z. Electrochim Acta 2006, 51, 3758–3762.
104. Guo, Y. P.; Zhou, Y. Eur Polym J 2007, 43, 2292–2297.
105. Fernandes, E. G. R.; Soares, D. A. W.; De Queiroz, A. A. A. J Mater Sci: Mater Electron 2008, 19, 457–462.
106. Cho, S. I.; Lee, S. B. Acc Chem Res 2008, 41, 699–707.
107. Zhang, H. B.; Li, H. L.; Zhang, F. B.; Wang, J. X.; Wang, Z.; Wang, S. C. J Mater Res 2008, 23, 2326–2332.
108. Roy, S.; Kargupta, K.; Chakraborty, S.; Ganguly, S. Mater Lett 2008, 62, 2535–2538.
109. Mu, S. L.; Yang, Y. F. J Phys Chem B 2008, 112, 11558–11563.
110. Anderson, R. E.; Ostrowski, A. D.; Gran, D. E.; Fowler, J. D.; Hopkins, A. R.; Villahermosa, R. M. Polym Bull 2008, 61, 563–568.
111. Lee, I.; Park, H. I.; Park, S.; Kim, M. J.; Yun, M. Nano 2008, 3, 75–82.
112. Xavier, M. G.; Venancio, E. C.; Pereira, E. C.; Leite, F. L.; Edson, R.; MacDiarmid, A. G.; Mattoso, L. H. C. J Nanosci Nanotechnol 2009, 9, 2169–2172.
113. Zhang, L.; Zhang, J.; Zhang, C. H. Biosens Bioelectron 2009, 24, 2085–2090.
114. Yu, X. F.; Li, Y. X.; Kalantar-Zadeh, K. Sens Actuator, B 2009, 136, 1–7.
115. Berti, F.; Todros, S.; Lakshmi, D.; Whitcombe, M. J.; Chianella, I.; Ferroni, M.; Piletsky, S. A.; Turner, A. P. F.; Marrazza, G. Biosens Bioelectron 2010, 26, 497–503.
116. Jiang, H. F.; Liu, X. X. Electrochim Acta 2010, 55, 7175–7181.
117. Ndangili, P. M.; Waryo, T. T.; Muchindu, M.; Baker, P. G. L.; Ngila, C. J.; Iwuoha, E. I. Electrochim Acta 2010, 55, 4267–4273.
118. Zhang, L. J.; Zujovic, Z. A.; Peng, H.; Bowmaker, G. A.; Kilmartin, P. A.; Travas-Sejdic, J. Macromolecules 2008, 41, 8877–8884.
119. Ciri-Marjanovic, G.; Trchova, M.; Stejskal, J. J Raman Spectrosc 2008, 39, 1375–1387.

120. Stejskal, J.; Sapurina, I.; Trchova, M.; Konyushenko, E. N. Macromolecules 2008, 41, 3530–3536.
121. Laslau, C.; Zujovic, Z. D.; Zhang, L. J.; Bowmaker, G. A.; Travas-Sejdic, J. Chem Mater 2009, 21, 954–962.
122. Meng, L. H.; Lu, Y.; Wang, X. D.; Zhang, J.; Duan, Y. Q.; Li, C. X. Macromolecules 2007, 40, 2981–2983.
123. Yan, X.; Liu, N.; Jin, E.; Zhang, W. J. Chem J Chin Univ 2007, 28, 391–393.
124. Zhou, C. Q.; Han, J.; Song, G. P.; Guo, R. Eur Polym J 2008, 44, 2850–2858.
125. Sreedhar, B.; Radhika, P.; Neelima, B.; Hebalkar, N.; Rao, M. V. B.; Polym Adv Technol 2009, 20, 950–958.
126. Zhang, Y.; Mu, S. L.; Zhai, J. P. Synth Met 2009, 159, 1844–1851.
127. Sun, Q. H.; Deng, Y. L. Eur Polym J 2008, 44, 3402–3408.
128. Xu, P.; Han, X. J.; Wang, C.; Zhang, B.; Wang, X. H.; Wang, H. L. Macromol Rapid Commun 2008, 29, 1392–1397.
129. Bian, C. Q.; Yu, Y. J.; Xue, G. J Appl Polym Sci 2007, 104, 21–26.
130. Tong, Y. C.; Hu, C. L.; Wang, Q. Y.; Bai, J.; Lei, Z. Q.; Su, B. T. Chem J Chin Univ 2008, 29, 415–418.
131. Phang, S. W.; Tadokoro, M.; Watanabe, J.; Kuramoto, N. Curr Appl Phys 2008, 8, 391–394.
132. Bian, C. Q.; Yu, A. H.; Wu, H. Q. Electrochem Commun 2009, 11, 266–269.
133. Ciric-Marjanovic, G.; Dragicevic, L.; Milojevic, M.; Mojovic, M.; Mentus, S.; Dojcinovic, B.; Marjanovic, B.; Stejskal, J. J Phys Chem B 2009, 113, 7116–7127.
134. Radoicic, M.; Saponjic, Z.; Nedeljkovic, J.; Ciric-Marjanovic, G.; Stejskal, J. Synth Met 2010, 160, 1325–1334.
135. Reddy, K. R.; Sin, B. C.; Ryu, K. S.; Noh, J.; Lee, Y. Synth Met 2009, 159, 1934–1939.
136. Borriello, A.; Agoretti, P.; Cassinese, A.; Angelo, P. D.; Mohanraj, G. T.; Sanguigno, L. J Nanosci Nanotechnol 2009, 9, 6307–6314.
137. Malta, M.; Silva, L. H.; Galembeck, A.; Korn, M. Macromol Rapid Commun 2008, 29, 1221–1225.
138. Mo, Z. L.; Zhang, P.; Zuo, D. D.; Sun, Y. L.; Chen, H. Mater Res Bull 2008, 43, 1664–1669.
139. Li, X.; Gao, Y.; Gong, J.; Zhang, L.; Qu, L. Y. J Phys Chem C 2009, 113, 69–73.
140. Zhou, Z.; He, D. L.; Guo, Y. N.; Cui, Z. D.; Wang, M. H.; Li, G. X.; Yang, R. H. Thin Solid Films 2009, 517, 6767–6771.
141. Gao, Y.; Shan, D. C.; Cao, F.; Gong, J.; Li, X.; Ma, H. Y.; Su, Z. M.; Qu, L. Y. J Phys Chem C 2009, 113, 15175–15181.
142. Mallick, K.; Witcomb, M.; Scurrell, M.; Strydom, A. J Phys D: Appl Phys 2009, 42, 095409.
143. Xia, H. B.; Chung, H. J.; Sow, C. H.; Chan, S. H. O. J Nanosci Nanotechnol 2010, 10, 2409–2415.
144. Huang, L. M.; Liao, W. H.; Ling, H. C.; Wen, T. C. Mater Chem Phys 2009, 116, 474–478.
145. Ciric-Marjanovic, G.; Dondur, V.; Milojevic, M.; Mojovic, M.; Mentus, S.; Radulovic, A.; Vukovic, Z.; Stejskal, J. Langmuir 2009, 25, 3122–3131.
146. Binitha, N. N.; Sugunan, S. J Appl Polym Sci 2008, 107, 3367–3372.
147. Mo, Z. L.; Shi, H. F.; Chen, H.; Niu, G. P.; Zhao, Z. L.; Wu, Y. B. J Appl Polym Sci 2009, 112, 573–578.
148. Zhang, K.; Zhang, L. L.; Zhao, X. S.; Wu, J. S. Chem Mater 2010, 22, 1392–1401.
149. Maser, W. K.; Jimenez, P.; Payne, N. O.; Shepherd, R. L.; Castell, P.; Panhuis, M. I. H.; Benito, A. M. J Nanosci Nanotechnol 2009, 9, 6157–6163.
150. Jimenez, P.; Maser, W. K.; Castell, P.; Martinez, M. T.; Benito, A. M. Macromol Rapid Commun 2009, 30, 418–422.
151. Cabezas, A. L.; Zhang, Z. B.; Zheng, L. R.; Zhang, S. L. Synth. Met. 2010, 160, 664–668.
152. Kumar, S.; Singh, V.; Aggarwal, S.; Mandal, U. K.; Kotnala, R. K. Compos Sci Technol 2010, 70, 249–254.
153. Zhang, L. J.; Wan, M. X.; Wei, Y. Macromol Rapid Commun 2006, 27, 366–371.
154. Ding, H. J.; Liu, X. M.; Wan, M. X.; Fu, S. Y. J Phys Chem B 2008, 112, 9289–9294.
155. Ding, H. J.; Zhu, C. J.; Zhou, Z. M.; Wan, M. X. Acta Polym Sin 2007, 462–466.
156. Zhang, Z. M.; Deng, J. Y.; Shen, J. Y.; Wan, M. X.; Chen, Z. J. Macromol Rapid Commun 2007, 28, 585–590.
157. Zhang, Z. M.; Deng, J. Y.; Wan, M. X. Mater Chem Phys 2009, 115, 275–279.
158. Li, G. C.; Jiang, L.; Peng, H. R. Macromolecules 2007, 40, 7890–7894.
159. Han, J.; Song, G. P.; Guo, R. Eur Polym J 2007, 43, 4229–4235.
160. Wang, Z.; Yuan, J.; Han, D.; Zhang, Y.; Shen, Y.; Kuehner, D.; Niu, L.; Ivaska, A. Cryst Growth Des 2008, 8, 1827–1832.
161. Zhang, X. T.; Chechik, V.; Smith, D. K.; Walton, P. H.; Duhme-Klair, A. K. Macromolecules 2008, 41, 3417–3421.
162. Blinova, N. V.; Stejskal, J.; Trchova, M.; Sapurina, I.; Ciric-Marjanovic, G. Polymer 2009, 50, 50–56.
163. Li, X. X.; Li, X. W. Mater Lett 2007, 61, 2011–2014.
164. Pan, L. J.; Pu, L.; Shi, Y.; Song, S. Y.; Xu, Z.; Zhang, R.; Zheng, Y. D. Adv Mater 2007, 19, 461–464.
165. Wang, Y. Y.; Jing, X. L.; Kong, J. H. Synth Met 2007, 157, 269–275.
166. Surwade, S. P.; Agnihotra, S. R.; Dua, V.; Manohar, N.; Jain, S.; Ammu, S.; Manohar, S. K. J Am Chem Soc 2009, 131, 12528–12529.
167. Chiou, N. R.; Lee, L. J.; Epstein, A. J. Chem Mater 2007, 19, 3589–3591.
168. Ding, H. J.; Long, Y. Z.; Shen, J. Y.; Wan, M. X. J Phys Chem B 2010, 114, 115–119.
169. Bai, X. L.; Li, X. T.; Li, N.; Zuo, Y.; Wang, L. F.; Li, J. X.; Qiu, S. L. Mater Sci Eng C 2007, 27, 695–699.
170. Mavundla, S. E.; Malgas, G. F.; Baker, P.; Iwuoha, E. I. Electroanalysis 2008, 20, 2347–2353.
171. Mi, H. Y.; Zhang, X. G.; Yang, S. D.; Ye, X. G.; Luo, J. M. Mater Chem Phys 2008, 112, 127–131.
172. Jia, Q. M.; Shan, S. Y.; Jiang, L. H.; Wang, Y. M. J Appl Polym Sci 2010, 115, 26–31.
173. Rahy, A.; Yang, D. J. Mater Lett 2008, 62, 4311–4314.
174. Rahy, A.; Sakrout, M.; Manohar, S.; Cho, S. J.; Ferraris, J.; Yang, D. J. Chem Mater 2008, 20, 4808–4814.
175. Zhou, C. F.; Du, X. S.; Liu, Z.; Ringer, S. P.; Mai, Y. W. Synth Met 2009, 159, 1302–1307.
176. Du, X. S.; Zhou, C. F.; Wang, G. T.; Mai, Y. W. Chem Mater 2008, 20, 3806–3808.

177. Bhadra, S.; Kim, N. H.; Rhee, K. Y.; Lee, J. H. Polym Int 2009, 58, 1173–1180.
178. Zhang, X. Y.; Goux, W. J.; Manohar, S. K. J Am Chem Soc 2004, 126, 4502–4503.
179. Teoh, G. L.; Liew, K. Y.; Mahmood, W. A. K. Mater Lett 2007, 61, 4947–4949.
180. Xing, S. X.; Zhao, C.; Jing, S. Y.; Wang, Z. C. Polymer 2006, 47, 2305–2313.
181. Xing, S. X.; Zheng, H. W. e-Polymers 2008, 106.
182. Thanpitcha, T.; Sirivat, A.; Jamieson, A.M.; Rujiravanit, R. Synth Met 2008, 158, 695–703.
183. Wang, D. H.; Ma, F. H.; Qi, S. H.; Song, B. Y. Synth Met 2010, 160, 2077–2084.
184. Pillalamarri, S. K.; Blum, F. D.; Tokuhiro, A. T.; Story, J. G.; Bertino, M. F. Chem Mater 2005, 17, 227–229.
185. Li, Z. F.; Blum, F. D.; Bertino, M. F.; Kim, C. S.; Pillalamarri, S. K. Sens Actuator, B 2008, 134, 31–35.
186. Liu, S.; Wang, J. Q.; Ou, J. F.; Zhou, J. F.; Chen, Y. F.; Yang, S. R. J Nanosci Nanotechnol 2010, 10, 933–940.
187. Li, J.; Tang, H. Q.; Zhang, A. Q. Macromol Rapid Commun 2007, 28, 740–745.
188. Gizdavic-Nikolaidis, M. R.; Stanisavljev, D. R.; Easteal, A. J.; Zujovic, Z. D. J Phys Chem C 2010, 114, 18790–18796.
189. Gizdavic-Nikolaidis, M. R.; Stanisavljev, D. R.; Easteal, A. J.; Zujovic, Z. D. Macromol Rapid Commun 2010, 31, 657–661.
190. Tiwari, A.; Kumar, R.; Prabaharan, M.; Pandey, R. R.; Kumari, P.; Chaturvedi, A.; Mishra, A. K. Polym Adv Technol 2010, 21, 615–620.
191. Chiou, N. R.; Lee, L. J.; Epstein, A. J. J Mater Chem 2008, 18, 2085–2089.
192. Bhadra, S.; Lee, J. H. J Appl Polym Sci 2009, 114, 331–340.
193. Nadagouda, M. N.; Varma, R. S. Green Chem 2007, 9, 632–637.
194. King, R. C. Y.; Roussel, F. Synth Met 2009, 159, 2512–2518.
195. Zhang, S. L.; Kan, S. Q.; Kan, J. Q. J Appl Polym Sci 2006, 100, 946–953.
196. Manigandan, S.; Jain, A.; Majumder, S.; Ganguly, S.; Kargupta, K.; Sens Actuator, B 2008, 133, 187–194.
197. Manigandan, S.; Majumder, S.; Ganguly, S.; Kargupta, K. Mater Lett 2008, 62, 2758–2761.
198. Zhang, H. M.; Wang, X. H.; Li, J.; Wang, F. S. Synth Met 2009, 159, 1508–1511.
199. Chiou, N. R.; Epstein, A. J. Adv Mater 2005, 73, 1679–1683.
200. Lu, Q. F.; Cheng, X. S. e-Polymers 2009, 084 .
201. Ding, Z. F.; Yanag, D. L.; Currier, R. P.; Obrey, S. J.; Zhao, Y. S. Macromol Chem Phys 2010, 211, 627–634.
202. Adetunji, O. O.; Chiou, N. R.; Epstein, A. J. Synth Met 2009, 159, 2263–2265.
203. Majumdar, D.; Maiti, R. P.; Basu, S.; Saha, S. K. J Nanosci Nanotechnol 2009, 9, 6896–6901.
204. He, Y. J.; Lu, J. H. React Funct Polym 2007, 67, 476–480.
205. Wang, J. X.; Wang, J. S.; Zhang, X. Y.; Wang, Z. Macromol Rapid Commun 2007, 28, 84–87.
206. Pham, Q. M.; Kim, J. S.; Kim, S. Synth Met 2010, 160, 394–399.
207. Ding, H. J.; Wan, M. X.; Wei, Y. Adv Mater 2007, 19, 465–469.
208. Wang, J. S.; Wang, J. X.; Yang, Z.; Wang, Z.; Zhang, F. B.; Wang, S. C. React Funct Polym 2008, 68, 1435–1440.
209. Li, Y.; Jing, X. L. React Funct Polym 2009, 69, 797–807.
210. Ding, Z. F.; Currier, R. P.; Zhao, Y. S.; Yang, D. L. Macromol Chem Phys 2009, 210, 1600–1606.
211. Li, G. C.; Zhang, C. Q.; Li, Y. M.; Peng, H. R.; Chen, K. Z. Polymer 2010, 51, 1934–1939.
212. Anilkumar, P.; Jayakannan, M. Langmuir 2006, 22, 5952–5957.
213. Anilkumar, P.; Jayakannan, M. J Phys Chem C 2007, 111, 3591–3600.
214. Anilkumar, P.; Jayakannan, M. Macromolecules 2007, 40, 7311–7319.
215. Anilkumar, P.; Jayakannan, M. Macromolecules 2008, 41, 7706–7715.
216. Antony, M. J.; Jayakannan, M. J Polym Sci, Part B: Polym Phys 2009, 47, 830–846.
217. Anilkumar, P.; Jayakannan, M. J Appl Polym Sci 2009, 114, 3531–3541.
218. Antony, M. J.; Jayakannan, M. J Phys Chem B 2010, 114, 1314–1324.
219. Anilkumar, P.; Jayakannan, M. J Phys Chem B 2009, 113, 11614–11624.
220. Anilkumar, P.; Jayakannan, M. J Phys Chem B 2010, 114, 728–736.
221. Wang, X. C.; Liu, J.; Huang, X. G.; Men, L. H.; Guo, M. J.; Sun, D. L. Polym Bull 2008, 60, 1–6.
222. Amarnath, C. A.; Kim, J.; Kim, K.; Choi, J.; Sohn, D. Polymer 2008, 49, 432–437.
223. Zhang, Z. M.; Wan, M. X.; Wei, Y. Adv Funct Mater 2006, 16, 1100–1104.
224. Zhang, L. X.; Zhang, L. J.; Wan, M. X.; Wei, Y. Synth Met 2006, 156, 454–458.
225. Zhong, W. B.; Chen, X. H.; Liu, S. M.; Wang, Y. X.; Yang, W. T. Macromol Rapid Commun 2006, 27, 563–569.
226. Zhong, W. B.; Wang, Y. X.; Yan, Y.; Sun, Y. F.; Deng, J. P.; Yang, W. T. J Phys Chem B 2007, 111, 3918–3926.
227. Janosevic, A.; Ciric-Marjanovic, G.; Marjanovic, B.; Holler, P.; Trchova, M.; Stejskal, J. Nanotechnology 2008, 19, 135606.
228. Garai, A.; Nandi, A. K. Synth Met 2009, 159, 757–760.
229. Jing, X. L.; Wang, Y. Y.; Wu, D.; She, L.; Guo, Y. J Polym Sci, Part A: Polym Chem 2006, 44, 1014–1019.
230. Jing, X. L.; Wang, Y. Y.; Wu, D.; Qiang, J. P. Ultrason Sonochem 2007, 14, 75–80.
231. Li, Y.; Wang, Y. Y.; Wu, D.; Jing, X. L. J Appl Polym Sci 2009, 13, 868–875.
232. Li, W.; Zhu, M. F.; Zhang, Q. H.; Chen, D. J. Appl Phys Lett 2006, 89, 103110.
233. Sun, Q. H.; Park, M. C.; Deng, Y. L. Mater Chem Phys 2008, 110, 276–279.
234. Ding, H. J.; Shen, J. Y.; Wan, M. X.; Chen, Z. J. Macromol Chem Phys 2008, 209, 864–871.
235. Song, S. Y.; Pan, L. J.; Li, Y.; Shi, Y.; Pu, L.; Zhang, R.; Zheng, Y. D. Chin J Chem Phys 2008, 21, 187–192.
236. Laslau, C.; Zujovic, Z. D.; Travas-Sejdic, J. Macromol Rapid Commun 2009, 30, 1663–1668.
237. Schulz, B.; Dietzel, B.; Orgzall, I.; Díez, I.; Xu, C. G. High Perform Polym 2009, 21, 633–652.

238. Ho, K. S.; Han, Y. K.; Tuan, Y. T.; Huang, Y. J.; Wang, Y. Z.; Ho, T. H.; Hsieh, T. H.; Lin, J. J.; Lin, S. C. Synth Met 2009, 159, 1202–1209.
239. Kemp, N. T.; Cochrane, J. W.; Newbury, R. Synth Met 2009, 159, 435–444.
240. Huang, J. X.; Kaner, R. B. Angew Chem, Int Ed 2004, 43, 5817–5821.
241. Li, D.; Kaner, R. B. J Am Chem Soc 2006, 128, 968–975.
242. Huang, J. X.; Kaner, R. B. Chem Commun 2006, 367–376.
243. Li, D.; Kaner, R. B. J Mater Chem 2007, 17, 2279–2282.
244. Chiou, N. R.; Epstein, A. J. Synth Met 2005, 153, 69–72.
245. Zhang, X. Y.; Kolla, H. S.; Wang, X. H.; Raja, K.; Manohar, S. K. Adv Funct Mater 2006, 16, 1145–1152.
246. Laslau, C.; Zujovic, Z. D.; Travas-Sejdic, J. Prog Polym Sci 2010, 35, 1403–1419.
247. Zujovic, Z. D.; Laslau, C.; Bowmaker, G. A.; Kilmartin, P. A.; Webber, A. L.; Brown, S. P.; Travas-Sejdic, J. Macromolecules 2010, 43, 662–670.
248. Stejskal, J.; Sapurina, I.; Trchova, M. Prog Polym Sci 2010, 35, 1420–1481.
249. Wang, Y. Y.; Jing, X. L. J Phys Chem B 2008, 112, 1157–1162.
250. Huang, Y. F.; Lin, C. W. Synth Met 2009, 159, 1824–1830.
251. Huang, Y. F.; Lin, C. W. Polym Int 2010, 59, 1226–1232.
252. Wang, P. C.; Venancio, E. C.; Sarno, D. M.; MacDiarmid, A. G. React Funct Polym 2009, 69, 217–223.
253. Zhang, H. B.; Wang, J. X.; Wang, Z.; Zhang, F. B.; Wang, S. C. Synth Met 2009, 159, 277–281.
254. Li, J.; Zhu, L. H.; Luo, W.; Liu, Y.; Tang, H. Q. J Phys Chem C 2007, 111, 8383–8388.
255. Stejskal, J.; Spirkova, M.; Ridde, A.; Helmstedt, M.; Mokreva, P.; Prokes, J. Polymer 1999, 40, 2487–2492.
256. Tran, H. D.; Kaner, R. B. Chem Commun 2006, 3915–3917.
257. Tran, H. D.; Wang, Y.; D'Arcy, J. M.; Kaner, R. B. ACS Nano 2008, 2, 1841–1848.
258. Surwade, S. P.; Manohar, N.; Manohar, S. K. Macromolecules 2009, 42, 1792–1795.
259. Tran, H. D.; Norris, I.; D'Arcy, J. M.; Tsang, H.; Wang, Y.; Mattes, B. R.; Kaner, R. B. Macromolecules 2008, 41, 7405–7410.
260. Wang, Y.; Tran, H. D.; Kaner, R. B. J Phys Chem C 2009, 113, 10346–10349.
261. Konyushenko, E. N.; Stejskal, J.; Sedenkova, I.; Trchova, M.; Sapurina, I.; Cieslar, M.; Prokes, J. Polym Int 2006, 55, 31–39.
262. Trchova, M.; Sedenkova, I.; Konyushenko, E. N.; Stejskal, J.; Holler, P.; Ciric-Marjanovic, G. J Phys Chem B 2006, 110, 9461–9468.
263. Stejskal, J.; Sapurina, I.; Trchova, M.; Konyushenko, E. N.; Holler, P.; Polymer 2006, 47, 8253–8262.
264. Wu, C. G.; Chiang, C. H.; Jeng, U. S. J Phys Chem B 2008, 112, 6772–6778.
265. Zhu, Y.; Li, J. M.; Wan, M. X.; Jiang, L. Polymer 2008, 49, 3419–3423.
266. Zhu, Y.; Li, J. M.; Wan, M. X.; Jiang, L. Macromol Rapid Commun 2008, 29, 239–243.
267. Zhang, Z. M.; Deng, J. Y.; Yu, L. M.; Wan, M. X. Synth Met 2008, 158, 712–716.
268. Petrov, P.; Mokreva, P.; Tsvetanov, C. B.; Terlemezyan, L. Colloid Polym Sci 2008, 286, 691–697.
269. Xing, S. X.; Jing, S. Y.; Zhao, C.; Wang, Z. C. e-Polymers 2007, 044.
270. Liu, B. Y.; Liu, L.; Shi, N. L.; Gong, J.; Sun, C. J Mater Sci Technol 2010, 26, 39–44.
271. Sapurina, I. Y.; Stejskal, J. Russ Chem Rev 2010, 79, 1123–1143.
272. Huang, Y. F.; Lin, C. W. Polymer 2009, 50, 775–782.
273. Konyushenko, E. N.; Trchova, M.; Stejskal, J.; Sapurina, I. Chem Pap 2010, 64, 56–64.
274. Zimbovskaya, N. A. J Chem Phys 2007, 126, 184901.
275. Tseng, R. J.; Baker, C. O.; Shedd, B.; Huang, J. X.; Kaner, R. B.; Ouyang, J. Y.; Yang, Y. Appl Phys Lett 2007, 90, 053101.
276. Zimbovskaya, N. A. J Chem Phys 2008, 129, 114705.
277. Hopkins, A. R.; Lipeles, R. A.; Hwang, S. J. Synth Met 2008, 158, 594–601.
278. Zujovic, Z. D.; Bowmaker, G. A.; Tran, H. D.; Kaner, R. B. Synth Met 2009, 159, 710–714.
279. Lahiff, E.; Woods, T.; Blau, W.; Wallace, G. G.; Diamond, D. Synth Met 2009, 159, 741–748.
280. Yin, Z. H.; Long, Y. Z.; Gu, C. Z.; Wan, M. X.; Duvail, J. L. Nanoscale Res Lett 2009, 4, 63–69.
281. Jain, M.; Annapoorni, S. Synth Met 2010, 160, 1727–1732.
282. Weng, S. H.; Zhou, J. Z.; Lin, Z. H. Synth Met 2010, 160, 1136–1142.
283. Laslau, C.; Henderson, W.; Zujovic, Z. D.; Travas-Sejdic, J. Synth Met 2010, 160, 1173–1178.
284. Lee, S. Y.; Lim, H.; Choi, G. R.; Kim, J. D.; Suh, E. K.; Lee, S. K. J Phys Chem C 2010, 114, 11936–11939.
285. Majumdar, D.; Saha, S. K. Appl Phys Lett 2010, 96, 183113.
286. Bozdag, K. D.; Chiou, N. R.; Prigodin, V. N.; Epstein, A. J. Synth Met 2010, 160, 271–274.
287. Li, G. C.; Pang, S. P.; Xie, G. W.; Wang, Z. B.; Peng, H. R.; Zhang, Z. K. Polymer 2006, 47, 1456–1459.
288. Long, Y. Z.; Chen, Z. J.; Shen, J. Y.; Zhang, Z. M.; Zhang, L. J.; Huang, K.; Wan, M. X.; Jin, A. Z.; Gu, C. Z.; Duvail, J. L. Nanotechnology 2006, 17, 5903–5911.
289. Nandan, B.; Hsu, J. Y.; Chiba, A.; Chen, H. L.; Liao, C. S.; Chen, S. A.; Hasegawa, H. Macromolecules 2007, 40, 395–398.
290. Kemp, N. T.; Cochrane, J.; Newbury, R. Nanotechnology 2007, 18, 145610.
291. Nandan, B.; Chen, H. L.; Liao, C. S.; Chen, S. A. Macromolecules 2004, 37, 9561–9570.
292. Yang, M.; Yao, X. X.; Wang, G.; Ding, H. J. Colloids Surf A 2008, 324, 113–116.
293. Chen, J. Y.; Chao, D. M.; Lu, X. F.; Zhang, W. J. Mater Lett 2007, 61, 1419–1423.
294. Chiou, N. R.; Lui, C. M.; Guan, J. J.; Lee, L. J.; Epstein, A. J. Nat Nanotechnol 2007, 2, 354–357.
295. Sun, Q. H.; Bi, W.; Fuller, T. F. Macromol Rapid Commun 2009, 30, 1027–1032.
296. Jiang, L. X.; Cui, Z. L. Polym Bull 2006, 56, 529–537.
297. Zou, X. H.; Zhang, S.; Shi, M. H.; Kong, J. L. J Solid State Electrochem 2007, 11, 317–322.
298. Kuila, B. K.; Stamm, M. J Mater Chem 2010, 20, 6086–6094.

299. Wang, X. H.; Shao, M. W.; Shao, G.; Wu, Z. C.; Wang, S. W. J Colloid Interf Sci 2009, 332, 74–77.
300. Zhang, C. Q.; Li, G. C.; Peng, H. R. Mater Lett 2009, 63, 592–594.
301. Li, G. C.; Zhang, C. Q.; Peng, H. R.; Chen, K. Z.; Zhang, Z. K. Macromol Rapid Commun 2008, 29, 1954–1958.
302. Lee, R. H.; Lai, H. H.; Wang, J. J.; Jeng, R. J.; Lin, J. J. Thin Solid Films 2008, 517, 500–505.
303. Deore, B. A.; Yu, I.; Woodmass, J.; Freund, M. S. Macromol Chem Phys 2008, 209, 1094–1105.
304. Han, D. X.; Song, J. J.; Ding, X. F.; Xu, X. Y.; Niu, L. Mater Chem Phys 2007, 105, 380–384.
305. Bhandari, H.; Bansal, V.; Choudhary, V.; Dhawan, S. K. Polym Int 2009, 58, 489–502.
306. Li, W. G.; Wang, H. L. J Am Chem Soc 2004, 126, 2278–2279.
307. Yan, Y.; Yu, Z.; Huang, Y. W.; Yuan, W. X.; Wei, Z. X. Adv Mater 2007, 19, 3353–3357.
308. Zhang, X. T.; Chechik, V.; Smith, D. K.; Walton, P. H.; Duhme-Klair, A. K.; Luo, Y. J. Synth Met 2009, 159, 2135–2140.
309. Weng, S. H.; Lin, Z. H.; Chen, L. X.; Zhou, J. Z. Electrochim Acta 2010, 55, 2727–2733.
310. Li, W. G.; Bailey, J. A.; Wang, H. L. Polymer 2006, 47, 3112–3118.
311. Lee, K. P.; Gopalan, A. I.; Lee, S. H.; Kim, M. S. Nanotechnology 2006, 17, 375–380.
312. Yan, Y.; Deng, K.; Yu, Z.; Wei, Z. X. Angew Chem, Int Ed 2009, 48, 2003–2006.
313. Zhang, D. H.; Shi, Y. J Polym Mater 2007, 24, 107–112.
314. Han, J.; Liu, Y.; Guo, R. J Polym Sci, Part A: Polym Chem 2008, 46, 740–746.
315. Mao, H.; Lu, X. F.; Chao, D. M.; Cui, L. L.; Zhang, W. J. Mater Lett 2008, 62, 998–1001.
316. Mu, S. L. Electrochim Acta 2006, 51, 3434–3440.
317. Li, G. X.; Lian, J. L.; Zheng, X. W.; Cao, J. Biosens Bioelectron 2010, 26, 643–648.
318. Langer, J. J.; Golczak, S. Polym Degrad Stabil 2007, 92, 330–334.
319. Trchova, M.; Konyushenko, E. N.; Stejskal, J.; Kovarova, J.; Ciric-Marjanovic, G. Polym Degrad Stabil 2009, 94, 929–938.
320. Mentus, S.; Ciric-Marjanovic, G.; Trchova, M.; Stejskal, J. Nanotechnology 2009, 20, 245601.
321. do Nascimento, G. M.; Silva, C. H. B.; Temperini, M. L. A. Polym Degrad Stabil 2008, 93, 291–297.
322. Yang, M. M.; Cheng, B.; Song, H. H.; Chen, X. H. Electrochim Acta 2010, 55, 7021–7027.
323. Yin, J. B.; Xia, X. A.; Xiang, L. Q.; Zhao, X. P. Carbon 2010, 48, 2958–2967.
324. Sun, Q. H.; Park, M. C.; Deng, Y. L. Mater Lett 2007, 61, 3052–3055.
325. Du, X. S.; Zhou, C. F.; Mai, Y. W. J Phys Chem C 2008, 112, 19836–19840.
326. Wang, Y. Y. PhD Dissertation, Xi'an Jiaotong University, Xi'an, People's Republic of 2007.
327. Massi, M.; Albonetti, C.; Facchini, M.; Cavallini, M.; Biscarini, F. Adv Mater 2006, 18, 2739–2742.
328. Virji, S.; Weiller, B. H.; Huang, J. X.; Blair, R.; Shepherd, H.; Faltens, T.; Haussmann, P. C.; Kaner, R. B.; Tolbert, S. H. J Chem Educ 2008, 85, 1102-1104.
329. Sutar, D. S.; Padma, N.; Aswal, D. K.; Deshpande, S. K.; Gupta, S. K.; Yakhmi, J. V. Sens Actuator, B 2007, 128, 286–292.
330. Liu, C. J.; Hayashi, K.; Toko, K. Synth Met 2009, 159, 1077–1081.
331. Chen, J. T.; Yang, J.; Yan, X. B.; Xue, Q. J. Synth Met 2010, 160, 2452–2458.
332. Li, W.; Hoa, N. D.; Cho, Y.; Kim, D.; Kim, J. S. Sens Actuator, B 2009, 143, 132–138.
333. Lekha, P. C.; Balaji, M.; Subramanian, S.; Padiyan, D. P. Curr Appl Phys 2010, 10, 457–467.
334. Liu, M. C.; Dai, C. L.; Chan, C. H.; Wu, C. C. Sensors 2009, 9, 869–880.
335. Ma, X. F.; Li, G.; Wang, M.; Cheng, Y. N.; Bai, R.; Chen, H. Z.; Chem-Eur J 2006, 12, 3254–3260.
336. Shirsat, M. D.; Bangar, M. A.; Deshusses, M. A.; Myung, N. V.; Mulchandani, A. Appl Phys Lett 2009, 94, 083502.
337. Virji, S.; Fowler, J. D.; Baker, C. O.; Huang, J. X.; Kaner, R. B.; Weiller, B. H. Small 2005, 1, 624–627.
338. Virji, S.; Kaner, R. B.; Weiller, B. H. Inorg Chem 2006, 45, 10467–10471.
339. Yan, X. B.; Han, Z. J.; Yang, Y.; Tay, B. K. Sens Actuator, B 2007, 123, 107–113.
340. Sadek, A. Z.; Wlodarski, W.; Shin, K.; Kaner, R. B.; Kalantar-zadeh, K. Nanotechnology 2006, 17, 4488–4492.
341. Sadek, A. Z.; Wlodarski, W.; Shin, K.; Kaner, R. B.; Kalantar-zadeh, K. Synth Met 2008, 158, 29–32.
342. Arsat, R.; Yu, X. F.; Li, Y. X.; Wlodarski, W.; Kalantar-zadeh, K. Sens Actuator, B 2009, 137, 529–532.
343. Arsat, R.; Tan, J.; Sadek, A. Z. Sens Lett 2008, 6, 947–950.
344. Sadek, A. Z.; Baker, C. O.; Powell, D. A.; Wlodarski, W.; Kaner, R. B.; Kalantar-zadeh, K.; IEEE Sens J 2007, 7, 213–218.
345. Atashbar, M. Z.; Sadek, A.Z.; Wlodarski, W.; Sriram, S.; Bhaskaran, M.; Cheng, C. J.; Kaner, R. B.; Kalantar-zadeh, K. Sens Actuator, B 2009, 138, 85–89.
346. Sadek, A. Z.; Wlodarski, W.; Kalantar-zadeh, K.; Baker, C.; Kaner, R. B. Sens Actuator, A 2007, 139, 53–57.
347. Virji, S.; Kaner, R. B.; Weiller, B. H. J Phys Chem B 2006, 110, 22266–22270.
348. Fowler, J. D.; Virji, S.; Kaner, R. B.; Weiller, B. H. J Phys Chem C 2009, 113, 6444–6449.
349. Al-Mashat, L.; Shin, K.; Kalantar-zadeh, K.; Plessis, J. D.; Han, S. H.; Kojima, R. W.; Kaner, R. B.; Li, D.; Gou, X. L.; Ippolito, S. J.; Wlodarski, W. J Phys Chem C 2010, 114, 16168–16173.
350. Virji, S.; Kojima, R.; Fowler, J. D.; Villanueva, J. G.; Kaner, R. B.; Weiller, B. H. Nano Res 2009, 2, 135–142.
351. Virji, S.; Kojima, R.; Fowler, J. D.; Kaner, R. B.; Weiller, B. H. Chem Mater 2009, 21, 3056–3061.
352. Maddu, A.; Zain, H.; Sardy, S. J Optoelectron Adv Mater 2007, 9, 2362–2366.
353. Xie, G. Z.; Sun, P.; Yan, X. L.; Du, X. S.; Jiang, Y. D. Sens Actuator, B 2010, 145, 373–377.
354. Pal, S.; Alocilja, E. C.; Downes, F. P. Biosens Bioelectron 2007, 22, 2329–2336.
355. Liu, Y.; Gore, A.; Chakrabartty, S.; Alocilja, E. C. Microchim Acta 2008, 163, 49–56.

356. Somerset, V.; Klink, M.; Akinyeye, R.; Michira, I.; Sekota, M.; Al-Ahmed, A.; Baker, P. G. L.; Iwuoha, E. Macromol Symp 2007, 255, 36–49.
357. Michira, I.; Akinyeye, R.; Somerset, V.; Klink, M. J.; Sekota, M.; Al-Ahmed, A.; Baker, P. G. L.; Iwuoha, E. Macromol Symp 2007, 255, 57–69.
358. Rajesh; Ahuja, T.; Kumar, D. Sens Actuator, B 2009, 136, 275–286.
359. Yang, T.; Zhou, N.; Zhang, Y. C.; Zhang, W.; Jiao, K.; Li, G. C. Biosens Bioelectron 2009, 24, 2165–2170.
360. Yang, T.; Jiang, C.; Zhang, W.; Jiao, K. Sci China-Chem 2010, 53, 1371–1377.
361. Xia, L.; Wei, Z. X.; Wan, M. X. J Colloid Interf Sci 2010, 341, 1–11.
362. Du, Z. F.; Li, C. C.; Li, L. M.; Zhang, M.; Xu, S. J.; Wang, T. H. Mater Sci Eng C 2009, 29, 1794–1797.
363. Horng, Y. Y.; Hsu, Y. K.; Ganguly, A.; Chen, C. C.; Chen, L. C.; Chen, K. H. Electrochem Commun 2009, 11, 850–853.
364. Zhao, M.; Wu, X. M.; Cai, C. X. J Phys Chem C 2009, 113, 4987–4996.
365. Santos, A. N.; Soares, D. A. W.; de Queiroz, A. A. A. Mater Res -Ibero-Am J Mater, 2010, 13, 5–10.
366. Xu, L. H.; Zhu, Y. H.; Tang, L. H.; Yang, X. L.; Li, C. Z. J Appl Polym Sci 2008, 109, 1802–1807.
367. Lee, G.; Kim, J.; Lee, J. H. Enzyme Microb Technol 2008, 42, 466–472.
368. Fernandes, E. G. R.; De Queiroz, A. A. A. J Mater Sci: Mater Med 2009, 20, 473–479.
369. Cao, F. M.; Liao, J.; Yang, K. G.; Bai, P. L.; Wei, Q.; Zhao, C. S. Anal Lett 2010, 43, 2790–2797.
370. Xian, Y. Z.; Hu, Y.; Liu, F.; Xian, Y.; Wang, H. T.; Jin, L. T. Biosens Bioelectron 2006, 21, 1996–2000.
371. Wang, Z. Y.; Liu, S. N.; Wu, P.; Cai, C. X. Anal Chem 2009, 81, 1638–1645.
372. Joo, H.; Lee, J. H. J Mol Catal B, Enzym 2010, 67, 179–183.
373. Zhang, W.; Yang, T.; Li, X.; Wang, D. B.; Jiao, K. Biosens Bioelectron 2009, 25, 428–434.
374. Zhou, N.; Yang, T.; Jiang, C.; Du, M.; Jiao, K. Talanta 2009, 77, 1021–1026.
375. Chang, H. X.; Yuan, Y.; Shi, N. L.; Guan, Y. F. Anal Chem 2007, 79, 5111–5115.
376. Feng, Y. Y.; Yang, T.; Zhang, W.; Jiang, C.; Jiao, K. Anal Chim Acta 2008, 616, 144–151.
377. Dhand, C.; Solanki, P. R.; Sood, K. N.; Datta, M.; Malhotra, B. D. Electrochem Commun 2009, 11, 1482–1486.
378. Ren, R.; Leng, C. C.; Zhang, S. S. Biosens Bioelectron 2010, 25, 2089–2094.
379. Fan, Y.; Chen, X. T.; Trigg, A. D.; Tung, C. H.; Kong, J. M.; Gao, Z. Q. J Am Chem Soc 2007, 129, 5437–5443.
380. Zhang, L. J.; Peng, H.; Hsu, C. F.; Kilmartin, P. A.; Travas-Sejdic, J. Nanotechnology 2007, 18, 115607.
381. Zhang, L. J.; Peng, H.; Sui, J.; Kilmartin, P. A.; Travas-Sejdic, J. Curr Appl Phys 2008, 8, 312–315.
382. Zhang, L. J.; Peng, H.; Kilmartin, P. A.; Soeller, C.; Travas-Sejdic, J. Electroanalysis 2007, 19, 870–875.
383. Hu, Z. C.; Xu, J. J.; Tian, Y.; Peng, R.; Xian, Y. Z.; Ran, Q.; Jin, L. T. Electrichim Acta 2009, 54, 4056–4061.
384. Wang, X. L.; Yang, T.; Feng, Y. Y.; Jiao, K.; Li, G. C. Electroanalysis 2009, 21, 819–825.
385. Langer, K.; Barczynski, P.; Baksalary, K.; Filipiak, M.; Golczak, S.; Langer, J. J. Microchim Acta 2007, 159, 201–206.
386. Langer, J. J.; Langer, K.; Barczynski, P.; Warchoł, J.; Bartkowiak, K. H. Biosens Bioelectron 2009, 24, 2947–2949.
387. Dhand, C.; Solanki, P. R.; Pandey, M. K.; Datta, M.; Malhotra, B. D. Electrophoresis 2010, 31, 3754–3762.
388. Barik, A.; Solanki, P. R.; Kaushik, A.; Ali, A.; Pandey, M. K.; Kim, C. G.; Malhotra, B. D. J Nanosci Nanotechnol 2010, 10, 6479–6488.
389. Venancio, E. C.; Mattoso, L. H. C.; Herrmann, P. S. D.; MacDiarmid, A. G. Sens Actuator, B 2008, 130, 723–729.
390. Wu, T. T.; Chen, Y. Y.; Chou, T. H. J Phys D: Appl Phys 2008, 41, 085101.
391. Zeng, F. W.; Liu, X. X.; Diamond, D.; Lau, K. T. Sens Actuator, B 2010, 143, 530–534.
392. Wang, F.; Wang, W. B.; Liu, B. H.; Wang, Z. Y.; Zhang, Z. P. Talanta 2009, 79, 376–382.
393. Medeiros, E. S.; Gregorio, R.; Martinez, R. A.; Mattoso, L. H. C. Sens Lett 2009, 7, 24–30.
394. Ayad, M. M.; Prastomo, N.; Matsuda, A.; Stejskal, J. Synth Met 2010, 160, 42–46.
395. Ayad, M. M.; Abu El-Nasr, A. J Phys Chem C 2010, 114, 14377–14383.
396. Mallick, K.; Witcomb, M.; Scurrell, M. Platinum Met Rev 2007, 51, 3–15.
397. Wang, H. L.; Li, W. G.; Jia, Q. X.; Akhadov, E. Chem Mater 2007, 19, 520–525.
398. Liu, F. J.; Huang, L. M.; Wen, T. C.; Yin, K. C.; Hung, J. S.; Gopalan, A. Polym Compos 2007, 28, 650–656.
399. Liu, F. J.; Huang, L. M.; Wen, T. C.; Gopalan, A. Synth Met 2007, 157, 651–658.
400. Huang, H. P.; Feng, X. M.; Zhu, J. J. Nanotechnology 2008, 19, 145607.
401. Gallon, B. J.; Kojima, R. W.; Kaner, R. B.; Diaconescu, P. L. Angew Chem, Int Ed 2007, 46, 7251–7254.
402. Kong, L. R.; Lu, X. F.; Jin, E.; Jiang, S.; Wang, C.; Zhang, W. J. Compos Sci Technol 2009, 69, 561–566.
403. Jiang, C. M.; Lin, X. Q. J Appl Electrochem 2008, 38, 1659–1664.
404. Jiang, C. M.; Lin, X. Q. J Power Sources 2007, 164, 49–55.
405. Chen, Z. W.; Xu, L. B.; Li, W. Z.; Waje, M.; Yan, Y. S. Nanotechnology 2006, 17, 5254–5259.
406. Liu, F. J.; Huang, L. M.; Wen, T. C.; Li, C. F.; Huang, S. L.; Gopalan, A. Synth Met 2008, 158, 603–609.
407. Ma, S. J.; Luo, S. L.; Zhou, H. H.; Kuang, Y. F.; Ning, X. H. J Cent South Univ Technol 2008, 15, 170–175.
408. Zhang, L. J.; Peng, H.; Kilmartin, P. A.; Soeller, C.; Travas-Sejdic, J. Macromolecules 2008, 41, 7671–7678.
409. Mu, S. L. Synth Met 2006, 156, 202–208.
410. Likhar, P. R.; Arundhathi, R.; Ghosh, S.; Kantam, M. L. J Mol Catal, A: Chem 2009, 302, 142–149.
411. Gharibi, H.; Zhiani, M.; Mirzaie, R. A.; Kheirmand, M.; Entezami, A. A.; Kakaei, K.; Javaheri, M. J Power Sources 2006, 157, 703–708.

412. Wang, J.; Qi, X.; Meng, F. J Phys Chem C 2009, 113, 1459–1465.
413. Arundhathi, R.; Kumar, D. C.; Sreedhar, B. J Org Chem 2010, 3621–3630.
414. Lam, T. L.; Tran, H.; Yuan, W.; Yu, Z. B.; Ha, S. M.; Kaner, R. B.; Pei, Q. B. In Proceedings of the Society of Photo-Optical Instrumentation Engineers (SPIE), Conference on Electroactive Polymer Actuators and Devices (EAPAD 2008), Mar 10–13, 2008, San Diego, CA, O9270 (2008).
415. Kim, S. H.; Oh, K. W.; Choi, J. H. J Appl Polym Sci 2010, 116, 2601–2609.
416. Baker, C. O.; Shedd, B.; Innis, P. C.; Whitten, P. G.; Spinks, G. M.; Wallace, G. G.; Kaner, R. B. Adv Mater 2008, 20, 155–158.
417. Shedd, B.; Baker, C. O.; Heller, M. J.; Kaner, R. B.; Hahn, H. T. Mater Sci Eng B 2009, 162, 111–115.
418. Gao, H. N.; Zhang, J. H.; Yu, W. L.; Li, Y. F.; Zhu, S. J.; Li, Y.; Wang, T. Q.; Yang, B. Sens Actuator, B 2010, 145, 839–846.
419. Amarnath, C. A.; Chang, J.; Lee, J.; Kim, D. Y.; Mane, R. S.; Han, S. H.; Sohn, D. Electrochem Solid State Lett 2008, 11, A167–A169.
420. Subramania, A.; Devi, S. L. Polym Adv Technol 2008, 19, 725–727.
421. Sun, L. J.; Liu, X. X.; Lau, K. K. T.; Chen, L.; Gu, W. M. Electrochim Acta 2008, 53, 3036–3042.
422. Ghenaatian, H. R.; Mousavi, M. F.; Kazemi, S. H.; Shamsipur, M. Synth Met 2009, 159, 1717–1722.
423. Guan, H.; Fan, L. Z.; Zhang, H. C.; Qu, X. H. Electrochim Acta 2010, 56, 964–968.
424. Pan, L. J.; Qiu, H.; Dou, C. M.; Li, Y.; Pu, L.; Xu, J. B.; Shi, Y. Int J Mol Sci 2010, 11, 2636–2657.
425. Li, G. R.; Feng, Z. P.; Zhong, J. H.; Wang, Z. L.; Tong, Y. X. Macromolecules 2010, 43, 2178–2183.
426. Liu, X. X.; Dou, Y. Q.; Wu, J.; Peng, X. Y. Electrochim Acta 2008, 53, 4693–4698.
427. Gupta, V.; Miura, N. Mater Lett 2006, 60, 1466–1469.
428. Dhawale, D. S.; Salunkhe, R. R.; Jamadade, V. S.; Dubal, D. P.; Pawar, S. M.; Lokhande C. Curr Appl Phys 2010, 10, 904–909.
429. Zhao, G. Y.; Li, H. L. Micropor Mesopor Mater 2008, 110, 590–594.
430. Dhawale, D. S.; Dubal, D. P.; Jamadade, V. S.; Salunkhe, R. R.; Lokhande, C. D. Synth Met 2010, 160, 519–522.
431. Kuila, B. K.; Nandan, B.; Bohme, M.; Janke, A.; Stamm, M. Chem Commun 2009, 5749–5751.
432. Amarnath, C. A.; Chang, J. H.; Kim, D.; Mane, R. S.; Han, S. H.; Sohn, D. Mater Chem Phys 2009, 113, 14–17.
433. Xu, J. J.; Wang, K.; Zu, S. Z.; Han, B. H.; Wei, Z. X. ACS Nano 2010, 4, 5019–5026.
434. Wang, K.; Huang, J. Y.; Wei, Z. X. J Phys Chem C 2010, 114, 8062–8067.
435. Hung, P. J.; Chang, K. H.; Lee, Y. F.; Hu, C. C.; Lin, K. M. Electrochim Acta 2010, 55, 6015–6021.
436. Wu, Q.; Xu, Y. X.; Yao, Z. Y.; Liu, A. R.; Shi, G. Q. ACS Nano 2010, 4, 1963–1970.
437. Horng, Y. Y.; Lu, Y. C.; Hsu, Y. K.; Chen, C. C.; Chen, L. C.; Chen, K. H. J Power Sources 2010, 195, 4418–4422.
438. Kim, B. C.; Kwon, J. S.; Ko, J. M.; Park, J. H.; Too, C. O.; Wallace, G. G. Synth Met 2010, 160, 94–98.
439. Bian, C. Q.; Yu, A. S. Synth Met, 2010, 160, 1579–1583.
440. Sivakkumar, S. R.; Kim, W. J.; Choi, J. A.; MacFarlane, D. R.; Forsyth, M.; Kim, D. W. J Power Sources 2007, 171, 1062–1068.
441. Sivakkumar, S. R.; Oh, J. S.; Kim, D. W. J Power Sources 2006, 163, 573–577.
442. Michel, M.; Ettingshausen, F.; Scheiba, F.; Wolz, A.; Roth, C. Phys Chem Chem Phys 2008, 10, 3796–3801.
443. Zhiani, M.; Gharibi, H.; Kakaei, K. Int J Hydrogen Eng 2010, 35, 9261–9268.
444. Zhiani, M.; Rezaei, B.; Jalili, J. Int J Hydrogen Eng 2010, 35, 9298–9305.
445. Chang, M. Y.; Wu, C. S.; Chen, Y. F.; Hsieh, B. Z.; Huang, W. Y.; Ho, K. S.; Hsieh, T. H.; Han, Y. K. Org Electron 2008, 9, 1136–1139.
446. Ameen, S.; Akhtar, M. S.; Kim, Y. S.; Yang, O. B.; Shin, H. S. J Phys Chem C 2010, 114, 4760–4764.
447. Chen, J. Z.; Li, B.; Zheng, J. F.; Zhao, J. H.; Jing, H. W.; Zhu, Z. P. Electrochim Acta 2011, 56, 4624–4630.
448. Wanekaya, A. K.; Bangar, M. A.; Yun, M.; Chen, W.; Myung, N. V.; Mulchandani, A. J Phys Chem C 2007, 111, 5218–5221.
449. Aw, K. C.; Salim, N. T.; Peng, H.; Zhang, L. J.; Travas-Sejdic, J.; Gao, W. J Mater Sci: Mater Electron 2008, 19, 996–999.
450. Lee, S. Y.; Choi, G. R.; Lim, H.; Lee, K. M.; Lee, S. K. Appl Phys Lett 2009, 95, 013113.
451. Lee, S. Y.; Lee, S. K.; Lim, H.; Choi, G. R. J Korean Phys Soc 2010, 57, 1416–1420.
452. Bangar, M. A.; Chen, W.; Myung, N. V.; Mulchandani, A. Thin Solid Films 2010, 519, 964–973.
453. Hangarter, C. M.; Bangar, M.; Mulchandani, A.; Myung, N. V. J Mater Chem 2010, 20, 3131–3140.
454. Yu, X. F.; Li, Y. X.; Zhu, N. F.; Yang, Q. B.; Kalantar-zadeh, K. Nanotechnology 2007, 18, 015201.
455. Niemann, M. U.; Srinivasan, S. S.; Phani, A. R.; Kumar, A.; Goswami, D. Y.; Stefanakos, E. K. J Nanosci Nanotechnol 2009, 9, 4561–4565.
456. Qu, M. N.; Zhao, G. Y.; Cao, X. P.; Zhang, J. Y. Langmuir 2008, 24, 4185–4189.
457. Zhang, H. B.; Wang, J. X.; Zhou, Z. B.; Wang, Z.; Zhang, F. B.; Wang, S. C. Macromol Rapid Commun 2008, 29, 68–73.
458. Li, X. W.; Li, X. H.; Dai, N.; Wang, G. C. Appl Surf Sci 2009, 255, 8276–8280.
459. Li, D.; Kaner, R. B. Chem Commun 2005, 3286–3288.
460. Yao, B.; Wang, G. C.; Ye, J. K.; Li, X. W. Mater Lett 2008, 62, 1775–1778.
461. Bhandari, H.; Srivastav, R.; Choudhary, V.; Dhawan, S. K. Thin Solid Films 2010, 519, 1031–1039.
462. Yang, X. G.; Li, B.; Wang, H. Z.; Hou, B. R. Prog Org Coat 2010, 69, 267–271.
463. Hu, L.; Gruner, G.; Jenkins, J.; Kim, C. J. J Mater Chem 2009, 19, 5845–5849.
464. Wang, Y.; Jing, X. L. Mater Sci Eng B 2007, 138, 95–100.
465. Banerjee, S.; Kumar, A. J Phys Chem Solids 2010, 71, 381–388.
466. Choi, J. H.; Kim, S. H.; Oh, K. W. Mol Cryst Liq Cryst 2007, 464, 863–871.
467. Jia, Q. M.; Li, J. B.; Wang, L. F.; Zhu, J. W.; Zheng, M. S. Mater Sci Eng A 2007, 448, 356–360.

468. Niu, Y. H. Polym Eng Sci 2008, 48, 355–359.
469. Su, C.; Wang, G. C.; Huang, F. R.; Li, X. W. Polym Compos 2008, 29, 1177–1182.
470. Bhadra, J.; Sarkar, D. Mater Lett 2009, 63, 69–71.
471. Kim, H. S.; Hobbs, H. L.; Wang, L.; Rutten, M. J.; Wamser, C. C. Synth Met 2009, 159, 1313–1318.
472. Borriello, A.; Guarino, V.; Schiavo, L.; Alvarez-Perez, M. A.; Ambrosio, L. J Mater Sci: Mater Med 2011, 22, 1053–1062.
473. Wang, C. C.; Song, J. F.; Bao, H. M.; Shen, Q. D.; Yang, C. Z. Adv Funct Mater 2008, 18, 1299–1306.
474. Deka, M.; Nath, A. K.; Kumar, A. Indian J Phys 2010, 84, 1299–1305.
475. Nath, A. K.; Deka, M.; Kumar, A. Indian J Phys 2010, 84, 1307–1313.
476. Fan, Z. F.; Wang, Z.; Duan, M. R.; Wang, J. X.; Wang, S. C. J Membr Sci 2008, 310, 402–408.
477. Fan, Z. F.; Wang, Z.; Sun, N.; Wang, J. X.; Wang, S. C. J Membr Sci 2008, 320, 363–371.
478. Araujo, P. L. B.; Santos, R. F. S.; Araujo, E. S. eXPRESS Polym Lett 2007, 1, 385–390.
479. Wang, J.; Zhu, L. H.; Li, J.; Tang, H. Q. Chin Chem Lett 2007, 18, 1005–1008.
480. Banerjee, S.; Saikia, J. P.; Kumar, A.; Konwar, B. K. Nanotechnology 2010, 21, 045101.
481. Kumar, A.; Banerjee, S.; Saikia, J. P.; Konwar, B. K. Nanotechnology 2010, 21, 175102.
482. Guo, S. J.; Dong, S. J.; Wang, E. K. Small 2009, 5, 1869–1876.
483. Han, J.; Li, L. Y.; Guo, R. Macromolecules 2010, 43, 10636–10644.
484. Hung, C. C.; Wen, T. C.; Wei, Y. Mater Chem Phys 2010, 122, 392–396.
485. Wang, X. X.; Yang, T.; Jiao, K. Chin Sci Bull 2010, 55, 4125–4131.
486. Stejskal, J.; Prokes, J.; Sapurina, I. Mater Lett 2009, 63, 709–711.
487. Trchova, M.; Stejskal, J. Synth Met 2010, 160, 1479–1486.
488. Choi, H. J.; Jhon, M. S. Soft Matter 2009, 1562–1567.
489. Yin, J. B.; Zhao, X. P.; Xia, X.; Xiang, L. Q.; Qiao, Y. P. Polymer 2008, 49, 4413–4419.
490. Yin, J. B.; Xia, X.; Xiang, L. Q.; Qiao, Y. P.; Zhao, X. P. Smart Mater Struct 2009, 18, 095007.
491. Deka, M.; Nath, A. K.; Kumar, A. J Membr Sci 2009, 327, 188–194.
492. Baker, C. O.; Shedd, B.; Tseng, R. J.; Martinez-Morales, A. A.; Ozkan, C. S.; Ozkan, M.; Yang, Y.; Kaner, R. B. ACS Nano 2011, 5, 3469–3474.